POLYIMIDES
AS ELECTRODE MATERIALS FOR ELECTROCHEMICAL CELLS

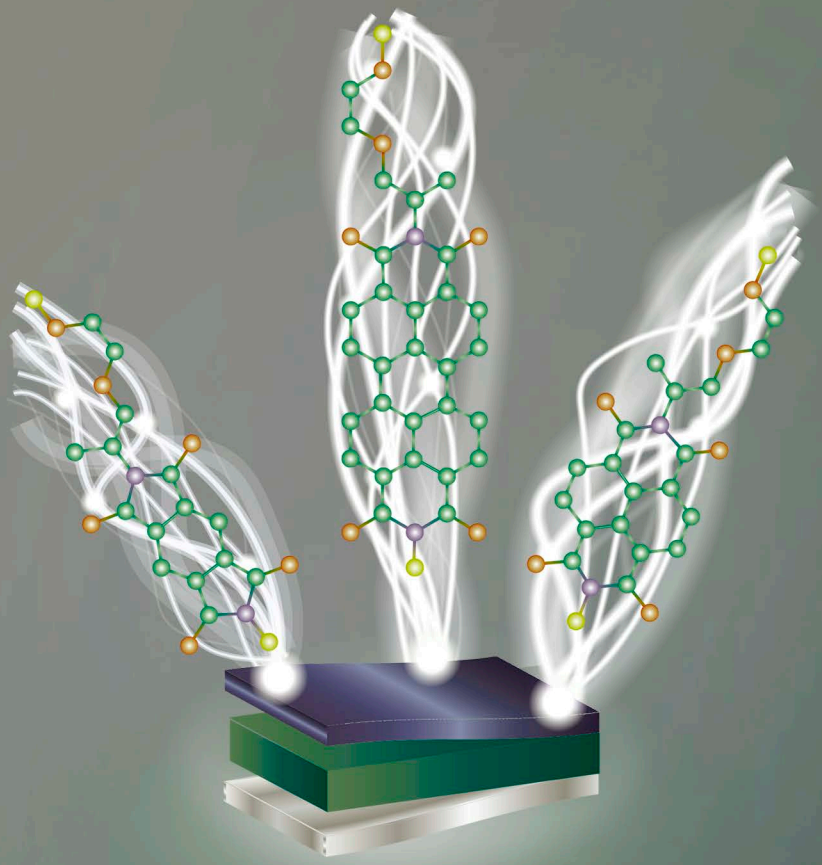

GUIOMAR HERNÁNDEZ GUTIÉRREZ

JULY 6, 2017

eman ta zabal zazu
Universidad del País Vasco
Euskal Herriko Unibertsitatea

POLYMAT

POLYIMIDES AS ELECTRODE MATERIALS FOR ELECTROCHEMICAL CELLS

Guiomar Hernández Gutiérrez

Thesis Advisor:

Prof. David Mecerreyes

University of the Basque Country UPV/EHU

Donostia-San Sebastián

2017

Table of contents

CHAPTER 1.
INTRODUCTION

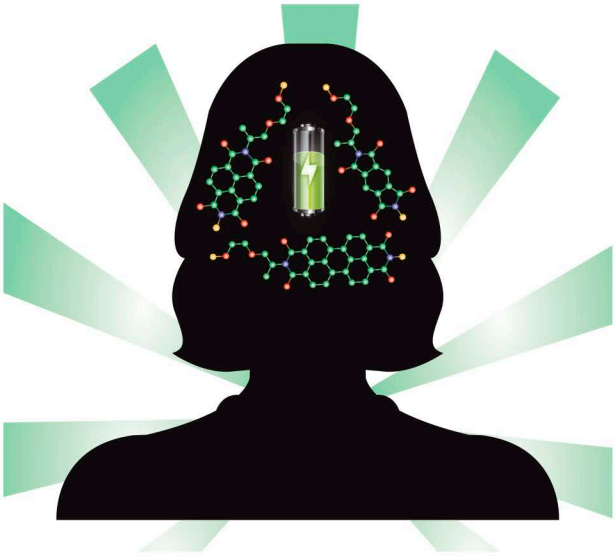

Chapter 1. Introduction

1.1. Electrochemical energy storage

Transition from fossil fuels to renewable energy is an immediate global necessity and challenge to combat global warming and climate change. A sustainable modern society must be able to store cleanly energy coming from wind and radiant solar energy. Unfortunately, these renewable energy sources are inherently erratic and generally dispersed. Thus, there is an important and growing need for efficient energy storage technologies in order to make the best use of these energy sources.[1,2] Electrochemical energy storage applications are growing enormously from portable electronics, to the widespread implementation of electric transportation systems and even grid-level energy storage.

However, the major bottleneck of these technologies is the relatively poor battery performance. The slow progress in the battery field, in comparison with the area of electronics, is due to the lack of suitable electrode materials and electrolytes.[3-6] Nevertheless, energy density and power capability at any price should not be the ultimate goal. Indeed, new concepts such as environmental

impact, cost effectiveness, sustainability and safety of the materials and devices are arising; providing new challenges and opportunities towards the development of novel electrode materials (Figure 1.1).[5,7] Furthermore, requirements such as flexibility, rapid charging, excellent cycle life and easy processing techniques are vital for the electrochemical energy storage devices used in applications related to the Internet of Things (IoT)[3] (mobile devices,[8] healthcare,[9] smart surfaces[10] and packaging[11] and wearable electronics).[12]

Lithium-ion batteries (Li-ion), with high energy density and design flexibility, are extensively employed in portable electronic devices and their application has

Figure 1.1. Future challenges in batteries.

expanded to the electric vehicle market.[13] However, several drawbacks of this technology should be recognize, such as the presence of toxic metal salts, low relative abundance of materials and the large energy cost of battery manufacture and recycling.[2,3] Therefore, other technologies beyond lithium-ion batteries, such as lithium-air (Li-air),[14] lithium-sulfur (Li-S),[15,16] sodium-ion (Na-ion),[17] zinc (Zn),[18] magnesium (Mg),[19] Li-organic[3] and organic redox flow (RFB)[20,21] batteries, have gained much attention due to their advantageous sustainability, cost-effectiveness and/or high capacity.[2,7,22]

1.1.1. Rechargeable batteries

An electrochemical cell is a device able to convert chemical energy directly into electric energy. The chemical energy is stored in the active materials and it is accessed by means of an electrochemical oxidation-reduction (redox) reaction. In the case of a rechargeable system this reaction is reversible. It is worth noting that while the term “battery” is often used, the appropriate term for the basic electrochemical unit is “cell”. A battery consists of one or more of these cells, connected in series or parallel, or both, depending on the desired output voltage and capacity.[23] However, for the sake of simplicity, the term battery (when used) will refer to a reversible electrochemical cell.

The cell consists of three major components: anode, cathode and electrolyte. The anode and cathode are the active materials of the cell, able to undergo a reversible redox reaction. Anode is the electrode that is oxidized during discharge (negative electrode), whereas the cathode is reduced during discharge (positive electrode). During the charge step, opposite redox reactions are taking place at each electrode; therefore, the terms anode and cathode are only valid during the discharge process of rechargeable batteries. However, negative electrodes are often regarded as anodes and positive electrodes as cathodes throughout the battery literature.[3,23] The two electrodes are separated by a solid electrolyte or by an insulating separator permeable to a liquid electrolyte. The

electrolyte conducts ions between the electrodes, enabling charge balance; therefore high ionic conductivity is desirable. Nevertheless, it has to be an electronic insulator to force electrons generated during the chemical reactions to flow through the external circuit where they can do work, and avoid short-circuiting of the cell.

Figure 1.2 depicts a schematic representation of the discharge and charge processes of a secondary or rechargeable metal-organic battery. During the discharge process (Figure 1.2a), the electrons flow from the anode, which is oxidized, through the external circuit to the cathode which is reduced accepting the electrons. At the same time, to ensure the charge balance, cations from the electrolyte flow to the cathode and anions to the anode. During the charge process (Figure 1.2b), the current flow is reversed; when the so-called cathode is oxidized, electrons flow from this electrode to the opposite one which is simultaneously reduced. Ions also flow in the reverse direction during charge, cations move from the cathode to the anode and *vice versa* for anions. While discharge is a spontaneous process, during charging a voltage in the opposite direction should be applied.[6]

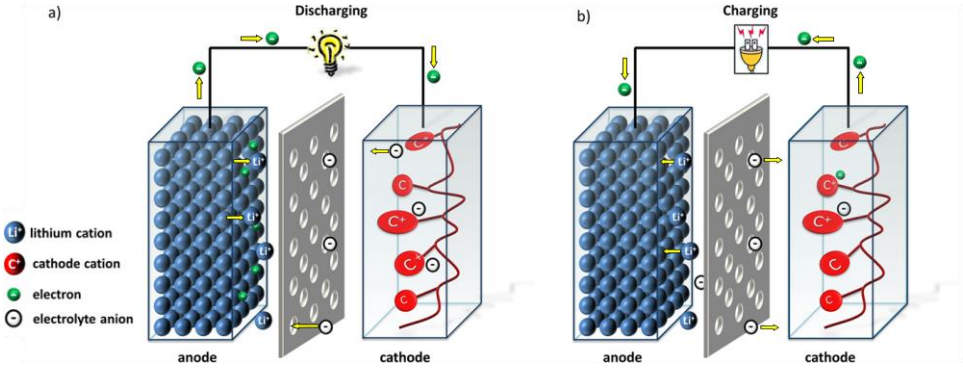

Figure 1.2. Schematic representation of (a) discharge and (b) charge processes in a metal-polymer cell.[3]

The amount of electrical energy per mass or volume (W h kg^{-1}) that a battery can deliver is the product of the cell's voltage and capacity. Another important parameter is power, which is related to how quickly the energy of the cell can be accessed (W kg^{-1}). These parameters are mostly dependent on the chemistry of the system. The cell voltage (V) is the difference between the cathode potential and the anode potential. The capacity (mA h g^{-1}) is the amount of electric charge that can be stored per unit mass in the cell. The theoretical specific capacity of a single electrode can be calculated according to Equation (1-1).

$$\text{Theoretical capacity (mA h g}^{-1}) = \frac{n\,F}{3.6 \times MW} \qquad \text{Equation 1-1}$$

where n is the number of transferred electrons per redox reaction, F the Faraday constant, 3.6 the conversion factor and MW the molar mass of the structural unit. There are three ways to maximize the energy of the battery: (1) larger chemical potential difference between the two electrodes; (2) lighter molecular or atomic weights of the reactants; and (3) increasing the number of electrons transferred per molecule of the active materials.[6,24]

Regarding the electrochemical characterization methods, cyclic voltammetry (CV) is the technique used to study the redox properties of electrochemically active compounds. This technique allows the determination of redox potentials at which the oxidation and reduction reactions take place. The potential of the working electrode is ramped linearly with time while measuring the current. In a cyclic voltammogram current is plotted versus the applied voltage, an example of a reversible redox reaction is depicted in Figure 1.3a. The current increases or decreases when the oxidation or reduction reactions, respectively, are taking place. In addition to potential values, cyclic voltammetry also provides valuable information about reversibility, stability and kinetics.

Another important battery characterization method is the galvanostatic charge-

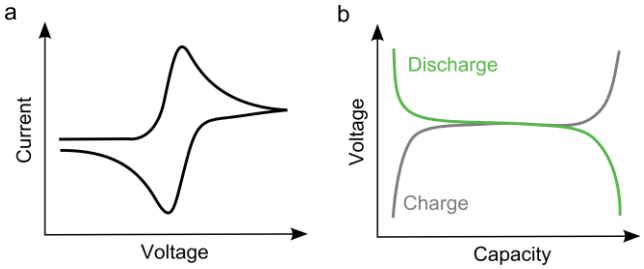

Figure 1.3. (a) Cyclic voltammogram for a reversible redox process and (b) typical voltage profiles for charge (grey) and discharge (green).

discharge. In this experiment, the cell voltage is monitored during time while applying a constant current, known as C-rate, which is the current needed to obtain the complete (dis)charge capacity in an established number of hours. The product of time and current gives the capacity of the device. A single, pronounced plateau, as depicted in Figure 1.3b, indicates a charge/discharge process that shows negligible changes of the system until complete conversion of the active material. The operating voltage of the device can be directly read from the plateau. The difference between the charge and discharge voltages indicates the polarization (and energy loss) during the whole process. Other information obtained from this experiment is the active mass utilization, which is the ratio between the experimental capacity delivered by the cell and the theoretical capacity. Coulombic efficiency is the ratio between discharge and charge capacities, and it is related to the energy that can be delivered in comparison with the energy required to charge the cell. Finally, the stability of the cell is determined by the capacity retention which is the ratio between the capacity at a specific cycle number and the initial capacity.

1.1.2. Role of polymers in batteries

Besides the three main components of the battery, anode, cathode and electrolyte; there are many other parts such as binders, separators, conductive

additives and current collectors, which play an important role although they do not contribute to the overall energy of the cell. In general, active materials are insulating, therefore conductive additives, mainly (nanostructured) carbon materials are required to ensure a good electronic conductivity. Those two components are integrated together by a polymer binder ensuring a good mechanical contact also with the current collector which is in charge of transferring electrons from the composite electrode to the external circuit and *vice versa*.

The application of polymeric materials is ubiquitous throughout all those components. Polymers have been widely used as binder materials. Fluorinated polymers such as poly(tetrafluoroethylene) (PTFE) and poly(vinylidene fluoride) (PVDF) feature good electrochemical stability and binding capability; however, they require the usage of toxic organic solvents, such as *N*-methyl-2-pyrrolidone (NMP). Therefore, alternative water-soluble binders are arising, being carboxymethylcellulose (CMC) one example.[25]

The majority of separators are based on microporous polyolefins films (*e.g.*, Celgard)[26] which physically isolate the cathode from the anode while allowing the flow of electrolyte ions. One example of alternative electrolyte systems with enhanced safety are solid polymer electrolytes composed of salts dissolved in a polymer matrix, usually poly(ethylene oxide) (PEO);[27] or gel electrolytes based on a polymer matrix providing mechanical support swollen with liquid electrolyte.[28]

Furthermore, conducting polymers have been used as conductive additives in the electrode formulation due to their inherent high electrical conductivity. Some examples are polypyrrole (PPy),[29] polyaniline (PANI)[30] and poly(3,4-ethylenedioxythiophene) (PEDOT).[31]

Nowadays, research is focusing on a new application of polymers in batteries, in

particular as active materials. For several reasons, redox polymers are promising alternative substitutes of conventional inorganic materials.[32] Polymers are potentially low-cost because abundant and inexpensive elements are involved. They feature sustainability and environmentally friendliness due to the low CO_2 footprint as high temperatures are not required and the absence of metals facilitates their disposal by low temperature combustion.[7,33,34] Although polymers are synthesized from fossil oil, research is also focusing on developing polymers coming from renewable sources.[35,36] Another important aspect of polymers is the low heat generation of the simple one-electron redox reaction with a minimized risk of thermal runaway in contrast to intercalation electrodes.[3]

In addition, they display many other advantages such as their inherent flexibility, light weight, high thermal and mechanical stability and their industrial scale production and processing. The wide structure diversity of polymers allows their redox properties to be tailored in a straightforward way, given that they depend on the electrochemically active groups, which can be modified by organic chemistry.[33] In contrast to inorganic materials, whose redox reactions are based on complex intercalation mechanisms, the electrochemical behavior of polymers is based on simple conversion reactions, allowing the exchange of other metals (Na, Mg, Zn) besides lithium as well as leading to high rate performance.

Research on polymer batteries started with the discovery of the electronic conductivity of doped conjugated polymers in 1977 by Shirakawa and co-workers. Afterwards, research focused mainly on conjugated polymers such as PANI, PPy, poly(carbazole),[37] and more recently PEDOT.[38] However, these polymers do not feature a distinct redox potential as it depends on the doping level resulting in a sloping voltage profile. To circumvent this drawback, polymers with isolated redox-active units attached to an insulating or conductive backbone have been developed.[3,32,34] Electrochemical properties of these materials are determined by the redox-active groups, leading to a distinct redox potential.

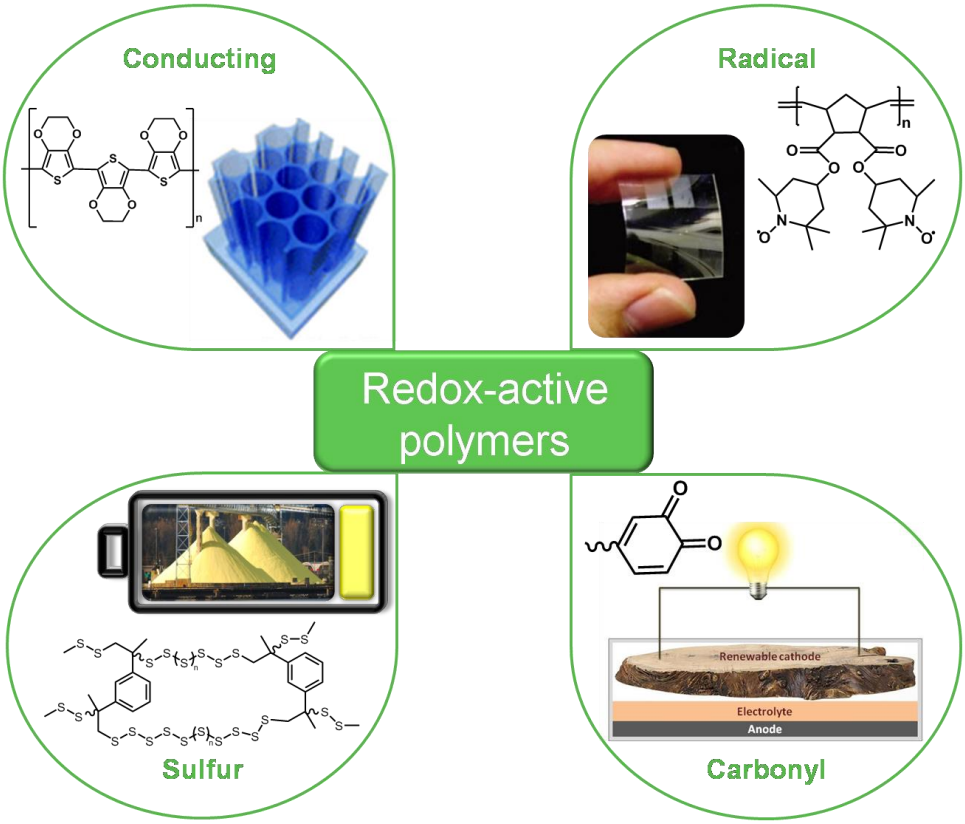

Figure 1.4. Types of redox-active polymers.[32]

These redox-active polymers can be divided into four types (Figure 1.4): conducting, radical, sulfur and carbonyl polymers.

Radical polymers contain radical species as redox-active units, the most studied one is 2,2,6,6-tetramethylpiperidine-1-oxyl (TEMPO).[39] They feature excellent electrochemical properties, in particular regarding their fast redox kinetics. Despite the high amount of radical polymers reported in literature, the number of different types of radicals that could be used for battery applications is rather limited.

Sulfur is an environmentally friendly and highly abundant element on earth; due to its redox activity it has emerged as a candidate for battery applications. Starting with the sodium/sulfur battery, numerous sulfur-based organic materials have been developed, mostly having disulfides or thioether groups.[16,40,41] Although they are able to provide high charge-storage capacity, the main drawback to be overcome is the strong capacity and voltage fading upon repeated cycling.[3]

Carbonyl-based polymers for electrochemical energy storage applications require functional moieties to stabilize the negatively charged carbon-oxygen groups.[33] Among many types of carbonyl groups, they can be classified in quinones,[42] imides[43] and other carbonyl derivatives, *e.g.* conjugated carboxylates.[44] Carbonyl polymers feature wide structure diversity, high theoretical capacity due to their ability to undergo multielectron redox reactions, in addition to good capacity stability upon cycling, which make them excellent candidates for electrochemical energy storage in comparison with conducting, radical or sulfur polymers. Given all these advantages, this thesis is based on electroactive carbonyl polymers.

1.2. Carbonyl polymers for batteries

The carbonyl group is a common organic structural specie featuring oxidative ability. It is able to undergo a one-electron reduction depending on its stabilizing substituents, even extending to more electrons if further carbonyl groups are connected in direct conjugation. Stabilization mechanism of the anion categorizes carbonyl moieties into three groups (Figure 1.5).[33,45] Compounds from group I employ neighboring carbonyls to form stable enolates upon reduction. Group II encompasses compounds based on aromatic carbonyl derivatives; carbonyl units are directly connected to an aromatic core which stabilizes the reduced specie by charge delocalization. Group III comprises

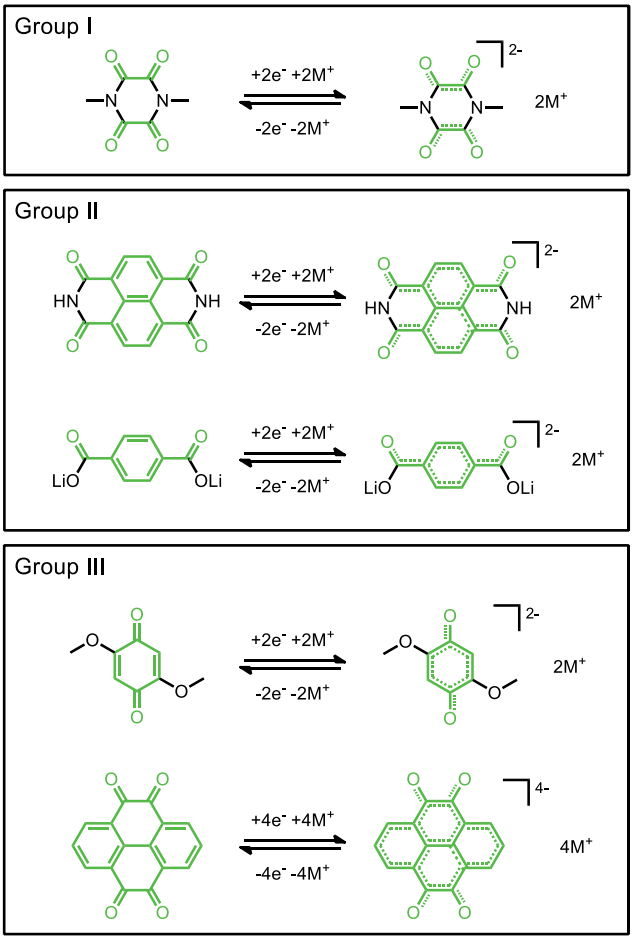

Figure 1.5. Representative structures of the carbonyl-based active electrode materials.[33]

normally quinone sub-structures, although they share some characteristics with compounds from group I and II, their main stabilizing force comes from the formation of an additional aromatic system after reduction.

Redox reaction of carbonyl compounds is based on the charge state of the carbon and oxygen atoms of the carbonyl group. Normally, the carbonyl compounds undergo one or more electron reductions, depending on the number

of carbonyl units and chemical structure, forming a charge anion during the discharge process. The negative charge is balanced by a suitable counter ion from the electrolyte. The characteristic redox potential of the carbonyl-based compounds can be tailored through different approaches, while introducing electron-donating groups decreases the redox potential, electron-withdrawing groups as well as extending the π-conjugation core lead to higher potentials.[46-48] However, introduction of substituents that are not directly involved in the redox reaction decreases the theoretical capacity due to the increment in the molar mass. Furthermore, the choice of the appropriate amount and type of conductive additive plays an important role in the activity of the material and the cell performance, although it is an inactive component that decreases the overall capacity of the cell.[49]

Carbonyl compounds started to be used as electroactive materials as small organic molecules. However, the main drawback is their significant solubility in the electrolyte solution with the consequent capacity loss. One approach to overcome this problem is the incorporation of the redox-active carbonyl groups into a polymeric backbone. Carbonyl polymers can be divided into three main groups: quinone polymers, polyimides and other carbonyl derivatives.

In general, quinone polymers and their derivatives feature redox potentials in the range of 2 to 3 V *vs.* Li^+/Li as the system gains aromaticity and promotes the reduction. Due to their high redox potential they are usually applied as cathode materials, mostly against lithium or lithium intercalation anodes. Polyimides are reversibly reduced in the range of 1.5 to 2.5 V *vs.* Li^+/Li and are mainly used as cathode materials in sodium or lithium-ion batteries. Among the carbonyl derivatives, several groups have reported the substitution of the carbonyl function in anthraquinones providing different redox potentials and capacities.[44,50] Furthermore, another type of carbonyl molecules are the ones based on conjugated dicarboxylates. They feature reduction potentials between 0.5 and

1 V *vs.* Li^+/Li making them good candidates as anode materials in lithium and sodium batteries. Although they are not polymers, their sufficient insolubility is enough to overcome the solubility problems of small molecules.[3,33]

Among the different types of carbonyl-based polymers, electroactive polyimides were studied in this thesis. Besides their good electrochemical properties regarding high capacity and redox voltage; their easy and scalable synthesis, as well as their excellent thermal properties, make them great candidates for practical battery applications.

1.3. Polyimides and their electrochemical activity

Polyimides are derived from the reaction of dianhydrides and diamines creating a heterocyclic imide unit in their polymer backbone. They were successfully introduced as commercial polymeric materials by DuPont in the early 1960s.[51] Since then, a broad variety of polyimides have been synthesized and reported in literature. Their scientific and commercial importance resides in their outstanding key properties, including thermal and thermo-oxidative stability, high mechanical strength, excellent electrical properties and superior chemical resistance. In addition, they are lightweight, flexible, insulator and heat resistant polymers. Therefore, they have been widely used as engineering plastics mostly in the electronics industry as well as for high temperature adhesives, aerospace, automotive and packaging industries.

The classical synthetic route pioneered at DuPont, consisting on a two step reaction *via* poly(amic acid)s, is still the most popular technique for the preparation of polyimides.[51] Figure 1.6 illustrates the reaction scheme of a polyimide polycondensation reaction, using the structure of a Kapton® polyimide as an example. The first step involves a very fast, exothermic stepwise

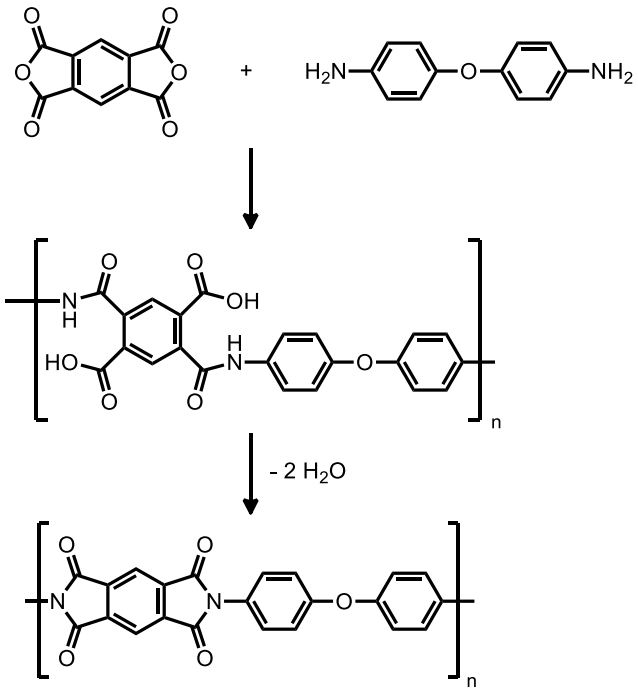

Figure 1.6. Polycondensation reaction scheme of Kapton® polyimide.

polymerization at room temperature to form poly(amic acid)s from dianhydrides and diamines. Subsequently, the poly(amic acid)s undergo an intramolecular cyclization (imidization) releasing water condensate and forming the corresponding polyimides. The second step can be carried out using chemical, azeotropical or thermal imidization techniques.[52] Chemical imidization requires a chemical dehydrating agent, usually an acid anhydride, to promote the ring closure reaction in temperature ranges of 20-80 °C.[53] In the azeotropic imidization the cyclodehydration is conducted in the presence of an azeotropic agent by heating the poly(amic acid) solution in a high boiling point solvent at temperatures of 160-200 °C.[54] In contrast, thermal imidization involves gradual heating of the poly(amic acid) to 250-350 °C, depending on the stability and glass transition temperature of the polymer. The latter technique is useful for the

preparation of thin materials such as films, coatings, fibers and powders. Thermal imidization method produces polyimides with enhanced thermal stability; however, their solubility decreases in comparison with the chemical or azeotropical techniques.[52]

Research on polyimides has been focused on improving their mechanical properties by preparing high molecular weight polyimides[55] as well as exploring other application areas such as membranes for gas separation,[56] electrochromic devices[57] and fiber reinforce composites.[58] Another less known application is their use as electroactive materials for electrochemical energy storage.[43,48,59] Electrochemical properties of polyimides with aromatic imide groups were first discovered in the late 1980s by Mazur *et al.*[60] and early 1990s by Viehbeck *et al.*[61] However, only in the early 2010s were polyimides first reported as electroactive materials in lithium batteries by Song *et al.*[43]

Redox reaction of carbonyl groups and polyimides in particular can be described as enolization. Polyimides, being in the oxidized state, can be electrochemically reduced with the consequent gain of electrons and association of ions with the oxygen atom. Afterwards, in a reversible manner, they can be oxidized recovering the original state while releasing electrons and ions. Ideally, each formula unit is able to transfer four electrons, one per carbonyl group. However, it has been reported that only two electrons can be reversibly transferred between 2.5 and 1.5 V *vs.* Li^+/Li. Although the other two electrons can be transferred by a deep reduction below 1 V *vs.* Li^+/Li;[62] unfortunately, that process is accompanied by serious structural damage and inactivation of the polymer. This could be caused by the big repulsion of four negative charges in the imide group.[43]

Therefore, polyimides are able to undergo a reversible two-electron redox reaction, generally in two steps. The first one-electron reduction yields a radical anion followed by a second one-electron step which generates the dianion form.

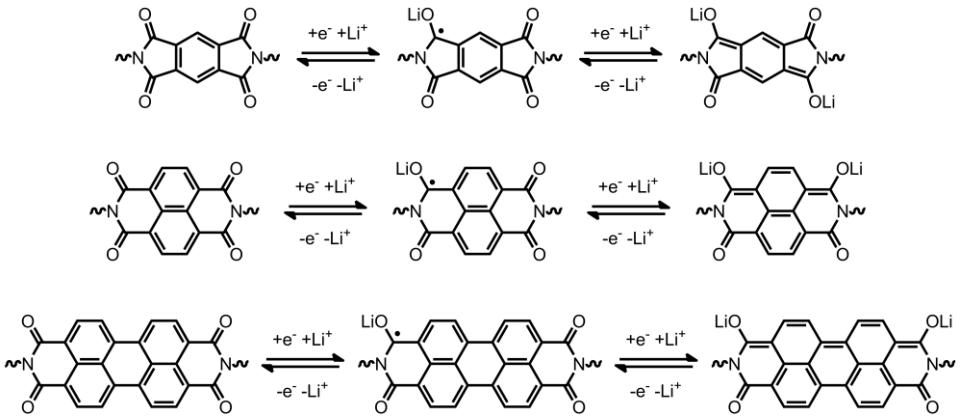

Figure 1.7. Proposed redox reaction mechanisms for pyromellitic (top), naphthalene (middle) and perylene (bottom) based polyimides.

Figure 1.7 represents a possible redox reaction mechanism for the three most studied polyimides derived from pyromellitic, naphthalene and perylene dianhydrides. In the case of pyromellitic polyimide, the dominant form of the dianionic state is expected to involve carbonyls in *trans* position providing the largest separation between the two negative charges. In contrast, reduction of *trans*-carbonyls in naphthalene and perylene polyimides would require the loss of aromaticity, thus a *cis*-carbonyl reduction is proposed.[61]

Electrochemical properties such as voltage and capacity are determined by the chemical structure of polyimides. While voltage and redox reaction mechanism is mostly dependent on the imide groups, the whole structure plays an important role towards the theoretical capacity of the polyimide.[60] The main structural difference between the three polyimides based on pyromellitic, naphthalene and perylene dianhydrides resides in the conjugation and separation of both imide groups. Increasing this separation diminishes the coulombic repulsion between the negative charges gained upon reduction. In addition, an increase in the conjugating structure between the two imide moieties results in the stabilization

of the reduced specie facilitating the reaction. This stabilization enhances the kinetics of the second one-electron reaction, overlapping with the first one and leading to a one step two-electron reaction mechanism.[43,61] Furthermore, increasing the conjugated backbone of polyimides lowers the LUMO (lower unoccupied molecular orbital) energy level shifting the redox potential towards more positive values.[43,48] Regarding the theoretical capacity of polyimides and taking into consideration Equation (1-1) (see page 7), the whole structure plays an important role. Therefore, increasing the number of electrons taking place in the redox reaction and lowering the molecular weight of the formula unit will lead to higher capacity values. These two characteristics can be tuned by the diamine part of the polyimides.

Research on polyimides for battery applications has been mostly focused on studying the electrochemical properties of different dianhydrides minimizing the molecular weight of diamines.[43,48] Recently, several groups have reported the incorporation of redox-active diamines in order to increase the number of electrons taking place in the redox reaction and to rise the theoretical capacity.[63-66]

Nevertheless, there is still room for improvement in the field of polyimides for electrochemical energy storage. The main disadvantage of redox-active polyimides reported in literature is their intractability; generally insoluble powders are obtained requiring the addition of extra binders to prepare electrode films. One way to overcome this drawback is by the incorporation of diamines able to improve the solubility issue and film forming properties. Furthermore, investigating other functional diamines with redox-active moieties to increase the theoretical capacity or using them as redox-active additives for different energy storage systems would open new possibilities for these polymers.

1.4. Applications of polyimides in electrochemical energy storage

Polyimides, as versatile polymers, can be used in many parts of the battery components, such as separators and binders, as well as anode and cathode materials. Spongy-like porous polyimide membranes with good wettability and low thermal shrinkage have been reported as separators for lithium-ion batteries.[67] Furthermore, due to their strong adhesive characteristics, good mechanical properties and high thermal stability, polyimides have been used as binders mostly for silicon electrodes but also in lithium and sodium cells. Polyimides are able to accommodate volume changes in electroactive materials upon charging and discharging as well as to enhance battery safety.[68-70]

Electrochemical activity of polyimides broadened the applications of polyimides to be used as redox-active materials. Redox potential of polyimides can be tuned varying their chemical structure. Furthermore, depending on the characteristic potential of the opposite electrode, polyimides can be used as anode or cathode materials. In general, polyimides have been mostly studied as cathodes in lithium or sodium cells because their potential is higher than that of those metals.[43,48] In contrast, polyimides can be used as anodes with high voltage electroactive materials.[59,71,72]

Versatility of redox-active polyimides is demonstrated by their use in different electrochemical energy storage systems, such as lithium-ion, sodium-ion, aqueous and lithium-sulfur batteries.

1.4.1. Polyimides in lithium batteries

The first polyimide-lithium cell was reported by Song *et al.* in 2010.[43] Five different polyimides based on pyromellitic and naphthalene dianhydrides with low molecular weight aliphatic and aromatic diamines were investigated. Although

theoretical capacity of pyromellitic polyimides is higher than the naphthalene ones, electrochemical performance of the latter is better. Furthermore, voltage of naphthalene polyimide was higher than the pyromellitic polyimide due to the increased in the conjugation structure. Afterwards, a perylene-hydrazine polyimide was reported featuring higher redox potential although slightly poorer battery performance.[64]

Despite the fact that a good performance at high rates allows faster charge-discharge processes, it also involves a larger charge-discharge voltage gap. Rate performance can be significantly improved by the incorporation of carbon-based materials; despite them being inactive and therefore diminishing the overall energy density of the device. Nevertheless, many groups have reported the use of different carbon materials to enhance the electrochemical performance of polyimides. Some examples of these carbon materials are 3D reduced graphene oxide network,[73] single-walled carbon nanotube (SWCNT)[74,75] and functionalized graphene sheets.[76]

Additionally, other ways to improve the cell performance consist in incorporating additional redox-active groups into the polymer backbone to increase the theoretical capacity and thus specific energy. Urea with one carbonyl group and anthraquinone with two carbonyl moieties surrounded by two aromatic rings are the two examples reported in literature. Polyimide containing urea groups featured a three-electron redox reaction,[63,64] whereas anthraquinone-based polyimide was able to transfer four electrons.[66]

Furthermore, a full organic battery was assembled using perylene-hexamethylenediamine as cathode and a prelithiated perylene tetracarboxylate as anode materials.[77] The full organic cell featured an operating voltage average of 1.2 V and good electrochemical performance.

1.4.2. Polyimides in sodium batteries

Sodium-ion batteries have been gaining increasing attention thanks to the natural abundance and low toxicity of sodium resources. Due to the redox mechanism of polyimides based on conversion reactions, they are electroactive not only to lithium, but sodium as well. Polyimides were first reported in sodium batteries in 2013 by Wang *et al*.[48] Redox potential of pyromellitic, naphthalene and perylene polyimides exhibited the same trend as seen in lithium batteries, although the voltage is slightly lower due to the different anode material. Among them, perylene polyimide showed the best cell performance.

A full sodium-ion cell using a naphthalene-ethylenediamine polyimide as anode coupled with $Na_3V_4(PO_4)_3$/C and $Na_4Fe(CN)_6$/C as cathodes presented a discharge plateau at 1 V and 75 % of the material activity at 1C, although a capacity fade was observed upon cycling.[78] An organic full sodium battery was reported using perylene polyimide as cathode and disodium terephthalate as anode materials, showing similar results to the previous one.[79]

Polyimides synthesized from anthraquinone derivatives have been also tested in sodium batteries in order to increase the specific capacity.[80-81] High material utilization was reported for all of them, however, the best capacity retention (95 %) was obtained by naphthalene-2,6-diaminoanthraquinone polyimide.[80]

1.4.3. Polyimides in aqueous batteries

Aqueous rechargeable batteries are an emerging energy storage technology due to the enhanced safety in comparison with flammable organic solvents used in conventional Li-ion batteries. Polyimides have been investigated as anode materials in lithium and sodium aqueous batteries. A naphthalene-hydrazine polyimide was characterized in 5 M $LiNO_3$ aqueous electrolyte showing a discharge potential at -0.5 V *vs.* SCE (Saturated Calomel Electrode). The same

polyimide was also studied in 5 M $NaNO_3$, indicating the cation type has a negligible effect in the capacity performance of the polyimide anode. This polyimide was characterized in a full cell as anode material with Lithium cobalt oxide ($LiCoO_2$) or Sodium vanadium fluorophosphate ($NaVPO_4F$) as cathodes. The lithium cell exhibited an initial capacity of 70 mA h g^{-1} (based on both electrodes weight) and a cell potential of 1.17 V at a charging speed of 2C. However, poorer results were obtained for the sodium full cell which suffered a big capacity fade in the first 20 cycles due to the limiting performance of $NaVPO_4F$ cathode.[71]

Afterwards, high rate capability of a naphthalene-ethylenediamine polyimide in 1 M Na_2SO_4 was reported.[82] When the current increased from C/1.8 to 10C a 71 % of the initial capacity was still remaining. Furthermore, remarkable cycling stability was reported at 5C for 1000 cycles. Higher material utilization was reported when multi-walled carbon nanotubes (MWCNT) were added to a naphthalene-phenylene diamine polyimide anode.[83] Interestingly, this anode with $Na_{0.44}MnO_2$ as cathode showed a discharge voltage of 0.8 V and better electrochemical performance than the previously reported $NaVPO_4F$.

Finally, a fiber-shaped aqueous lithium-ion battery with high power density was reported using naphthalene-ethylenediamine polyimide with CNT as anode and $LiMn_2O_4$/CNT as cathode.[72] The full lithium-ion aqueous battery exhibited a discharge voltage platform of 1.4 V and a specific discharge capacity of 123 mA h g^{-1} based on the polyimide mass at 10C.

1.4.4. Polyimides in lithium-sulfur batteries

Besides electroactive material of cathodes or anodes, polyimides can be used as redox-active additives to other battery systems, such as the lithium-sulfur. Lithium-sulfur battery is an emerging technology towards building more sustainable, safer and cheaper batteries. However, there are still numerous

challenges to be overcome, some of them are the insulating characteristic of sulfur requiring big amounts of conductive additives and the low material utilization hindering the accessibility of the full theoretical capacity. Consequently, redox mediators able to enhance the electrochemical properties of the sulfur cathodes are arising. Polyimides, with a redox potential similar to sulfur, have been proven to act as redox mediators facilitating the accessibility of the sulfur active material.[84,85]

1.5. Motivation and objectives

In order to move away from fossil fuels emissions towards renewable energy sources, development of efficient, cheap, safe and sustainable electrochemical energy storage technologies is becoming a necessity. Currently, lithium-ion batteries based on inorganic oxides own the majority of the battery market. However, despite their outstanding energy density and power capability, they contain toxic metals and safety is compromised by the flammable organic solvents employed. Therefore, redox-active polymers are gaining attention as alternative active materials in electrochemical energy storage.

Among the numerous types of redox-active polymers, polyimides, belonging to carbonyl-based polymers, feature high specific capacity and redox voltage. Furthermore, their straightforward and scalable synthesis, as well as their excellent thermal properties, make them great candidates for electrochemical cells applications. However, electroactive polyimides are usually insoluble powders hindering their tractability. Therefore, the main goal of this thesis is to synthesize polyimides with functionalities to make them soluble materials as well as to enhance their electrochemical properties in different energy storage systems.

Within this scope, the specific objectives of this thesis are the following:

- Investigation of the dependency of the electrochemical properties on the chemical structure of polyimides.
- Synthesis and characterization of soluble polyimide-polyether copolymers.
- Battery performance characterization of these materials as cathodes in lithium-ion batteries.
- Study of the redox-mediating effect of polyimide-polyether copolymers as redox-active binders in lithium-sulfur batteries.
- Electrochemical characterization of polyimides as anode materials for high power aqueous sodium-ion batteries.

1.6. Outline of the thesis

Following this first chapter of introduction; in the second chapter, the electrochemical characterization of eight different polyimides is presented. The dependency of the redox properties on the chemical structure of polyimides is investigated. Three polyimides based on naphthalene, pyromellitic and hexafluoroisopropylidene dianhydrides are studied as cathodes in lithium-ion batteries. Besides, redox-active aromatic diamines, ionic diamines, together with two aliphatic diamines are characterized also as cathodes in lithium-ion batteries.

In the third chapter, synthesis and structural characterization of soluble polyimides containing oligoether diamines is reported. The conjugation structure of the dianhydride part varied from pyromellitic to naphthalene to perylene; while the molecular weight of the oligoether diamines changed from 600 to 900 to 2000 g mol^{-1}. Their electrochemical properties are studied in lithium-ion batteries.

In Chapter 4, oligoether-based polyimides are employed as redox-active

mediators for the lithium-sulfur batteries. The synergy between imide and ether groups is determined to enhance sulfur mass utilization, reduce polarization, accelerate reaction kinetics and increase capacity retention of the battery. Furthermore, the effect of the reduction of carbon content in the electrode composition is studied.

In Chapter 5, oligoether-based polyimides are used as anode materials for sustainable, cheap and safe aqueous sodium-ion batteries. Their electrochemical properties focusing on the redox potential, reaction kinetics and rate capability are determined in an aqueous sodium electrolyte.

Finally, in Chapter 6 the most relevant conclusions of this thesis are summarized.

1.7. References

(1) Goodenough, J. B. Electrochemical energy storage in a sustainable modern society. *Energy Environ. Sci.* **2014**, *7,* 14-18.

(2) Larcher, D.; Tarascon, J. M. Towards greener and more sustainable batteries for electrical energy storage. *Nat. Chem.* **2015**, *7,* 19-29.

(3) Muench, S.; Wild, A.; Friebe, C.; Häupler, B.; Janoschka, T.; Schubert, U. S. Polymer-based organic batteries. *Chem. Rev.* **2016**, *116,* 9438-9484.

(4) Schon, T. B.; McAllister, B. T.; Li, P.-F.; Seferos, D. S. The rise of organic electrode materials for energy storage. *Chem. Soc. Rev.* **2016**, *45,* 6345-6404.

(5) Song, Z.; Zhou, H. Towards sustainable and versatile energy storage devices: an overview of organic electrode materials. *Energy Environ. Sci.* **2013**, *6,* 2280-2301.

(6) Armand, M.; Tarascon, J. M. Building better batteries. *Nature* **2008**, *451,* 652-657.

(7) Poizot, P.; Dolhem, F. Clean energy new deal for a sustainable world: from non-CO_2 generating energy sources to greener electrochemical storage devices. *Energy Environ. Sci.* **2011**, *4,* 2003-2019.

(8) Nathan, A.; Ahnood, A.; Cole, M. T.; Lee, S.; Suzuki, Y.; Hiralal, P.; Bonaccorso, F.; Hasan, T.; Garcia-Gancedo, L.; Dyadyusha, A.; Haque, S.; Andrew, P.; Hofmann, S.; Moultrie, J.; Chu, D.; Flewitt, A. J.; Ferrari, A. C.; Kelly, M. J.; Robertson, J.; Amaratunga, G. A. J.; Milne, W. I. Flexible electronics: the next ubiquitous platform. *Proc. IEEE* **2012**, *100,* 1486-1517.

(9) Lochner, C. M.; Khan, Y.; Pierre, A.; Arias, A. C. All-organic optoelectronic sensor for pulse oximetry. *Nat. Commun.* **2014**, *5,* 5745.

(10) Roselli, L.; Carvalho, N. B.; Alimenti, F.; Mezzanotte, P.; Orecchini, G.; Virili, M.; Mariotti, C.; Gonçalves, R.; Pinho, P. Smart surfaces: Large area electronics systems for internet of things enabled by energy harvesting. *Proc. IEEE* **2014**, *102,* 1723-1746.

(11) Nilsson, H. E.; Unander, T.; Siden, J.; Andersson, H.; Manuilskiy, A.; Hummelgard, M.; Gulliksson, M. System integration of electronic functions in smart packaging applications. *IEEE Trans. Components, Packag. Manuf. Technol.* **2012**, *2,* 1723-1734.

(12) Ostfeld, A. E.; Gaikwad, A. M.; Khan, Y.; Arias, A. C. High-performance flexible energy storage and harvesting system for wearable electronics. *Sci. Rep.* **2016**, *6,* 26122.

(13) Andre, D.; Kim, S.-J.; Lamp, P.; Lux, S. F.; Maglia, F.; Paschos, O.; Stiaszny, B. Future generations of cathode materials: an automotive industry perspective. *J. Mater. Chem. A* **2015**, *3,* 6709-6732.

(14) Ogasawara, T.; Débart, A.; Holzapfel, M.; Novák, P.; Bruce, P. G. Rechargeable Li_2O_2 electrode for lithium batteries. *J. Am. Chem. Soc.* **2006**, *128,* 1390-1393.

(15) Manthiram, A.; Chung, S.-H.; Zu, C. Lithium–Sulfur batteries: progress and prospects. *Adv. Mater.* **2015**, *27,* 1980-2006.

(16) Dirlam, P. T.; Glass, R. S.; Char, K.; Pyun, J. The use of polymers in Li-S batteries: A review. *J. Polym. Sci., Part A: Polym. Chem.* **2017**, *55,* 1635-1668.

(17) Palomares, V.; Serras, P.; Villaluenga, I.; Hueso, K. B.; Carretero-Gonzalez, J.; Rojo, T. Na-ion batteries, recent advances and present challenges to become low cost energy storage systems. *Energy Environ. Sci.* **2012**, *5,* 5884-5901.

(18) Li, Y.; Dai, H. Recent advances in zinc-air batteries. *Chem. Soc. Rev.* **2014**, *43,* 5257-5275.

(19) Kim, Y. J.; Wu, W.; Chun, S.-E.; Whitacre, J. F.; Bettinger, C. J. Catechol-mediated reversible binding of multivalent cations in eumelanin half-cells. *Adv. Mater.* **2014**, *26,* 6572-6579.

(20) Janoschka, T.; Martin, N.; Martin, U.; Friebe, C.; Morgenstern, S.; Hiller, H.; Hager, M. D.; Schubert, U. S. An aqueous, polymer-based redox-flow battery using non-corrosive, safe, and low-cost materials. *Nature* **2015**, *527,* 78-81.

(21) Huskinson, B.; Marshak, M. P.; Suh, C.; Er, S.; Gerhardt, M. R.; Galvin, C. J.; Chen, X.; Aspuru-Guzik, A.; Gordon, R. G.; Aziz, M. J. A metal-free organic-inorganic aqueous flow battery. *Nature* **2014**, *505,* 195-198.

(22) Bruce, P. G.; Freunberger, S. A.; Hardwick, L. J.; Tarascon, J.-M. Li-O_2 and Li-S batteries with high energy storage. *Nat. Mater.* **2012**, *11,* 19-29.

(23) Linden, D.; Reddy, T. B. *Handbook of Batteries,* 3rd ed.; McGraw-Hill: New York, 2002.

(24) Gao, X.-P.; Yang, H.-X. Multi-electron reaction materials for high energy density batteries. *Energy Environ. Sci.* **2010**, *3,* 174-189.

(25) Guerfi, A.; Kaneko, M.; Petitclerc, M.; Mori, M.; Zaghib, K. $LiFePO_4$ water-soluble binder electrode for Li-ion batteries. *J. Power Sources* **2007**, *163,* 1047-1052.

(26) Arora, P.; Zhang, Z. Battery Separators. *Chem. Rev.* **2004**, *104,* 4419-4462.

(27) Bouchet, R.; Maria, S.; Meziane, R.; Aboulaich, A.; Lienafa, L.; Bonnet, J.-P.; Phan, T. N. T.; Bertin, D.; Gigmes, D.; Devaux, D.; Denoyel, R.; Armand, M. Single-ion BAB triblock copolymers as highly efficient electrolytes for lithium-metal batteries. *Nat. Mater.* **2013**, *12,* 452-457.

(28) Aihara, Y.; Appetecchi, G. B.; Scrosati, B. A new concept for the formation of homogeneous, poly(ethylene oxide) based, gel-type polymer electrolyte. *J. Electrochem. Soc.* **2002**, *149,* A849-A854.

(29) Wang, G. X.; Yang, L.; Chen, Y.; Wang, J. Z.; Bewlay, S.; Liu, H. K. An investigation of polypyrrole-$LiFePO_4$ composite cathode materials for lithium-ion batteries. *Electrochim. Acta* **2005**, *50,* 4649-4654.

(30) Shao, L.; Jeon, J.-W.; Lutkenhaus, J. L. Polyaniline nanofiber/vanadium pentoxide sprayed layer-by-layer electrodes for energy storage. *J. Mater. Chem. A* **2014**, *2,* 14421-14428.

(31) Casado, N.; Hernández, G.; Veloso, A.; Devaraj, S.; Mecerreyes, D.; Armand, M. PEDOT radical polymer with synergetic redox and electrical properties. *ACS Macro Lett.* **2016**, *5,* 59-64.

(32) Casado, N.; Hernández, G.; Sardon, H.; Mecerreyes, D. Current trends in redox polymers for energy and medicine. *Prog. Polym. Sci.* **2016**, *52,* 107-135.

(33) Häupler, B.; Wild, A.; Schubert, U. S. Carbonyls: Powerful organic materials for secondary batteries. *Adv. Energy Mater.* **2015**, *5,* 1402034.

(34) Liang, Y.; Tao, Z.; Chen, J. Organic electrode materials for rechargeable lithium batteries. *Adv. Energy Mater.* **2012**, *2,* 742-769.

(35) Zhang, L.; Liu, Z.; Cui, G.; Chen, L. Biomass-derived materials for electrochemical energy storages. *Prog. Polym. Sci.* **2015**, *43,* 136-164.

(36) Gandini, A.; Lacerda, T. M. From monomers to polymers from renewable resources: Recent advances. *Prog. Polym. Sci.* **2015**, *48,* 1-39.

(37) Novak, P.; Muller, K.; Santhanam, K. S. V.; Haas, O. Electrochemically active polymers for rechargeable batteries. *Chem. Rev.* **1997**, *97,* 207-281.

(38) Zhan, L.; Song, Z.; Zhang, J.; Tang, J.; Zhan, H.; Zhou, Y.; Zhan, C. PEDOT: Cathode active material with high specific capacity in novel electrolyte system. *Electrochim. Acta* **2008**, *53,* 8319-8323.

(39) Nakahara, K.; Iwasa, S.; Satoh, M.; Morioka, Y.; Iriyama, J.; Suguro, M.; Hasegawa, E. Rechargeable batteries with organic radical cathodes. *Chem. Phys. Lett.* **2002**, *359,* 351-354.

(40) Su, Y.-Z.; Dong, W.; Zhang, J.-H.; Song, J.-H.; Zhang, Y.-H.; Gong, K.-C. Poly[bis(2-aminophenyloxy)disulfide]: A polyaniline derivative containing disulfide bonds as a cathode material for lithium battery. *Polymer* **2007**, *48,* 165-173.

(41) Zhang, J.; Kong, L.; Zhan, L.; Tang, J.; Zhan, H.; Zhou, Y.; Zhan, C. Aliphatic thioether polymers as novel cathode active materials for rechargeable lithium battery. *Electrochem. Commun.* **2008**, *10,* 1551-1554.

(42) Choi, W.; Harada, D.; Oyaizu, K.; Nishide, H. Aqueous electrochemistry of poly(vinylanthraquinone) for anode-active materials in high-density and rechargeable polymer/air batteries. *J. Am. Chem. Soc.* **2011**, *133,* 19839-19843.

(43) Song, Z.; Zhan, H.; Zhou, Y. Polyimides: Promising energy-storage materials. *Angew. Chem. Int. Ed.* **2010**, *49,* 8444-8448.

(44) Häupler, B.; Burges, R.; Friebe, C.; Janoschka, T.; Schmidt, D.; Wild, A.; Schubert, U. S. Poly(exTTF): A novel redox-active polymer as active material for Li-organic batteries. *Macromol. Rapid Commun.* **2014**, *35,* 1367–1371.

(45) Liang, Y.; Zhang, P.; Chen, J. Function-oriented design of conjugated carbonyl compound electrodes for high energy lithium batteries. *Chem. Sci.* **2013**, *4,* 1330-1337.

(46) Vadehra, G. S.; Maloney, R. P.; Garcia-Garibay, M. A.; Dunn, B. Naphthalene diimide based materials with adjustable redox potentials: evaluation for organic lithium-ion batteries. *Chem. Mater.* **2014**, *26,* 7151-7157.

(47) Takeda, T.; Taniki, R.; Masuda, A.; Honma, I.; Akutagawa, T. Electron-deficient anthraquinone derivatives as cathodic material for lithium ion batteries. *J. Power Sources* **2016**, *328,* 228-234.

(48) Wang, H.-g.; Yuan, S.; Ma, D.-l.; Huang, X.-l.; Meng, F.-l.; Zhang, X.-b. Tailored aromatic carbonyl derivative polyimides for high-power and long-cycle sodium-organic batteries. *Adv. Energy Mater.* **2014**, *4,* 1301651.

(49) Chen, Z.; Dahn, J. R. Reducing carbon in $LiFePO_4$ / C composite electrodes to maximize specific energy, volumetric energy, and tap density. *J. Electrochem. Soc.* **2002**, *149,* A1184-A1189.

(50) Haupler, B.; Burges, R.; Janoschka, T.; Jahnert, T.; Wild, A.; Schubert, U. S. PolyTCAQ in organic batteries: enhanced capacity at constant cell potential using two-electron-redox-reactions. *J. Mater. Chem. A* **2014**, *2,* 8999-9001.

(51) Sroog, C. E.; Endrey, A. L.; Abramo, S. V.; Berr, C. E.; Edwards, W. M.; Olivier, K. L. Aromatic polypyromellitimides from aromatic polyamic acids. *J. Polym. Sci., Part A: Polym. Chem.* **1996**, *34,* 2069-2086.

(52) Liaw, D.-J.; Wang, K.-L.; Huang, Y.-C.; Lee, K.-R.; Lai, J.-Y.; Ha, C.-S. Advanced polyimide materials: Syntheses, physical properties and applications. *Prog. Polym. Sci.* **2012**, *37,* 907-974.

(53) Dabral, M.; Xia, X.; Gerberich, W. W.; Francis, L. F.; Scriven, L. E. Near-surface structure formation in chemically imidized polyimide films. *J. Polym. Sci., Part B: Polym. Phys.* **2001**, *39,* 1824-1838.

(54) Kim, Y. J.; Glass, T. E.; Lyle, G. D.; McGrath, J. E. Kinetic and mechanistic investigations of the formation of polyimides under homogeneous conditions. *Macromolecules* **1993**, *26,* 1344-1358.

(55) Muñoz, D. M.; Calle, M.; de la Campa, J. G.; de Abajo, J.; Lozano, A. E. An improved method for preparing very high molecular weight polyimides. *Macromolecules* **2009**, *42,* 5892-5894.

(56) Calle, M.; Lozano, A. E.; de Abajo, J.; de la Campa, J. G.; Álvarez, C. Design of gas separation membranes derived of rigid aromatic polyimides. 1. Polymers from diamines containing di-tert-butyl side groups. *J. Membr. Sci.* **2010**, *365,* 145-153.

(57) Chang, C.-H.; Wang, K.-L.; Jiang, J.-C.; Liaw, D.-J.; Lee, K.-R.; Lai, J.-Y.; Lai, K.-H. Novel rapid switching and bleaching electrochromic polyimides containing triarylamine with 2-phenyl-2-isopropyl groups. *Polymer* **2010**, *51,* 4493-4502.

(58) Ishida, Y.; Ogasawara, T.; Yokota, R. Development of highly soluble addition-type imide oligomers for matrix of carbon fiber composite (I): imide oligomers based on asymmetric biphenyltetracarboxylic dianhydride and 9,9-Bis(4-aminophenyl) fluorene. *High Perform. Polym.* **2006**, *18,* 727-737.

(59) Oyaizu, K.; Hatemata, A.; Choi, W.; Nishide, H. Redox-active polyimide/carbon nanocomposite electrodes for reversible charge storage at negative potentials: expanding the functional horizon of polyimides. *J. Mater. Chem.* **2010**, *20,* 5404-5410.

(60) Mazur, S.; Lugg, P. S.; Yarnitzky, C. Electrochemistry of aromatic polyimides. *J. Electrochem. Soc.* **1987**, *134,* 346-353.

(61) Viehbeck, A.; Goldberg, M. J.; Kovac, C. A. Electrochemical properties of polyimides and related imide compounds. *J. Electrochem. Soc.* **1990**, *137,* 1460-1466.

(62) Han, X.; Chang, C.; Yuan, L.; Sun, T.; Sun, J. Aromatic carbonyl derivative polymers as high-performance Li-Ion storage materials. *Adv. Mater.* **2007**, *19,* 1616-1621.

(63) Chen, C.; Zhao, X.; Li, H.-B.; Gan, F.; Zhang, J.; Dong, J.; Zhang, Q. Naphthalene-based polyimide derivatives as organic electrode materials for lithium-ion batteries. *Electrochim. Acta* **2017**, *229,* 387-395.

(64) Sharma, P.; Damien, D.; Nagarajan, K.; Shaijumon, M. M.; Hariharan, M. Perylene-polyimide-based organic electrode materials for rechargeable lithium batteries. *J. Phys. Chem. Lett.* **2013**, *4,* 3192-3197.

(65) Wu, H. P.; Yang, Q.; Meng, Q. H.; Ahmad, A.; Zhang, M.; Zhu, L. Y.; Liu, Y. G.; Wei, Z. X. A polyimide derivative containing different carbonyl groups for flexible lithium ion batteries. *J. Mater. Chem. A* **2016**, *4,* 2115-2121.

(66) Tian, B.; Ning, G.-H.; Tang, W.; Peng, C.; Yu, D.; Chen, Z.; Xiao, Y.; Su, C.; Loh, K. P. Polyquinoneimines for lithium storage: more than the sum of its parts. *Mater. Horiz.* **2016**, *3,* 429-433.

(67) Wang, H.; Wang, T.; Yang, S.; Fan, L. Preparation of thermal stable porous polyimide membranes by phase inversion process for lithium-ion battery. *Polymer* **2013**, *54,* 6339-6348.

(68) Wilkes, B. N.; Brown, Z. L.; Krause, L. J.; Triemert, M.; Obrovac, M. N. The electrochemical behavior of polyimide binders in Li and Na cells. *J. Electrochem. Soc.* **2016**, *163,* A364-A372.

(69) Qian, G.; Wang, L.; Shang, Y.; He, X.; Tang, S.; Liu, M.; Li, T.; Zhang, G.; Wang, J. Polyimide binder: A facile way to improve safety of lithium ion batteries. *Electrochim. Acta* **2016**, *187,* 113-118.

(70) Choi, J.; Kim, K.; Jeong, J.; Cho, K. Y.; Ryou, M.-H.; Lee, Y. M. Highly adhesive and soluble copolyimide binder: Improving the long-term cycle life of silicon anodes in lithium-ion batteries. *ACS Appl. Mater. Interfaces* **2015**, *7,* 14851-14858.

(71) Qin, H.; Song, Z. P.; Zhan, H.; Zhou, Y. H. Aqueous rechargeable alkali-ion batteries with polyimide anode. *J. Power Sources* **2014**, *249,* 367-372.

(72) Zhang, Y.; Wang, Y.; Wang, L.; Lo, C.-M.; Zhao, Y.; Jiao, Y.; Zheng, G.; Peng, H. A fiber-shaped aqueous lithium ion battery with high power density. *J. Mater. Chem. A* **2016**, *4,* 9002-9008.

(73) Meng, Y.; Wu, H.; Zhang, Y.; Wei, Z. A flexible electrode based on a three-dimensional graphene network-supported polyimide for lithium-ion batteries. *J. Mater. Chem. A* **2014**, *2,* 10842-10846.

(74) Wu, H.; Shevlin, S. A.; Meng, Q.; Guo, W.; Meng, Y.; Lu, K.; Wei, Z.; Guo, Z. Flexible and binder-free organic cathode for high-performance lithium-ion batteries. *Adv. Mater.* **2014**, *26,* 3338-3343.

(75) Wu, H.; Wang, K.; Meng, Y.; Lu, K.; Wei, Z. An organic cathode material based on a polyimide/CNT nanocomposite for lithium ion batteries. *J. Mater. Chem. A* **2013**, *1,* 6366-6372.

(76) Song, Z.; Xu, T.; Gordin, M. L.; Jiang, Y.-B.; Bae, I.-T.; Xiao, Q.; Zhan, H.; Liu, J.; Wang, D. Polymer–graphene nanocomposites as ultrafast-charge and -discharge cathodes for rechargeable lithium batteries. *Nano Lett.* **2012**, *12,* 2205-2211.

(77) Iordache, A.; Delhorbe, V.; Bardet, M.; Dubois, L.; Gutel, T.; Picard, L. Perylene-based all-organic redox battery with excellent cycling stability. *ACS Appl. Mater. Interfaces* **2016**, *8,* 22762-22767.

(78) Chen, L.; Li, W.; Wang, Y.; Wang, C.; Xia, Y. Polyimide as anode electrode material for rechargeable sodium batteries. *RSC Adv.* **2014**, *4,* 25369-25373.

(79) Banda, H.; Damien, D.; Nagarajan, K.; Hariharan, M.; Shaijumon, M. M. A polyimide based all-organic sodium ion battery. *J. Mater. Chem. A* **2015**, *3,* 10453-10458.

(80) Xu, F.; Xia, J.; Shi, W. Anthraquinone-based polyimide cathodes for sodium secondary batteries. *Electrochem. Commun.* **2015**, *60,* 117-120.

(81) Xu, F.; Wang, H.; Lin, J.; Luo, X.; Cao, S.-a.; Yang, H. Poly(anthraquinonyl imide) as a high capacity organic cathode material for Na-ion batteries. *J. Mater. Chem. A* **2016**, *4,* 11491-11497.

(82) Deng, W.; Shen, Y.; Qian, J.; Yang, H. A polyimide anode with high capacity and superior cyclability for aqueous Na-ion batteries. *Chem. Commun.* **2015**, *51,* 5097-5099.

(83) Gu, T.; Zhou, M.; Liu, M.; Wang, K.; Cheng, S.; Jiang, K. A polyimide-MWCNTs composite as high performance anode for aqueous Na-ion batteries. *RSC Adv.* **2016**, *6,* 53319-53323.

(84) Gu, P.-Y.; Zhao, Y.; Xie, J.; Binte Ali, N.; Nie, L.; Xu, Z. J.; Zhang, Q. Improving the performance of lithium–sulfur batteries by employing polyimide particles as hosting matrixes. *ACS Appl. Mater. Interfaces* **2016**, *8,* 7464-7470.

(85) Frischmann, P. D.; Hwa, Y.; Cairns, E. J.; Helms, B. A. Redox-active supramolecular polymer binders for lithium–sulfur batteries that adapt their transport properties in operando. *Chem. Mater.* **2016**, *28,* 7414-7421.

CHAPTER 2.

DEPENDENCY OF THE ELECTROCHEMICAL PROPERTIES ON THE CHEMICAL STRUCTURE OF POLYIMIDES

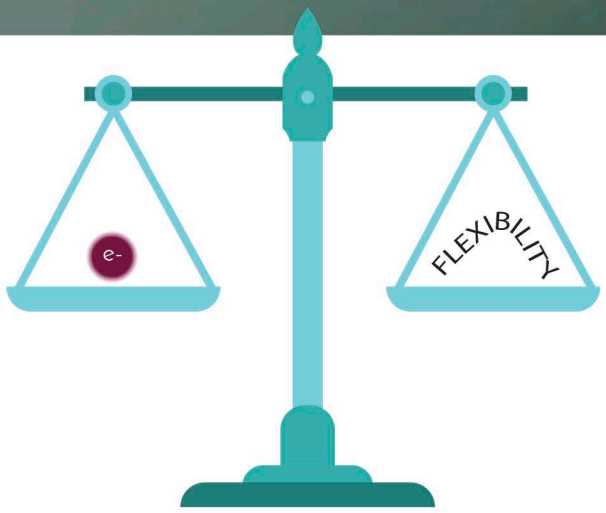

Chapter 2. Dependency of the electrochemical properties on the chemical structure of polyimides

2.1. Introduction

Polyimides are well known as engineering plastics with high mechanical strength and excellent thermal stability. Although their electrochemical properties were first reported in the late 1980s by Mazur *et al*.[1] and Viehbeck *et al.*[2]; it was not until 2010 when Song *et al.*[3] studied them as active materials in lithium batteries. Imide functional groups of aromatic polyimides are the centers for the electron transfer process. Each imide group accepts only one electron reversibly, thus each formula unit with two imide groups is able to transfer two electrons. These two electrons can be exchanged in one or two steps giving one or two

characteristic redox potentials, respectively. Generally, imide's structure determines the mechanism of the redox reaction. Increasing the separation of both imide groups through a conjugated structure would diminish the coulombic repulsion between the negative charges gained in the reduction reaction as well as stabilizing the reduced specie. The increase in conjugation enhances the kinetics of the redox reaction of polyimides occurring in only one step.[2,3] Furthermore, increasing the conjugated backbone lowers the LUMO energy level of the polyimides shifting the redox potentials towards more positive values.[3,4]

Although redox potential of polyimides is mostly determined by the imide structure, in terms of theoretical capacity the whole structure plays an important role. Theoretical capacity can be calculated from the following equation:

$$\text{Theoretical capacity (mA h g}^{-1}) = \frac{n\,F}{3.6 \times MW} \qquad \text{Equation 2-1}$$

where n is the number of electrons taking place in the redox reaction, F is the Faraday constant, 3.6 is the conversion factor and MW is the molecular weight of the repeating unit. Therefore, increasing the number of electrons taking place in the redox reaction and lowering the molecular weight of the formula unit will lead to higher capacity values.

Polyimides based on pyromellitic, naphthalene and perylene dianhydrides with low molecular weight diamines are the most studied ones due to their improved performance in batteries and higher theoretical capacity.[3-6] However, they commonly yield insoluble powders which are intractable and require the addition of binders to the electrode formulation. One example to overcome this drawback is to use 4,4'-(hexafluoroisopropylidene)diphthalic anhydride (6FDA), which is a dianhydride known to improve the solubility of the final polymer and therefore its tractability.[7]

Moving towards the possible diamines, not a lot of effort has been made to

incorporate functional diamines which could provide other advantages to the system such as solubility, additional redox-active sites, stability or enhancement of the rate capability. For example, diaminoanthraquinone[8-10] or urea[11,12] have been reported in the sinthesis of polyimides as additional redox-active cabonyl groups, increasing the theoretical capacity of the final polymer. Other possible redox-active diamines could be aniline phthalein (APh), aniline phthalimidine (APhI) and aniline anthrone (AAn), which possess a conjugated carbonyl group able to undergo a one-electron redox reaction, thus increasing the theoretical capacity of the polyimide. Furthermore, incorporation of ionic moieties into the polyimide backbone would increase the ionic conductivity as it is the case for poly(ionic liquid)s[13] and also improve the rate performance of the cell. Finally, aliphatic diamines could introduce flexibility to the polymer backbone facilitating the electrochemical reaction of the redox-active sites.

In this chapter, the electrochemical properties of polyimides with different dianhydride and diamine structures will be studied as well as their performance as cathode materials in lithium batteries. Different dianhydrides based on pyromellitic dianhydride (PMDA), naphthalene dianhydride (NTDA) and 4,4'-(hexafluoroisopropylidene) diphthalic anhydride (6FDA) will be investigated. Aromatic diamines with additional carbonyl groups, such as aniline phthalein (APh), aniline phthalimidine (APhI) and aniline anthrone (AAn), will be studied in this chapter. Furthermore, the aliphatic diamines to be explored in this chapter are 1,12-dodecanediamine (DDA) and 4,9-dioxa-1,12-dodecanediamine (DODDA).

2.2. Polymer synthesis and electrode preparation

Polyimides studied in this chapter were synthesized following the conventional polycondensation reaction.[14] Their synthesis and characterization was carried out

by Sofia M. Morozova and Dr. Alexander S. Shaplov from A. N. Nesmeyanov Institute of Organoelement Compounds of Russian Academy of Sciences

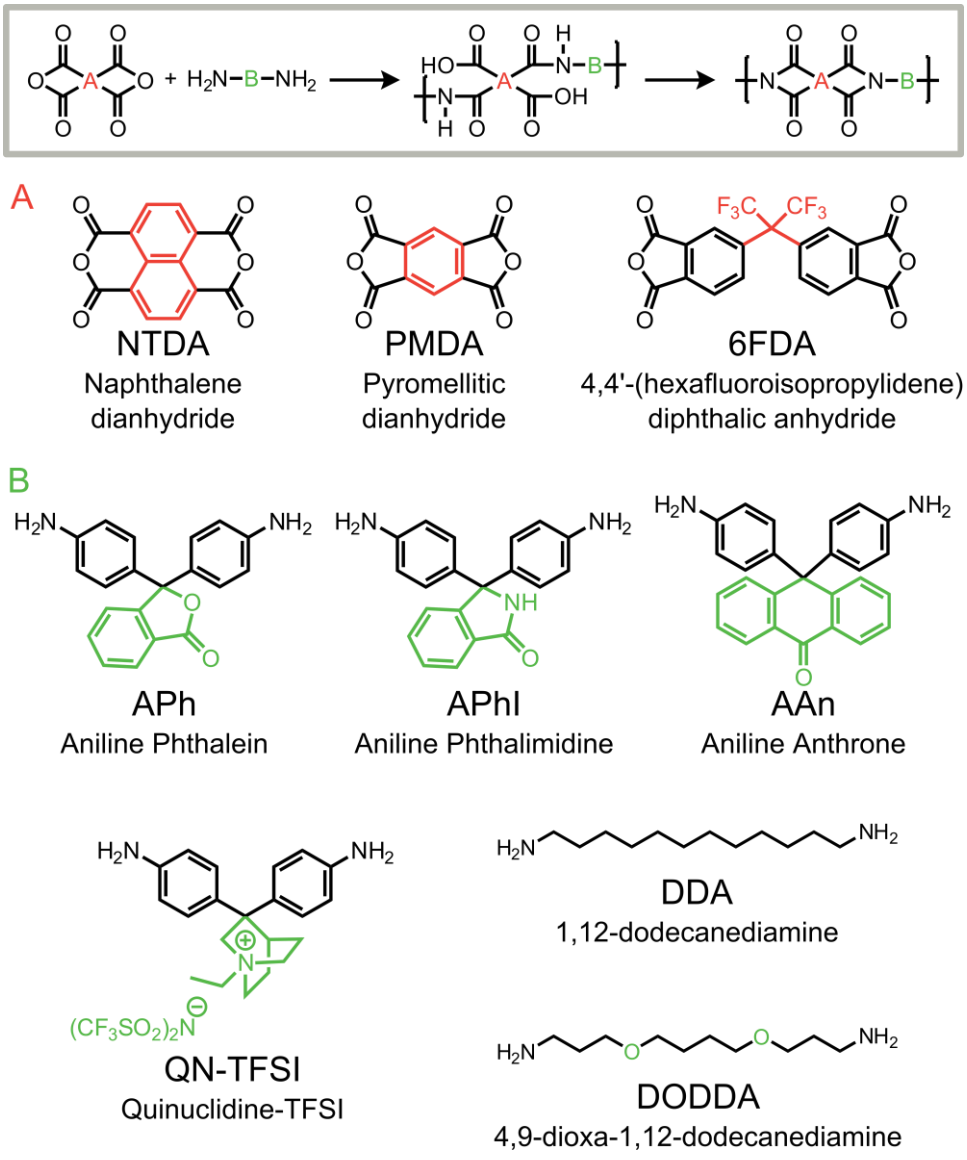

Figure 2.1. General synthesis scheme of polyimides and chemical structures of the monomers.

(INEOS RAS). Equimolar amounts of dianhydride and diamine were mixed at room temperature in *m*-cresol as solvent and benzoic acid as catalyst. The temperature of the reaction was increased to 180 °C in order to achieve complete imidization of polyimides. A general polycondensation reaction scheme of polyimides and chemical structures of starting monomers used in this work are depicted in Figure 2.1.

Electrode preparation started by mixing polyimides with Ketjenblack (KB) as conductive carbon by hand milling. Afterwards, the mixture was dispersed in a solution of poly(vinylidene fluoride) (PVDF) in *N*-metyl-2-pyrrolidone (NMP). The obtained slurry was casted over aluminum current collector and dried under vacuum at 100 °C. The final cathode composition was 50 wt% polyimide as active material, 45 wt% Ketjenblack and 5 wt% PVDF binder. The anode consisted in a lithium metal foil and the electrolyte 1M LiTFSI in dimethoxyethane and 1,3-dioxolane (DME/DOL, 1:1 v/v) soaking a glass fiber separator. Figure 2.2 illustrates the components of the cells studied in this chapter.

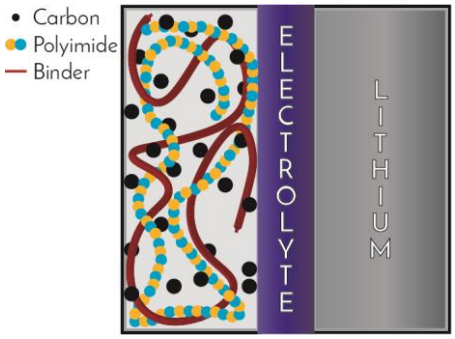

Figure 2.2. Schematic diagram of the polyimide-lithium cell studied in this chapter.

2.3. Electrochemical properties of polyimides with different imide groups

Electrochemical properties of polyimides based on pyromellitic, naphthalene and 6FDA dianhydrides were investigated using the same diamine: aniline phthalein (APh). Cyclic voltammetry of the three different polyimides was carried out in two-electrode cell (coin cell using lithium metal as anode and reference electrode and 1M LiTFSI solution in DME/DOL, 1:1 v/v as liquid electrolyte) at 0.1 mV s^{-1} between 1 and 3.5 V *vs.* Li^+/Li (Figure 2.3).

As it can be seen in Figure 2.3a, pyromellitic polyimide featured two pairs of redox peaks indicating a two-step reaction, the first one at 2.1/2.6 V *vs.* Li^+/Li and

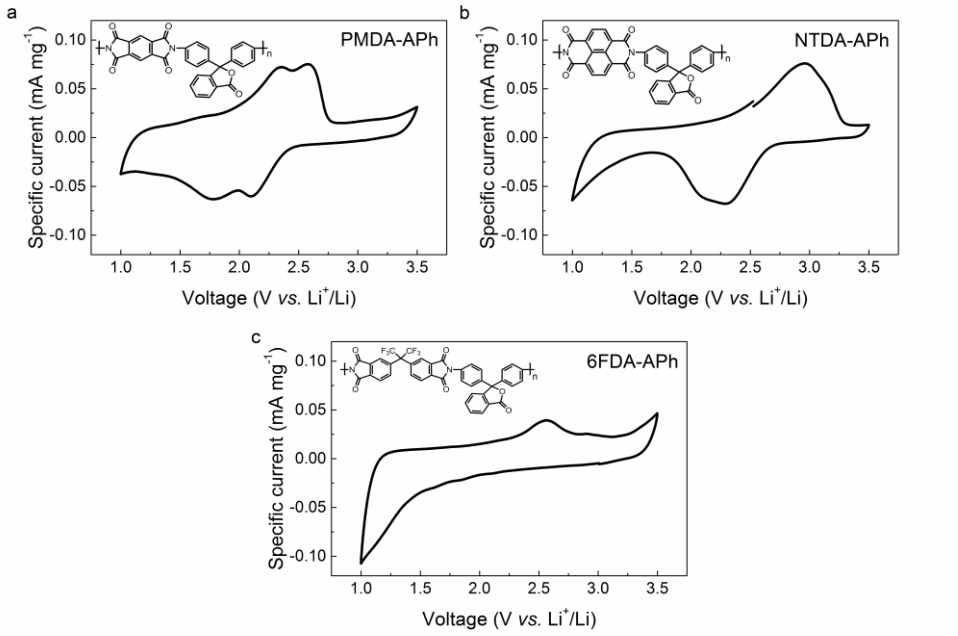

Figure 2.3. Cyclic voltammograms at 0.1 mV s^{-1} of (a) Pyromellitic-aniline phthalein (PMDA-APh), (b) Naphthalene-aniline phthalein (NTDA-APh) and (c) 4,4'-(hexafluoroisopropylidene)diphthalic anhydride-aniline phthalein (6FDA-APh).

the second one at 1.8/2.3 V *vs.* Li^+/Li. In the case of naphthalene polyimide (Figure 2.3b), the reaction took place in one step at higher voltages, 2.3 V *vs.* Li^+/Li for the reduction and 2.9 V *vs.* Li^+/Li for the oxidation reactions. The increase in the cathodic current below 1.5 V *vs.* Li^+/Li is probably coming from irreversible parasitic reactions occurring at lower voltages.

These two polyimides have a conjugated structure between the two imide groups which stabilizes the radical anion and dianion formed in the reduction reaction. Nevertheless, naphthalene polyimide presents higher conjugation than pyromellitic polyimide. Increasing the conjugation of the imide favors the delocalization of the gained electrons facilitating the redox reaction and shifting the voltage towards more positive values. In addition, the merging of the redox peaks into a broader one suggested a one step reaction for NTDA-APh polyimide (Figure 2.3a).[1,2]

In the case of 6FDA-APh polyimide, the main advantage was its solubility in NMP which facilitated the electrode preparation. However, the absence of reversible redox peaks within the voltage range used in the cyclic voltammetry (Figure 2.3c) impeded its use as cathode material for lithium batteries. The carbon of the hexafluoroisopropylidene (6F) moiety interrupts the conjugation across the imides hindering its reduction and shifting the voltage towards lower values.[2,15] Hence, 6FDA-APh polyimide would be more suitable for anode applications, which are beyond the scope of this thesis.

To further study the cycling performance of pyromellitic- and naphthalene-based polyimides bearing aniline phthalein groups, galvanostatic charge-discharge experiments were carried out. The theoretical capacity of both polyimides was calculated considering a three-electron reaction; two electrons from the imide groups and the third one from the phthalein, resulting in 161 mA h g^{-1} for PMDA-APh and 147 mA h g^{-1} for NTDA-APh. The current used to cycle the

batteries (generally known as the C-rate) was calculated taking into account the theoretical capacity for a given polyimide to charge-discharge the cell in 5 h, this value is referred as C/5 rate. The voltage profile of naphthalene polyimide (Figure 2.4a), shows a higher voltage plateau than the pyromellitic polyimide. Moreover, PMDA-APh polyimide featured two redox plateaus, which are in agreement with the two redox peaks in the cyclic voltammogram in Figure 2.3a.

Cycling stability (following the capacity values with cycling) of the two batteries is depicted in Figure 2.4b. Initial capacities for pyromellitic and naphthalene polyimides were 142 mA h g^{-1} and 137 mA h g^{-1}, respectively. The obtained values, close to the theoretical capacity, suggested a three-electron reaction, despite the absence of a third redox peak in the cyclic voltammograms. Similarty, a perylene-urea polyimide has been reported to undergo a three-electron reaction at the same redox voltage, *i.e.* without an additional redox peak.[12] Large differences in cycling stability were found for both polymers. On the one hand, pyromellitic polyimide showed a clear capacity fade in the first 20 cycles leading to 25 % capacity retention after 100 cycles. On the other hand, naphthalene polyimide aside from achieving an initial capacity closer to the theoretical value, also retains 64 % of its initial capacitance after 100 cycles. Despite the higher

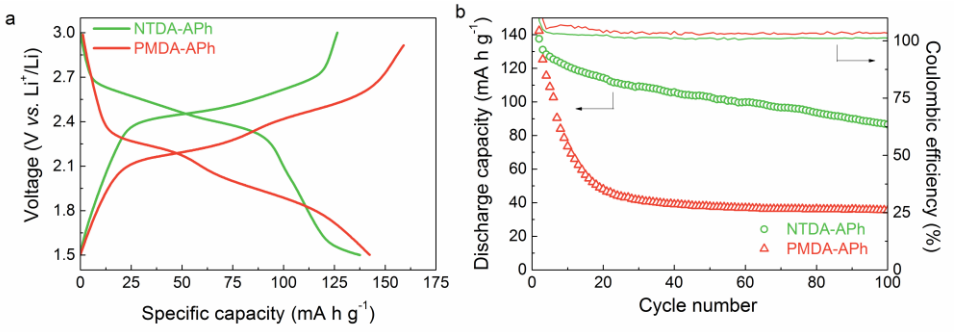

Figure 2.4. (a) Voltage profile of the second cycle and (b) cycling performance (left axis) and coulombic efficiency (right axis) of Naphthalene-aniline phthalein, NTDA-APh (green line/circles) and Pyromellitic-aniline phthalein, PMDA-APh (orange line/triangles) at C/5 rate.

capacity retention of NTDA-APh over PMDA-APh, naphthalene polyimide showed a continuous capacity fade with cycling. These differences for the two polyimides confirmed what other groups have reported, a better performance of naphthalene polyimides over pyromellitic polyimides.[3,4,16,17] The coulombic efficiency of these polymers was close to 100 % after 100 cycles, showing that no parasitic reactions were involved.

2.4. Electrochemical properties of polyimides varying diamines

Electrochemical properties of polyimides synthesized form different diamine monomers were investigated. Naphthalene dianhydride was used for all the polyimides in this section due to its better performance in comparison with PMDA and 6FDA. In order to confirm that the redox voltage is mostly dependent on the dianhydride part, cyclic voltammetry tests were performed on polyimides with different diamines in their structure. The naphthalene polyimides studied were: aniline phthalein (APh), with an additional redox-active carbonyl group (NTDA-APh); another aromatic diamine bearing an ionic functionality without redox activity (NTDA-QN-TFSI); and an aliphatic diamine containing ether groups (NTDA-DODDA). As it can be seen in Figure 2.5, the reduction voltage for the different polyimides is very similar. However, the main difference resides in the oxidation peak. The ionic polyimide (NTDA-QN-TFSI) featured the smallest difference between the reduction and oxidation peaks (0.27 V), followed by the polyimide with aliphatic diamine (NTDA-DODDA) (0.45 V) and finally the polyimide bearing aniline phthalein (NTDA-APh) (0.67 V). The separation of the reduction and oxidation voltages as well as the broadening of the redox peaks suggest a kinetic limitation.[18,19]

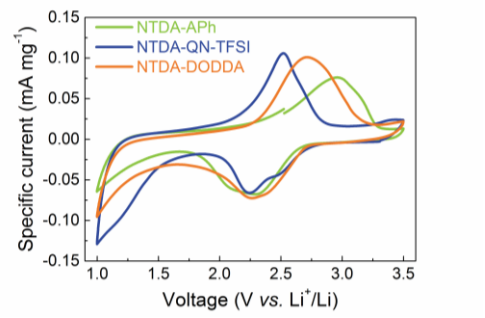

Figure 2.5. Cyclic voltammograms of naphthalene-aniline phthalein, NTDA-APh (green), naphthalene-quinuclidine-TFSI, NTDA-QN-TFSI (blue) and naphthalene-dioxadodecanediamine, NTDA-DODDA (orange) at 0.1 mV s^{-1}.

Due to the similarities in the cyclic voltammograms, cycling performance of the different polymers was investigated. In order to simplify the comparison, polyimides were divided into aromatic and aliphatic diamines. Aromatic diamines were: aniline phthalein (APh), aniline phthalimidine (APhI), aniline anthrone (AAn), and quaternized quinuclidine (QN-TFSI). Whereas 1,12-dodecanediamine (DDA) and 4,9-dioxa-1,12-dodecanediamine (DODDA) corresponded to the aliphatic diamines group.

2.4.1. Aromatic diamines

Polyimides were compared in terms of cycling stability and rate capability which is the measurement of the capacity when increasing the current density, *i.e.* decreasing the charge-discharge times.

Cycling stability of the polyimides coming from the aromatic diamines was characterized at C/5 between 1.5 and 3 V *vs.* Li^+/Li (Figure 2.6). The voltage range was adjusted in order to avoid the side reactions occurred below 1.5 V *vs.* Li^+/Li. Theoretical capacities of polyimides containing additional carbonyl groups, NTDA-APh (147 mA h g^{-1}), NTDA-APhI (147 mA h g^{-1}), and

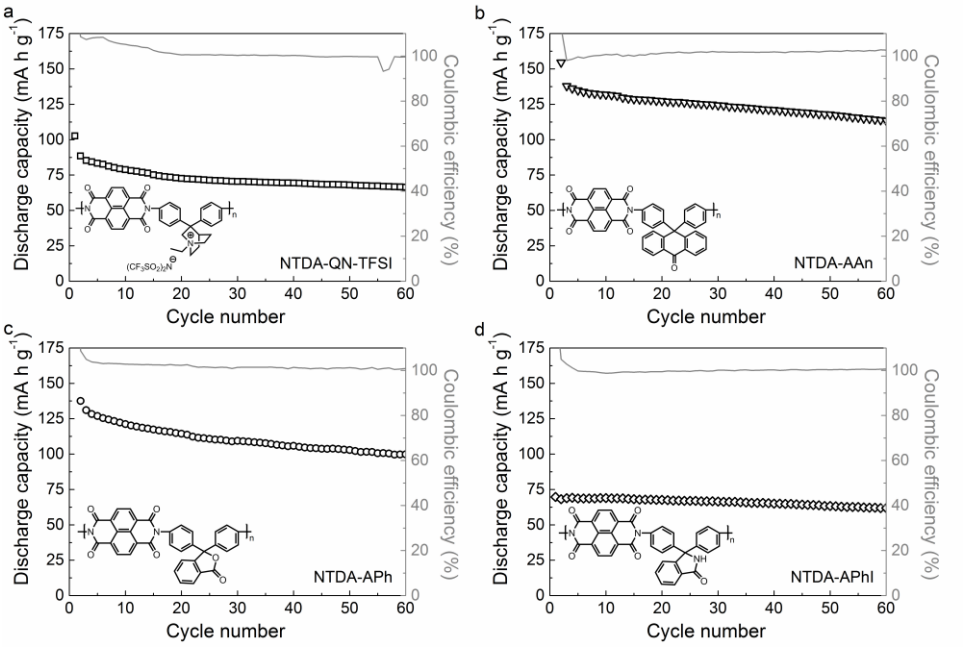

Figure 2.6. Cycling performance (left axis, black) and coulombic efficiency (right axis, grey) of (a) naphthalene-quinuclidine-TFSI, NTDA-QN-TFSI (squares), (b) naphthalene-aniline anthrone, NTDA-AAn (inverse triangles), (c) naphthalene-aniline phthalein, NTDA-APh (circles) and (d) naphthalene-aniline phthalimidine, NTDA-APhI (rhombi) at C/5 between 1.5 and 3 V *vs.* Li^+/Li.

NTDA-AAn (132 mA h g^{-1}) were higher than the ionic polyimide NTDA-QN-TFSI (64 mA h g^{-1}). This is caused by the extra electron considered in the redox reaction of the former polyimides and the very high molecular weight of the latter polyimide. The capacity observed in the first cycle in comparison with the corresponding theoretical capacity provides the percentage of active mass utilization. Surprisingly, as it can be seen in Figure 2.6a, the initial discharge capacity for the ionic polyimide (NTDA-QN-TFSI) (88 mA h g^{-1}) was higher than the theoretical value (64 mA h g^{-1}). One possible reason is that the theoretical capacity was not calculated properly. If the mass of the TFSI ion from the polyimide was not considered for the calculation of the theoretical capacity, the

corresponding value would rise to 97 mA h g^{-1} and the experimental discharge capacity would be lower.

The anthrone-based naphthalene polyimide (NTDA-AAn) showed the best results with 137 mA h g^{-1} discharge capacity, corresponding to the complete utilization of the electrode's mass (Figure 2.6b). It was followed by NTDA-APh (Figure 2.6c) and NTDA-QN-TFSI which achieved 93 and 91 % of their theoretical capacity, respectively. Despite the low capacity values observed for the NTDA-APhI polyimide (70 mA h g^{-1}, 48 % active mass utilization), a high capacity retention of 88 % was observed after 60 cycles (Figure 2.6d). Anthrone-based naphthalene polyimide exhibited higher stability (83 % capacity retention) than NTDA-APh and NTDA-QN-TFSI (both with 75 % capacity retention after 60 cycles). Excellent coulombic efficiency of 100 % was observed for all the samples.

Cell performance of NTDA-AAn (100 % material utilization and 83 % capacity retention) was improved in comparison with similar polymers reported in literature. As an example, Chen *et al.*[11] reported a naphthalene-urea polyimide able to undergo a three-electron reaction which featured 57 % material utilization and 93 % capacity retention. Another example reported by Tian *et al.*[10] consisted in a naphthalene-anthraquinone polyimide featuring a four-electron reaction with 92 % material utilization and 64 % capacity retention.

In order to further compare the performance of the different polyimides, rate capability was studied (Figure 2.7). In this experiment, the current density used to cycle the batteries was increased from 25 mA g^{-1} to 250 mA g^{-1} and back to 25 mA g^{-1}. The results would provide the capability of the polymers to charge and discharge at high currents as well as to recover their initial capacity at lower current. NTDA-AAn and NTDA-APhI polyimides displayed initial discharge capacities of 93 and 103 mA h g^{-1} at 25 mA g^{-1}, respectively. While increasing the current density to 250 mA g^{-1}, the discharge capacities dropped to 70 mA h g^{-1}

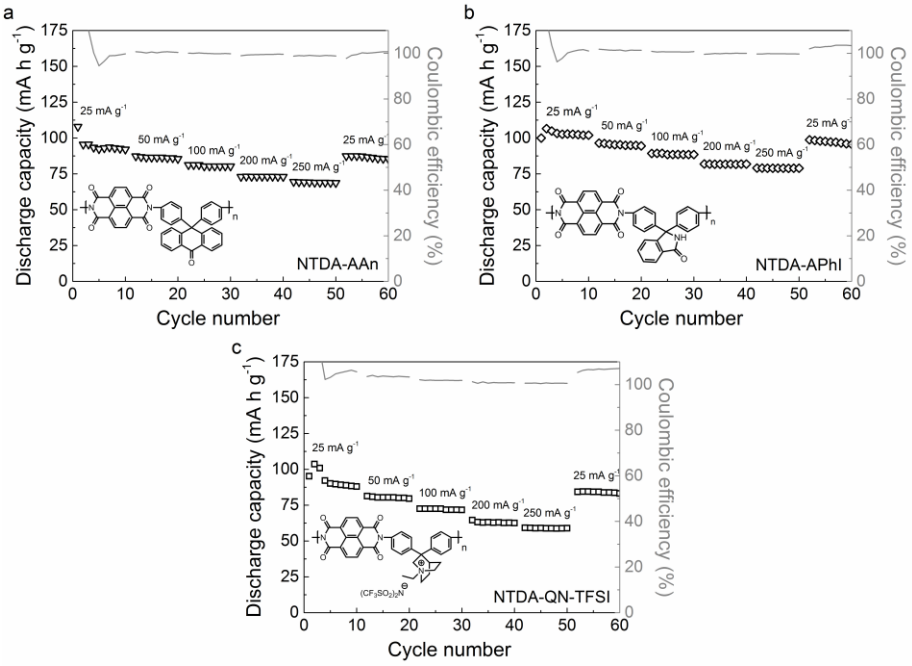

Figure 2.7. Rate capability (left axis, black) and coulombic efficiency (right axis, grey) of (a) naphthalene-aniline anthrone, NTDA-AAn (inverse triangles), (b) naphthalene-aniline phthalimidine, NTDA-APhI (rhombi) and (c) naphthalene-quinuclidine-TFSI, NTDA-QN-TFSI (squares) at 25, 50, 100, 200, 250 and 25 mA g^{-1} current densities between 1.5 and 3 V *vs.* Li^+/Li.

for NTDA-AAn and 80 mA h g^{-1} for NTDA-APhI, corresponding to 75 % and 78 % of the initial capacity, respectively, at 25 mA g^{-1}. Both polymers showed outstanding capacity recoveries of 94 % when cycling again at low current densities (Figure 2.7a and b). The same capacity recovery was observed for the ionic polyimide (NTDA-QN-TFSI); although the rate capability was worse than the other two polyimides, with 67 % capacity retention at 250 mA g^{-1} (Figure 2.7c). These results suggested that the ionic moiety of the polyimide backbone do not improve the rate capability of the polyimide.

2.4.2. Aliphatic diamines

Polyimides with aromatic diamines bearing redox-active carbonyl groups are able to exchange extra electrons. In contrast, polyimides synthesized from aliphatic diamines undergo a two-electron reaction coming from the diimide part. Therefore, theoretical capacities of the latter polyimides is lower, 123 mA h g^{-1} for 4,9-dioxa-1,12-dodecanediamine (NTDA-DODDA) and 124 mA h g^{-1} for 1,12-dodecanediamine (NTDA-DDA). Figure 2.8 shows that both polymers, NTDA-DDA and NTDA-DODDA, were able to access 100 % of their theoretical capacity at a low current density (25 mA g^{-1}). On the one hand, the ether-based polyimide (NTDA-DODDA) (Figure 2.8a) achieved 87 mA h g^{-1} discharge capacity at 250 mA g^{-1}, corresponding to 70 % capacity retention. On the other hand, NTDA-DDA featured 56 % capacity retention (Figure 2.8b). Although the latter polyimide was able to recover 93 % of the initial capacity when decreasing the current density back to 25 mA g^{-1}, NTDA-DODDA recovered 100 %. The better rate capability of NTDA-DODDA in comparison with NTDA-DDA could be explained due to the presence of ether groups known to solvate lithium ions and improve ionic conductivity resulting in faster reaction kinetics.[20-21]

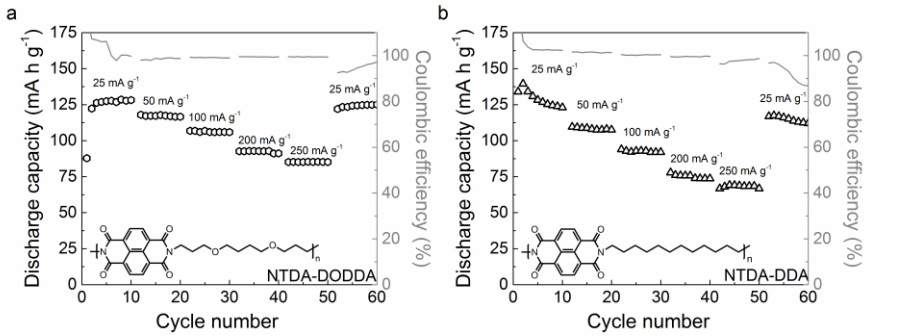

Figure 2.8. Rate capability (left axis, black) and coulombic efficiency (right axis, grey) of (a) naphthalene-dioxadodecanediamine, NTDA-DODDA (hexagons) and (b) naphthalene-dodecanediamine, NTDA-DDA (triangles) at 25, 50, 100, 200, 250 and 25 mA g^{-1} current densities between 1.5 and 3 V *vs.* Li^+/Li.

2.5. Conclusions

Electrochemical properties of different polyimides varying the structure of dianhydrides and diamines have been explored in this chapter. The redox potential of polyimides is mostly dependent on the imide part, *i.e.* the dianhydride precursor. Pyromellitic polyimide featured two redox peaks corresponding to a two-step reaction. Increasing the conjugation of the diimide to naphthalene polyimide, the redox reaction is facilitated resulting in a one-step reaction at higher potentials. Regarding battery performance, naphthalene polyimide showed higher capacity and stability than pyromellitic polyimide which presented a rapid capacity fade within the first 20 cycles. On the contrary, 6F polyimides did not show any redox activity in the cathode voltage range due to the disruption of aromaticity between the two imide groups.

Despite the scarce effect of diamines on the redox potential of polyimides, they played an important role in the battery performance. Naphthalene polyimide with aniline phthalein, phthalimidine and anthrone diamines were able to exchange a third electron. Among them, naphthalene polyimide with aniline anthrone (NTDA-AAn) featured better stability and rate capability. The high molecular weight of the ionic polyimide based on quinuclidine-TFSI decreased the theoretical capacity to meager values without enhancing the rate capability. Naphthalene polyimides synthesized with aliphatic diamines provided flexibility to the polymer chain making the active material more accessible and delivering the same capacity values as the theoretical. The presence of ether groups in the aliphatic diamines improved the performance of the battery at higher current densities with a complete recovery of the capacity afterwards. Therefore, there is a trade-off in the capacity between an increase in the number of electrons transferred and the flexibility of the polyimides.

2.6. Experimental part

2.6.1. Materials

Poly(vinylidene fluoride) (PVDF), *N*-Methyl-2-pyrrolidone (NMP), anhydrous dimethoxyethane (DME) and 1,3-dioxolane (DOL) were purchased from Sigma-Aldrich and used as received. Lithium bis(trifluoromethanesulfonyl)imide (LiTFSI) was purchased from Solvionic®.

2.6.2. Polymer synthesis

Polyimides were synthesized by a simple polycondensation reaction from equimolar amounts of dianhydride and diamine. Polyimides were synthesized and characterized by Sofia M. Morozova and Dr. Alexander S. Shaplov from A.N. Nesmeyanov Institute of Organoelement Compounds of Russian Academy of Sciences (INEOS RAS). Briefly, all polyimides were synthesized by adding equimolar amounts of the dianhydride and diamine monomers in *m*-cresol as solvent and benzoic acid as catalyst. The temperature was gradually increased to 180 °C under inert atmosphere for 10 h. The polymers were precipitated in excess of acetone and washed thoroughly in that solvent. Polyimides were dried under vacuum at 70 °C obtaining quantitative yield.

2.6.3. Electrode preparation and cell assembly

Cathodes were composed of polyimides as active materials (50 wt%), Ketjenblack (KB) (Ketjenblack® EC-600JD, AzkoNobel) as conductive additive (45 wt%) and PVDF as binder (5 wt%). First, polyimides and KB were mixed by hand milling and then added to a solution of PVDF in NMP. The obtained slurry was casted on aluminum foil using the doctor blade technique. Electrodes were punched into 12 mm diameter discs and dried under vacuum at 100 °C overnight.

Coin cells (CR2032) were assembled in an argon-filled glove box. Lithium foil

(Rockwood lithium) used as anode electrode was separated from the cathode by glass fiber (Glass fiber GFD/55, Whatman) imbibed with 1 M LiTFSI in dimethoxyethane and 1,3-dioxolane (DME/DOL, 1:1 v/v).

2.6.4. Methods

Cyclic voltammetry (CV) measurements were carried out on a VMP3 (Biologic®) electrochemical workstation at 20 °C. Scan rates of 0.1 mV s^{-1} were used between 1 and 3.5 V *vs.* Li^+/Li.

Galvanostatic charge-discharge experiments were conducted at 20 °C on a MACCOR® battery tester between 1.5 and 3.5 V *vs.* Li^+/Li at different current densities from 25 mA g^{-1} to 250 mA g^{-1}.

2.7. References

(1) Mazur, S.; Lugg, P. S.; Yarnitzky, C. Electrochemistry of aromatic polyimides. *J. Electrochem. Soc.* **1987**, *134,* 346-353.

(2) Viehbeck, A.; Goldberg, M. J.; Kovac, C. A. Electrochemical properties of polyimides and related imide compounds. *J. Electrochem. Soc.* **1990**, *137,* 1460-1466.

(3) Song, Z.; Zhan, H.; Zhou, Y. Polyimides: Promising energy-storage materials. *Angew. Chem. Int. Ed.* **2010**, *49,* 8444-8448.

(4) Wang, H.-g.; Yuan, S.; Ma, D.-l.; Huang, X.-l.; Meng, F.-l.; Zhang, X.-b. Tailored aromatic carbonyl derivative polyimides for high-power and long-cycle sodium-organic batteries. *Adv. Energy Mater.* **2014**, *4,* 1301651.

(5) Meng, Y.; Wu, H.; Zhang, Y.; Wei, Z. A flexible electrode based on a three-dimensional graphene network-supported polyimide for lithium-ion batteries. *J. Mater. Chem. A* **2014**, *2,* 10842-10846.

(6) Chen, L.; Li, W.; Wang, Y.; Wang, C.; Xia, Y. Polyimide as anode electrode material for rechargeable sodium batteries. *RSC Adv.* **2014**, *4,* 25369-25373.

(7) Liaw, D.-J.; Wang, K.-L.; Huang, Y.-C.; Lee, K.-R.; Lai, J.-Y.; Ha, C.-S. Advanced polyimide materials: Syntheses, physical properties and applications. *Prog. Polym. Sci.* **2012**, *37,* 907-974.

(8) Wu, H. P.; Yang, Q.; Meng, Q. H.; Ahmad, A.; Zhang, M.; Zhu, L. Y.; Liu, Y. G.; Wei, Z. X. A polyimide derivative containing different carbonyl groups for flexible lithium ion batteries. *J. Mater. Chem. A* **2016**, *4,* 2115-2121.

(9) Xu, F.; Wang, H.; Lin, J.; Luo, X.; Cao, S.-a.; Yang, H. Poly(anthraquinonyl imide) as a high capacity organic cathode material for Na-ion batteries. *J. Mater. Chem. A* **2016**, *4,* 11491-11497.

(10) Tian, B.; Ning, G.-H.; Tang, W.; Peng, C.; Yu, D.; Chen, Z.; Xiao, Y.; Su, C.; Loh, K. P. Polyquinoneimines for lithium storage: more than the sum of its parts. *Mater. Horiz.* **2016**, *3,* 429-433.

(11) Chen, C.; Zhao, X.; Li, H.-B.; Gan, F.; Zhang, J.; Dong, J.; Zhang, Q. Naphthalene-based polyimide derivatives as organic electrode materials for lithium-ion batteries. *Electrochim. Acta* **2017**, *229,* 387-395.

(12) Sharma, P.; Damien, D.; Nagarajan, K.; Shaijumon, M. M.; Hariharan, M. Perylene-polyimide-based organic electrode materials for rechargeable lithium batteries. *J. Phys. Chem. Lett.* **2013**, *4,* 3192-3197.

(13) Mecerreyes, D. Polymeric ionic liquids: Broadening the properties and applications of polyelectrolytes. *Prog. Polym. Sci.* **2011**, *36,* 1629-1648.

(14) Korshak, V. V.; Vinogradova, S. V.; Vygodskii, Y. S. Cardo Polymers. *J. Macromol. Sci., Rev. Macromol. Chem.* **1974**, *11,* 45-142.

(15) Hsiao, S.-H.; Yeh, S.-J.; Wang, H.-M.; Guo, W.; Kung, Y.-R. Synthesis and optoelectronic properties of polyimides with naphthyldiphenylamine chromophores. *J. Polym. Res.* **2014**, *21,* 407.

(16) Häupler, B.; Wild, A.; Schubert, U. S. Carbonyls: Powerful organic materials for secondary batteries. *Adv. Energy Mater.* **2015**, *5,* 1402034.

(17) Tian, D.; Zhang, H.-Z.; Zhang, D.-S.; Chang, Z.; Han, J.; Gao, X.-P.; Bu, X.-H. Li-ion storage and gas adsorption properties of porous polyimides (PIs). *RSC Adv.* **2014**, *4,* 7506-7510.

(18) Casado, N.; Hernández, G.; Sardon, H.; Mecerreyes, D. Current trends in redox polymers for energy and medicine. *Prog. Polym. Sci.* **2016**, *52,* 107-135.

(19) Muench, S.; Wild, A.; Friebe, C.; Häupler, B.; Janoschka, T.; Schubert, U. S. Polymer-based organic batteries. *Chem. Rev.* **2016**, *116,* 9438-9484.

(20) Wright, P. V. Ionic conductivity and organisation of macromolecular polyether-alkali-metal salt complexes. *J. Mater. Chem.* **1995**, *5,* 1275-1283.

(21) Porcarelli, L.; Shaplov, A. S.; Bella, F.; Nair, J. R.; Mecerreyes, D.; Gerbaldi, C. Single-ion conducting polymer electrolytes for lithium metal polymer batteries that operate at ambient temperature. *ACS Energy Lett.* **2016**, *1,* 678-682.

CHAPTER 3.

REDOX-ACTIVE POLYIMIDE-POLYETHER COPOLYMERS AS CATHODES FOR LITHIUM BATTERIES

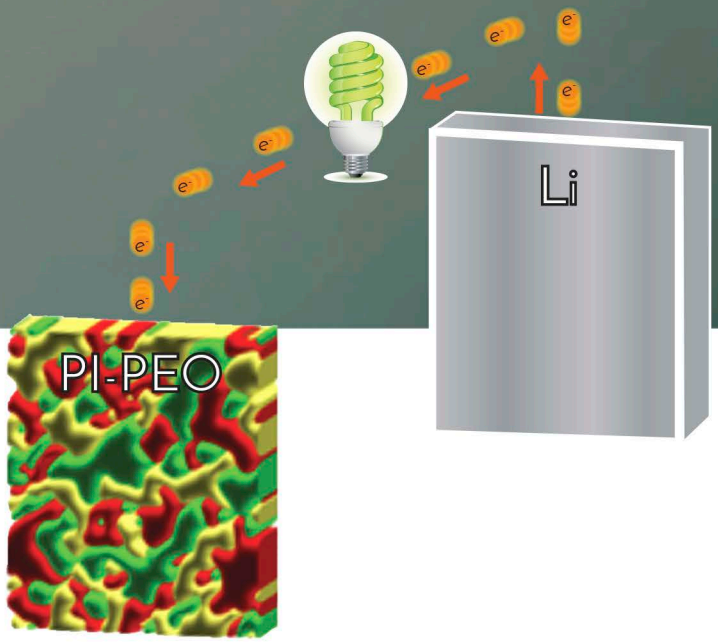

Chapter 3. Redox-active polyimide-polyether copolymers as cathodes for lithium batteries

3.1. Introduction

Polyimides have been widely known for their outstanding thermal stability, mechanical strength and insulating properties. Besides, these materials are able to become electronically conducting upon electrochemical reduction, owing to the relatively large electron affinity of the imide group.[1,2] The conductivity results from electron hoping between neighboring imide moieties.[3,4] Nevertheless, addition of conductive additives is necessary for a good electrochemical performance of the battery. Most papers reporting polyimides as cathodes for lithium-ion batteries have a composition of 60 wt% active material, 30 wt% conductive carbon and

10 wt% binder.[5-7] In some cases, the conductive carbon used were graphene or single-walled carbon nanotubes; expensive additives known to improve the rate capability of the active material.[8-11]

Although increasing electronic conductivity is one way to enhance the rate performance and accessibility of the active mass, it is not the only solution. Redox reactions not only involve the electron transfer but also the diffusion of the required charge-compensating ionic species (cations). In this context, incorporation of solvating agents such as ethylene oxide may enhance the ion mobility.[3] Poly(ethylene oxide) (PEO) is a widely used polymer in the battery field as polymer electrolyte and binder.[12-15] PEO contains ether coordination sites that enable the dissociation of salts, as well as the assistance in ionic transportation through a flexible macromolecular structure.[16]

Therefore, copolymers in which imide redox-active groups separated by PEO blocks could be interesting materials to be used as cathodes in lithium-ion batteries. Furthermore, the incorporation of PEO would enhance the solubility of the polyimide and thus facilitate its tractability. There are several ways to incorporate PEO into a polyimide backbone. PEO chains can be grafted onto a polyimide backbone by post-functionalization[17] or by the reaction of monomers already containing pendant PEO groups.[18] In contrast, linear polyimide-PEO copolymers can be synthesized using dianhydrides and linear α,ω-diamino oligopolyethers.[19-20] The main advantage of the latter type of polymers is the commercially available oligoether diamines with different lengths of PEO chains, allowing a one-step synthesis route.

The aim of this chapter is to synthesize soluble polyimide-polyether copolymers to be used as cathode materials in lithium-ion batteries. On the one hand, polyimides based on pyromellitic, naphthalene and perylene dianhydrides were chosen due to their different electrochemical properties. On the other hand, linear

α,ω-diamino oligopolyethers (Jeffamines®) with different molecular weights were used to investigate the effect of the ether length on the battery performance.

3.2. Polymer synthesis and characterization

Polyimide-polyether copolymers were synthesized by a conventional polycondensation reaction adding stoichiometric amounts of oligoether diamines and dianhydrides (pyromellitic, naphthalene or perylene). This reaction occurred in two steps *via* an intermediate poly(amic acid) and the consequent chemical imidization. The linear oligoether diamines used in this chapter, called Jeffamines®, are composed mostly of PEO with a few units of PPO. For simplicity they will be indicated as PEO followed by their molecular weight. PEO600 corresponds approximately to 9 units of ethylene oxide (EO), PEO900 to 12 EO units and PEO2000 to 39 units. Figure 3.1 depicts a general scheme reaction, the chemical structures of polyimide-polyether copolymers and physical aspect of polyimides bearing PEO2000. Pyromellitic and naphthalene

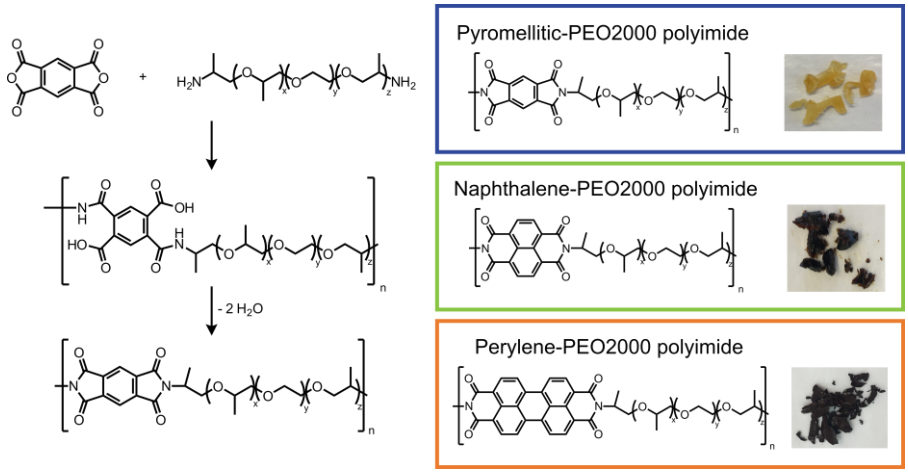

Figure 3.1. General scheme reaction, chemical structures and physical aspect of three different polyimides bearing PEO2000.

Table 3.1. Weight composition of both monomers in the final poly**imides**.

Entry	Polyimide	imide wt%	PEO wt%
1	Pyromellitic-PEO600	28.6	71.4
2	Pyromellitic-PEO900	19.5	80.5
3	Pyromellitic-PEO2000	10	90
4	Naphthalene-PEO600	32	68
5	Naphthalene-PEO900	23	77
6	Naphthalene-PEO2000	12	88
7	Perylene-PEO2000	16.4	83.6

dianhydrides reacted with the three different Jeffamines®; however, solubility of perylene dianhydride was limited and therefore perylene polyimide was only synthesized with PEO2000. The low solubility of perylene derivatives is due to the π-π stacking and its highly conjugated structure.

Appearance and consistency of the final polymers depended upon the PEO length, from transparent and sticky polyimides based on PEO600 and PEO900 to waxy opaque polyimides containing PEO2000. Similarly, the color of the final polymer is given by the imide segment; light yellow for pyromellitic, dark brown for naphthalene and deep red for perylene polyimides.

In spite of the equimolar amounts added of dianhydride and oligoether diamine, the weight composition of both monomers (imide and PEO) in the final polymer varied significantly (results are summarized in Table 3.1).

Structure characterization was carried out by ^{1}H NMR and Attenuated Total Reflectance Infrared Spectroscopy (ATR-FTIR). ^{1}H NMR spectra (Figure 3.2a-c)

showed the characteristic peaks of PEO at 0.9 ppm (protons from the CH_3 corresponding to the propylene units), and 3.6 ppm (from the CH_2), as well as the aromatic protons from the imide moieties at 8.2 ppm for pyromellitic polyimides (Figure 3.2a), 8.7 ppm for naphthalene polyimides (Figure 3.2b) and between

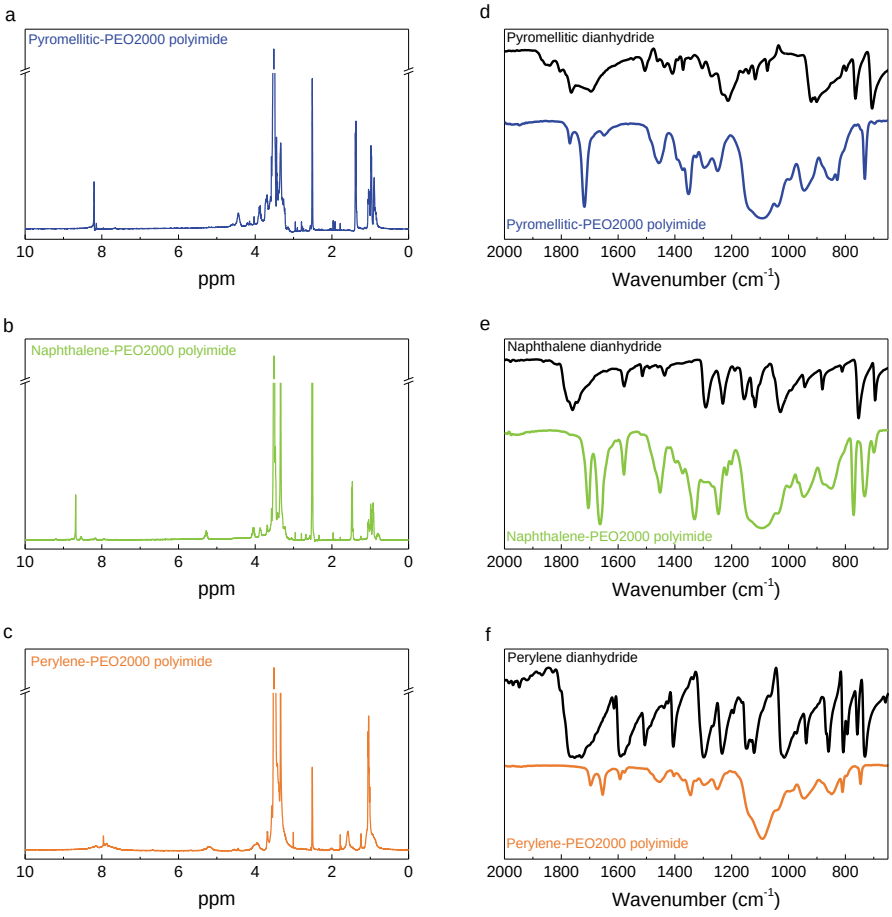

Figure 3.2. ^1H NMR spectra of (a) Pyromellitic-PEO2000, (b) Naphthalene-PEO2000 and (c) Perylene-PEO2000 polyimides. ATR-FTIR spectra of (d) pyromellitic dianhydride (black) and Pyromellitic-PEO2000 polyimide (blue), (e) Naphthalene dianhydride (black) and Naphthalene-PEO2000 polyimide (green) and (f) Perylene dianhydride (black) and Perylene-PEO2000 polyimide (orange).

7.4 and 8.6 ppm for perylene polyimides (Figure 3.2c). Besides ^{1}H NMR, imidization was also confirmed by ATR-FTIR (Figure 3.2d-f). The main difference between the dianhydride precursors and the final polyimides is the shift towards lower wavenumber of the carbonyl stretching bands and the appearance of the C–N asymmetric stretching bands. Increasing the conjugation of the imide groups from pyromellitic to naphthalene to perylene polyimides led to a decrease in the wavenumber of the bands. Typical bands for pyromellitic polyimides (Figure 3.2d) appeared at 1770 cm^{-1} (ν_{as} C=O), 1714 cm^{-1} (ν_{sym} C=O), 1350 cm^{-1} (ν_{as} C–N) and 730 cm^{-1} (δ C=O). In the case of naphthalene polyimide (Figure 3.2e) at 1705 cm^{-1} (ν_{as} C=O), 1662 cm^{-1} (ν_{sym} C=O), 1330 cm^{-1} (ν_{as} C–N) and 735 cm^{-1} (δ C=O). Finally, for perylene polyimide (Figure 3.2f) the bands appeared at 1695 cm^{-1} (ν_{as} C=O), 1654 cm^{-1} (ν_{sym} C=O), 1343 cm^{-1} (ν_{as} C–N) and 744 cm^{-1} (δ C=O).

Molecular weight (M_W) and dispersity of the polymers ($Đ$) were determined by Gel Permeation Chromatography (GPC) in tetrahydrofuran (THF) using polystyrene standards. Results are presented in Table 3.2, although there is not a clear trend.

Glass transition temperature (T_g) and melting temperature (T_m) of the synthesized polymers was determined by Differential Scanning Calorimetry (DSC). DSC curves of naphthalene polyimides with PEO600, PEO900 and PEO2000 are depicted in Figure 3.3, while experimental data for all the samples is summarized in Table 3.2. The DSC traces indicated that polymers containing PEO blocks of 600 g mol^{-1} and 900 g mol^{-1} were amorphous exhibiting well-defined glass transition temperatures. However, longer PEO blocks of 2000 g mol^{-1} yielded semi-crystalline polymers featuring T_g and T_m. As a general trend, the measured T_g decreased when the length of PEO blocks increased due to the longer flexible sequences.[21] As expected, T_g of the polymers was higher than the corresponding starting oligoethers. Semi-crystalline structure of

polyimides bearing PEO2000 can be explained due to the ability of long PEO segments to crystallize.

Table 3.2. Characteristics of the starting monomers and the final polyimide-polyether copolymers.

Entry	Sample	M_w[a] (g mol^{-1})	$Đ$[a]	T_g[b] (°C)	T_m[b] (°C)	T_d[c] (°C)
1	PEO600	-	-	-62	-12	-
2	PEO900	-	-	-62	18	-
3	PEO2000	-	-	-59	37	370
4	Pyromellitic dianhydride	-	-	-	-	230
5	Pyromellitic-PEO600	6500	3.3	-34	-	320
6	Pyromellitic-PEO900	15500	5.2	-47	-	330
7	Pyromellitic-PEO2000	25300	4.4	-49	29	280
8	Naphthalene dianhydride	-	-	-	-	330
9	Naphthalene-PEO600	30300	4.0	-26	-	385
10	Naphthalene-PEO900	83100	5.4	-43	-	380
11	Naphthalene-PEO2000	24700	3.7	-54	30	350
12	Perylene dianhydride	-	-	-	-	530
13	Perylene-PEO2000	11400	2	-55	25	360

[a] Molecular weight (M_w) and dispersity ($Đ=M_w/M_n$) of polymers determined by GPC calibrated relative to polystyrene standards. [b] Glass transition temperature (T_g) and melting temperature (T_m) determined from the second heating scan recorded by DSC at 10 °C min^{-1} heating rate. [c] Degradation temperature (T_d) determined by the onset point using Universal Analysis 2000 and obtained by TGA at a heating rate of 10 °C min^{-1} under nitrogen atmosphere.

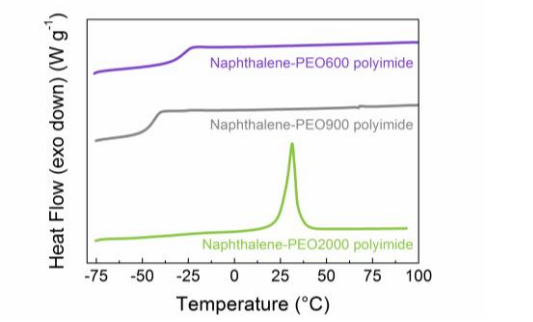

Figure 3.3. DSC traces of Naphthalene-PEO600 (purple), Naphthalene-PEO900 (grey) and Naphthalene-PEO2000 (green) polyimides.

Degradation temperature (T_d), determined by thermogravimetric analysis (TGA), was higher than 300 °C for all the polymers (values in Table 3.2). Although the length of PEO does not have a big effect on the degradation temperature of the polymers, it is not the case for the change in conjugation of the imide groups, as the T_d increased from pyromellitic to perylene polyimides (Figure 3.4).

Polyimide-polyether copolymers are composed of rigid segments from aromatic imide groups alternating with flexible oligoether blocks, possibly leading to microphase separation. Therefore, morphology of the samples was studied by atomic force microscopy (AFM). These measurements were done in

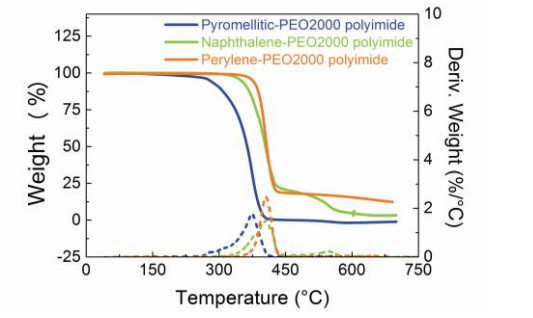

Figure 3.4. TGA curves (solid lines) and the derivatives (dashed lines) for Pyromellitic-PEO2000 (blue), Naphthalene-PEO2000 (green) and Perylene-PEO2000 (orange) polyimides.

collaboration with Raphaël Coste and Dr. Laurent Rubatat from the University of Pau (France). For the sample preparation, polyimide-polyether copolymers were dissolved in acetonitrile, solvent-casted on glass squares and dried under vacuum at 100 °C overnight. As an example, Figure 3.5 shows the AFM images of Naphthalene-PEO600 polyimide. As observed in the AFM image, a weak segregation is noticeable from the height and elastic modulus (log scale) images collected in the PeakForce mode. More specifically, on the mechanical modulus image, the clear domains correspond to aromatic parts (higher modulus); whereas darker domains are rich in aliphatic polyether segments (lower modulus). The nanodomains showed a non-regular structure formed by two co-continuous phases. Unfortunately, characterization by AFM of polyimide-polyether samples with PEO2000 was not possible due to their semi-crystalline morphology. Altogether, polyimide-polyether copolymers showed microphase separation.

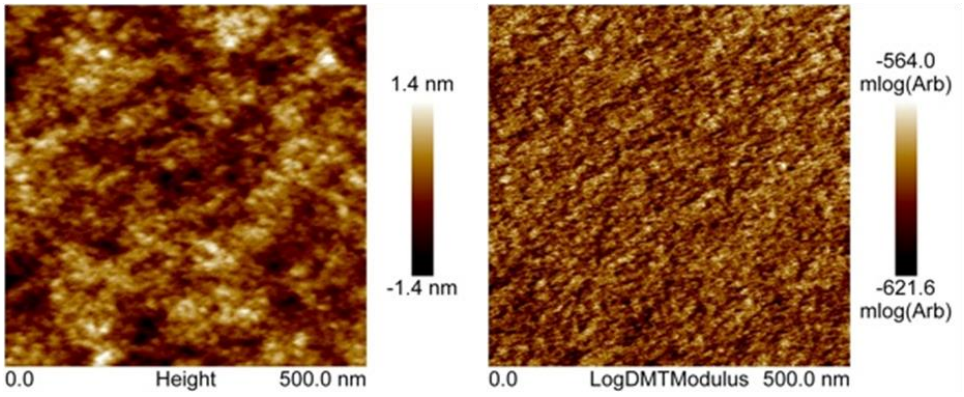

Figure 3.5. Height (left) and elastic modulus in log scale (right) AFM images of Naphthalene-PEO600 polyimide (collected in the PeakForce mode).

3.3. Electrode preparation and characterization

Polyimide-polyether copolymers were soluble in common organic solvents, such as dichloromethane, acetonitrile, and *N,N*-dimethylformamide, in comparison with fully aromatic polyimides which have a limited solubility. This enhanced solubility brings three important advantages regarding the battery electrode preparation. Firstly, given that the active material of the electrode is soluble it can be prepared by a simple solution method, instead of milling or other mixing techniques. Secondly, high boiling point and toxic solvents such as NMP could be avoided. Thirdly, due to the good film forming properties of polyimide-polyether copolymers, there is no need to add a binder to the electrode composition. Thus, for the electrode preparation, polyimide-polyether copolymers were dissolved in acetonitrile and then carbon Ketjenblack (KB) was dispersed in that solution. The obtained slurry was casted on aluminum foil using the doctor blade technique, dried under vacuum at 100 °C and punched into 12 mm diameter discs. The overall process is illustrated in Figure 3.6. Final composition of the electrodes was 85 wt% polyimide-polyether as active material and binder together with 15 wt% KB.

Morphology of the electrodes was investigated by PeakForce Tunnelling AFM (TUNA). This mode provides additional information about the conductivity of the samples as well as the elastic modulus and adhesion at the nanometer length

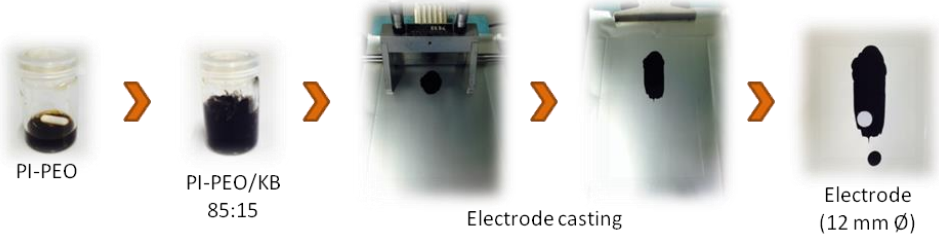

Figure 3.6. Graphical representation of polyimide-polyether (PI-PEO) film electrode preparation.

scale. This technique was used to characterize sample Naphthalene-PEO600 polyimide electrode loaded with 15 wt% KB and Figure 3.7 shows the corresponding topography, elastic modulus (log scale), adhesion and peak current AFM images. The electrode did not show an obvious phase segregation between the copolymer parts, but presents an aggregate-like morphology with small particles (few tens nm) surrounding bigger particles (few hundred nm). The correlation between the elastic modulus and the peak current images tends to demonstrate that the small particles correspond to the carbon black. Indeed, there is a strong spatial correlation between higher modulus and electron conducting area; *e.g.*, domains pointed by the red and green arrows. In addition,

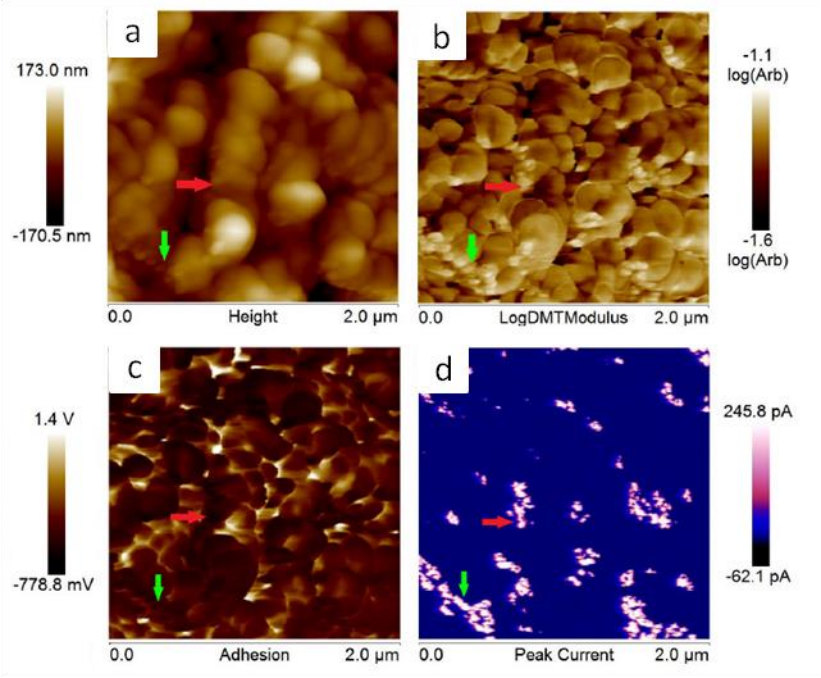

Figure 3.7. AFM images collected in PeakForce TUNA AFM, using a DC sample bias of 1 V on sample Naphthalene-PEO600 polyimide loaded with 15 wt% of carbon black. (a) Topography, (b) elastic modulus in log scale, (c) adhesion force and (d) peak current images. The red and green arrows are pointing on the same domains in all four pictures.

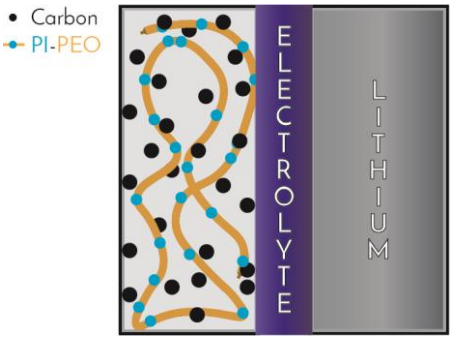

Figure 3.8. Schematic diagram of a lithium cell composed of polyimide-polyether copolymers and carbon as cathode.

the analysis (bearing analysis) on the peak current image indicates a conducting area of about 10 %, which is in reasonable agreement with the amount of carbon black loaded in the composite. However, carbon black is not very well distributed along the sample as it can be seen on the peak current image in Figure 3.7d.

Cells were assembled using polyimide-polyether copolymers (85 wt%) and Ketjenblack (15 wt%) as cathode, lithium metal as anode and glass fiber as separator soaked with 1M LiTFSI in 2-methyltetrahydrofuran (MeTHF). A schematic representation of the cell is illustrated in Figure 3.8.

3.4. Effect of the imide group on the electrochemical properties of polyimides

Redox reaction mechanism of imides can be described as an enolization process of the carbonyl group, facilitated by a conjugated structure able to disperse charge by delocalization.[22] As shown in the schemes on the right side of Figure 3.9, reversible redox reaction of imide groups occurs in two steps of one-electron each. Reduction (gain of electrons) is related to association of

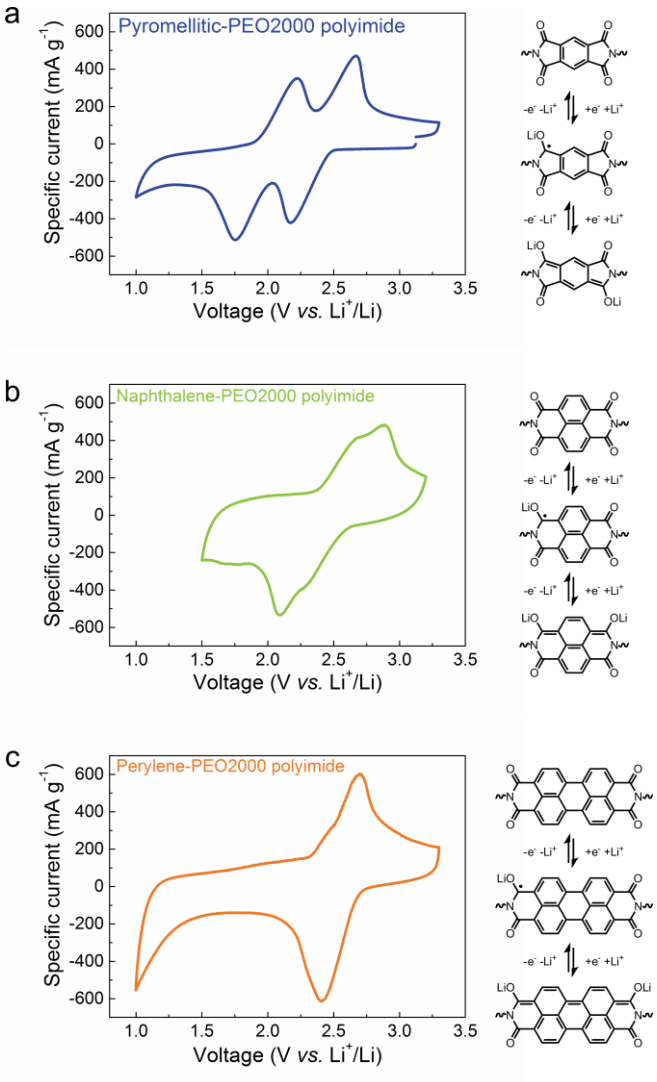

Figure 3.9. Cyclic voltammogram at 1 mV s^{-1} (left) and redox mechanism (right) of (a) Pyromellitic-PEO2000, (b) Naphthalene-PEO2000 and (c) Perylene-PEO2000 polyimides.

lithium ions with oxygen whereas dissociation occurs during oxidation (loss of electrons).[1,7] In the first reduction step a radical-anion is formed, followed by the second reduction step to generate a dianion specie. In order to study the redox

mechanism and to determine the redox voltage of the polyimides, cyclic voltammetry was performed in a coin cell against metallic lithium. In Figure 3.9a, cyclic voltammogram of Pyromellitic-PEO2000 polyimide shows two pairs of reduction/oxidation peaks at 2.17/2.67 V and 1.75/2.22 V *vs.* Li^+/Li. The first peak could be associated with the formation of the radical-anion followed by the generation of the dianion,[1,7] as it can be seen in the redox mechanism. However, when the conjugation of the imide group is increased to Naphthalene-PEO2000 polyimide (Figure 3.9b), the redox peaks tend to merge into a broader one shifted to higher voltages, 2.3/2.9 V and 2.1/2.7 V *vs.* Li^+/Li. Further increase in the conjugation to Perylene-PEO2000 polyimide resulted in one pair of redox peaks at 2.4/2.7 V *vs.* Li^+/Li (Figure 3.9c), although two electrons are being transferred. This increase in conjugation stabilizes the reduced specie as well as separates the negative charges gained upon reduction, facilitating the reaction occurring in only one step of two electrons and shifting the redox voltages to higher values.

To further investigate the battery performance of the polyimides containing different imide moieties, galvanostatic charge-discharge experiments were carried out. In this technique, a constant current is applied until a set voltage is reached. This current, known as C-rate, is calculated based on the theoretical capacity and mass of the active material, and the time chosen to completely charge or discharge the battery. For this experiment, a C-rate of C/10 was applied between 1.5 and 3.3 V *vs.* Li^+/Li. As it was explained in the introduction in Chapter 1, the theoretical capacity depends on the molecular weight of the active material. In this chapter the theoretical capacity is calculated taking into account only the molecular weight of the imide groups which is the active part. Thus, increasing the molecular weight of the imide moieties results in a decrease of the theoretical capacity, from 250 mA h g^{-1} for Pyromellitic polyimides to 200 mA h g^{-1} for Naphthalene polyimides and 140 mA h g^{-1} for Perylene polyimides. To be able to compare the three of them, the experimental capacities were represented as percentage of the theoretical capacity. Voltage profiles of

the three different polyimides are represented in Figure 3.10a. The reduction reaction of Pyromellitic-PEO2000 polyimide started at 2.4 V *vs.* Li^+/Li, in the case of Naphthalene-PEO2000 polyimide at 2.5 V *vs.* Li^+/Li following by Perylene-PEO2000 polyimide at 2.6 V *vs.* Li^+/Li. As it was seen by cyclic voltammetry, the voltage profiles also confirmed the increase in the redox voltage of polyimides when the conjugation of the active groups was extended. Regarding the capacity of the cells, a high active mass utilization over 90 % was observed for the three samples; although a slight decrease can be noted when increasing the conjugation.

Stability of the cells was studied over 100 cycles. Pyromellitic-PEO2000

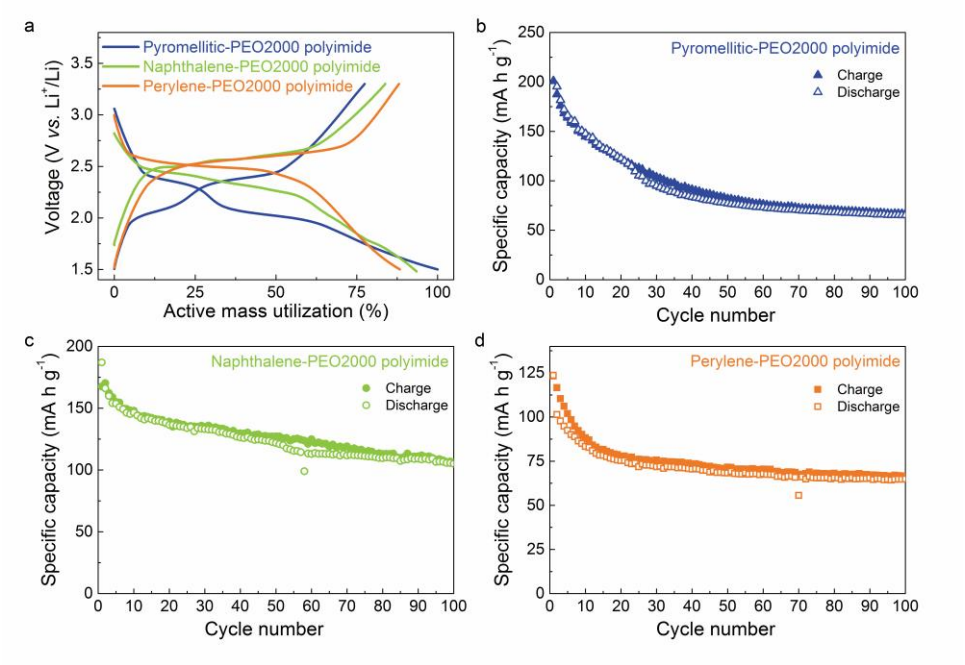

Figure 3.10. (a) Voltage profile of Pyromellitic-PEO2000 (blue), Naphthalene-PEO2000 (green) and Perylene-PEO2000 (orange) polyimides at C/10. Cycling stability, charge (filled symbols)-discharge (empty symbols), at C/10 between 1 and 1.5 V *vs.* Li^+/Li of (b) Pyromellitic-PEO2000 (blue triangles), (c) Naphthalene-PEO2000 (green circles) and (d) Perylene-PEO2000 (orange squares) polyimides.

polyimide showed a sharp capacity fade in the first 40 cycles leading to a 25 % capacity retention after 100 cycles (Figure 3.10b). Slight dissolution of the active material in the electrolyte could explain this surprising result. However, in the case of Naphthalene-PEO2000 polyimide (Figure 3.10c), despite the continuous capacity fade with the increasing number of cycles, the polyimide is able to retain a capacity of 105 mA h g^{-1} (56 % capacity retention) after 100 cycles. In contrast, Perylene-PEO2000 polyimide exhibited a rapid capacity decay in the first 10 cycles, but was able to deliver a stable capacity afterwards (Figure 3.10d). Additionally, the three polyimides featured high coulombic efficiencies, close to 100 %, meaning very similar charge-discharge capacities were obtained during cycling. Although other groups have reported the use of polyimides in lithium batteries with capacity retentions higher than 66 %,[6,7,23] usually arduous electrode preparation methods are required, whereas that is avoided with the use of polyimide-polyether copolymers.

Rate performance of the cells was investigated by increasing the C-rate gradually from C/5 to 2C (Figure 3.11a). Naphthalene-PEO2000 polyimide was able to retain 50 % of the theoretical capacity at 1C and 37 % at 2C. In contrast, Perylene-PEO2000 polyimide featured better rate performance with 60 % and

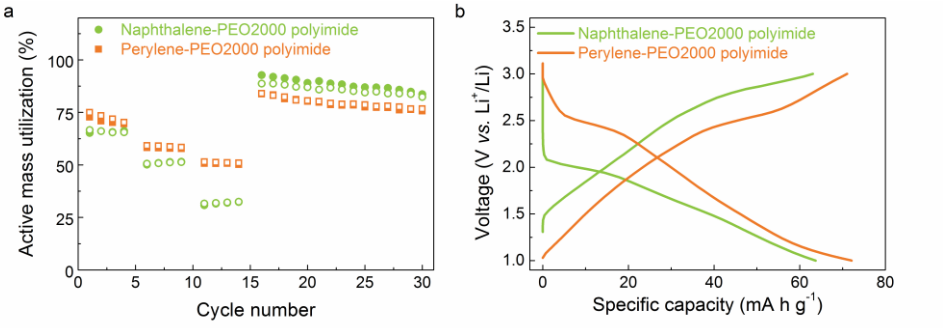

Figure 3.11. (a) Rate capability, charge (filled symbols)-discharge (empty symbols) and (b) voltage profiles at 2C for Naphthalene-PEO2000 (green circles/line) and Perylene-PEO2000 (orange squares/line) polyimides between 1 and 3 V *vs.* Li^+/Li.

50 % capacity retention at 1C and 2C, respectively. In contrast, higher capacity recovery was observed for Naphthalene polyimide in comparison with the analogous Perylene polyimide. Looking at the voltage profiles in Figure 3.11b, corresponding to a high current of 2C, a deep decrease in the discharge voltage and an increase in the charge voltage (high polarization) was only noticeable for Naphthalene-PEO2000 polyimide. Nevertheless, it has been reported in literature that rate capability of active materials and in particular of polyimides, can be improved by the application of functionalized graphene sheets[24] or carbon nanotubes.[9,10]

3.5. Effect of the PEO length on the cell performance

Poly(ethylene oxide) is a widely known polymer in the electrochemical research area, mainly due to its ability to solvate ions facilitating the ionic mobility.[3,25,26] Although polyether chains do not possess electrochemical activity, they may contribute to the overall cell performance Therefore, Naphthalene polyimides bearing PEO with three different chain lengths (PEO600, PEO900 and PEO2000) were synthesized and investigated in lithium batteries.

Cycling stability of the three different samples is presented in Figure 3.12. Initial discharge capacity of Naphthalene-PEO600 polyimide was 126 mA h g^{-1} corresponding to a low active mass utilization (63 %). Nevertheless, an increase in the initial discharge capacity was observed when lengthening the PEO chain, from 149 mA h g^{-1} for Naphthalene-PEO900 polyimide to 196 mA h g^{-1} for the corresponding polyimide with PEO2000 (Table 3.3 summarizes these results). The solvating effect of the ether chains could help the mobility of the lithium ions towards the imide moieties making them more accessible and facilitating its redox reaction. Despite this big difference in the active mass utilization of the three samples, all of them showed good stability with capacity retentions around

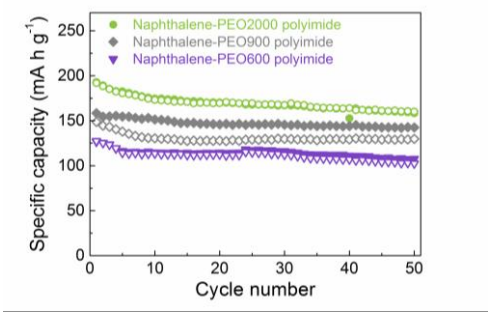

Figure 3.12. Cycling stability, charge (empty symbols)-discharge (filled symbols) of Naphthalene-PEO600 (purple inverse triangles), Naphthalene-PEO900 (grey rhombi) and Naphthalene-PEO2000 (green circles) polyimides at C/10 between 1 and 3 V *vs.* Li^+/Li.

85 % at the 50th cycle, corresponding to 105 mA h g^{-1}, 130 mA h g^{-1}, and 162 mA h g^{-1} discharge capacities for PEO600, PEO900 and PEO2000 Naphthalene-based polyimides, respectively. Surprisingly, coulombic efficiency of Naphthalene-PEO900 polyimide was lower than in the case of the other samples.

Furthermore, for practical applications the specific capacity of the overall electrode instead of the active material should be mentioned. Here, is where the length of the PEO plays an important role. As it could be expected, the overall cell capacity was lower when longer PEO chains were used. The discharge

Table 3.3. Initial specific capacities of Naphthalene polyimides with different PEO lengths considering the mass of the Naphthalene, the polymer and the whole electrode.

Entry	Polyimide	Initial specific capacity (mA h g^{-1})		
		(Naphthalene)	(Polymer)	(Electrode)
1	Naphthalene-PEO600	126	40	34
2	Naphthalene-PEO900	149	34	29
3	Naphthalene-PEO2000	196	23	19.5

capacities of the polyimide-polyether/KB electrodes varied from 20 mA h g^{-1} for Naphthalene-PEO2000 polyimide to 34 mA h g^{-1} for the corresponding PEO600-based polyimide (Table 3.3). As important as this result might be, it is not a commonly reported value in literature.

3.6. Conclusions

Polyimide-polyether copolymers combined the intrinsic properties of both materials, redox activity of imide moieties as well as solubility and ionic conductivity of polyether blocks. The copolymers showed by AFM a microphase separation morphology composed of rigid segments coming from the imide groups separated from soft polyether regions.

Solubility of the polyimide-polyether copolymers in acetonitrile and their film forming properties facilitated the electrode preparation, avoided the use of toxic and high boiling point solvents and permitted the removal of binder from the electrode composition.

Perylene-PEO2000 polyimide showed the highest discharge voltage followed by Naphthalene-PEO2000 and Pyromellitic-PEO2000 polyimides due to the higher conjugation of the imide moieties. Although Naphthalene-PEO2000 featured the highest active mass utilization, Perylene-PEO2000 presented better cycling stability over 100 cycles. On the other hand, Pyromellitic-PEO2000 suffered a rapid capacity fade upon cycling. Among the different PEO lengths, an increase in the molecular weight from 600 to 900 to 2000 g mol^{-1}, resulted in higher accessibility of the redox-active imide moieties and therefore higher capacity values.

Altogether polyimide-polyether combination strategy offers several advantages to engineer polyimide electrodes in batteries. Some of them are the facile solvent-based electrode processing due to the solubility of the copolymers, the withdrawal of high boiling point and toxic solvents, as well as the manufacture of high performance electrodes without the use of additional binders.

3.7. Experimental part

3.7.1. Materials

Pyromellitic dianhydride (PMDA) (97%), 1,4,5,8-naphthalenetetracarboxylic dianhydride (NTDA) (≥95%) and Perylene-3,4,9,10-tetracarboxylic dianhydride (PLDA) (97%) were obtained from Sigma-Aldrich and used as received. O,O'-Bis(2-aminopropyl)polyethylene glycol, with central PEO sequences of 500, 800 and 1900 molecular weights (Jeffamine® ED-600, ED-900 and ED-2003, respectively) were purchased also from Sigma-Aldrich and used as received.

Anhydrous *N,N*-dimethylacetamide (DMAc), anhydrous toluene, diethyl ether, dichloromethane, anhydrous acetonitrile and anhydrous 2-methyltetrahydrofuran (MeTHF) were purchased from Sigma-Aldrich and used as received. Lithium bis(trifluoromethanesulfonyl)imide (LiTFSI) was purchased from Solvionic®.

3.7.2. Polymer synthesis

Polyimides were synthesized by a simple polycondensation reaction from equimolar amounts of dianhydrides and diamines. PEO based diamines (5 mmol) were dissolved in anhydrous *N,N*-dimethylacetamide in a 100 mL three-necked flask blanketed with nitrogen. Afterwards, stoichiometric amount of dianhydride (5 mmol) was added and stirred overnight at room temperature. Azeotropic imidization was carried out at 130 °C using toluene as an azeotrope (Dean Stark)

to remove water generated from the polycondensation reaction. Polymers were obtained by precipitation of the reaction mixture into diethyl ether. Polyimides were dried under vacuum at 100 °C obtaining around 70 % yield.

3.7.3. Polymer characterization

^{1}H NMR measurement was carried out using deuterated dymethylsulfoxide (DMSO-d_6) on a Bruker Avance 500 (500 MHz) spectrometer. Attenuated Total Reflectance Fourier Transform Infrared Spectroscopy (ATR-FTIR) measurements were conducted on a Bruker ALPHA Spectrometer. Gel permeation chromatography (GPC) analysis was performed on a Shimadzu LC-20AD pump with an UV-visible detector (Waters 2410 differential refractometer), with Styragel HR series of columns (HR-6-HR-HR2). Tetrahydrofuran (THF) was used as eluent with a flow rate of 1 mL min^{-1} at 35 °C. Calibration relative to polystyrene standards was used to calculate molecular weights and dispersity.

Differential Scanning Calorimetry (DSC) measurements were carried out on a DSC Q2000 from TA Instruments in order to determine glass transition temperatures (T_g) and melting temperatures (T_m). Samples were heated to 100 °C, quenched to -80 °C and heated again to 100 °C, at a heating rate of 10 °C min^{-1}. Thermal stability of the samples was investigated with a thermogravimetric analysis (TGA) performed on a TGA Q500 from TA Instruments. Measurements were carried out by heating the sample at 10 °C min^{-1} under nitrogen atmosphere from room temperature to 700 °C.

Morphology of the samples was studied in collaboration with Raphaël Coste and Dr. Laurent Rubatat from the University of Pau (France), using Atomic Force Microscopy (AFM). The AFM used in this study was a Bruker Multimode VIII AFM used in PeakForce mode at 2 kHz. The cantilevers mounted were SCANASYST with a nominal spring constant of 0.4 N m^{-1} provided by Bruker probe. Since no cantilever calibration was initially performed, the z-scales on the elastic modulus

and adhesion images are purely qualitative (displayed in arbitrary units or in V).

3.7.4. Electrochemical characterization

Cathodes were prepared by dissolving polyimide-polyether copolymers in acetonitrile and then Ketjenblack (KB) (Ketjenblack® EC-600JD, AzkoNobel) was dispersed in that solution. The obtained slurries were casted on aluminum foil using the doctor blade technique, dried under vacuum at 100 °C and punched into 12 mm diameter discs with a material loading of *ca.* 5 mg. Final composition of the electrodes was 85 wt% polyimide-polyether as active material and binder and 15 wt% KB.

Morphology and conductivity of electrodes were studied with the Bruker Multimode VIII AFM under the PeakForce TUNA mode, at 2 kHz. This mode allows mapping of mechanical and conductivity properties of the samples at the nanometer length scale. The SCM-PIT conductive cantilevers, with a nominal spring constant ranging from 1 to 5 N m^{-1}, provided by Bruker probe were mounted. The peak current signal was measured in pA with DC sample bias of 1 V.

Coin cells (CR2032) were assembled in an argon-filled glove box. Lithium foil (Rockwood lithium) used as anode electrode was separated from the cathode by glass fiber (Glass fiber GFD/55, Whatman) imbibed with 1 M LiTFSI in 2-methyltetrahydrofuran (MeTHF). This electrolyte mixture exhibited the best performance among others due to the partial solubility of the copolymers in common organic solvents.

Cyclic voltammetry (CV) measurements were carried out on a VMP3 (Biologic®) electrochemical workstation at 20 °C. Scan rates of 1 mV s^{-1} were used between 1 and 3.3 V *vs.* Li^+/Li.

Galvanostatic charge-discharge experiments were conducted on a MACCOR® battery tester at 20 °C. The specific voltage range and C-rate used in each experiment is included in the corresponding figure caption.

3.8. References

(1) Viehbeck, A.; Goldberg, M. J.; Kovac, C. A. Electrochemical properties of polyimides and related imide compounds. *J. Electrochem. Soc.* **1990**, *137,* 1460-1466.

(2) Mazur, S.; Lugg, P. S.; Yarnitzky, C. Electrochemistry of aromatic polyimides. *J. Electrochem. Soc.* **1987**, *134,* 346-353.

(3) Michot, C.; Baril, D.; Armand, M. Polyimide polyether mixed conductors as switchable materials for electrochromic devices. *Sol. Energy Mater. Sol. Cells* **1995**, *39,* 289-299.

(4) Oyaizu, K.; Hatemata, A.; Choi, W.; Nishide, H. Redox-active polyimide/carbon nanocomposite electrodes for reversible charge storage at negative potentials: expanding the functional horizon of polyimides. *J. Mater. Chem.* **2010**, *20,* 5404-5410.

(5) Chen, C.; Zhao, X.; Li, H.-B.; Gan, F.; Zhang, J.; Dong, J.; Zhang, Q. Naphthalene-based polyimide derivatives as organic electrode materials for lithium-ion batteries. *Electrochim. Acta* **2017**, *229,* 387-395.

(6) Sharma, P.; Damien, D.; Nagarajan, K.; Shaijumon, M. M.; Hariharan, M. Perylene-polyimide-based organic electrode materials for rechargeable lithium batteries. *J. Phys. Chem. Lett.* **2013**, *4,* 3192-3197.

(7) Song, Z.; Zhan, H.; Zhou, Y. Polyimides: Promising energy-storage materials. *Angew. Chem. Int. Ed.* **2010**, *49,* 8444-8448.

(8) Meng, Y.; Wu, H.; Zhang, Y.; Wei, Z. A flexible electrode based on a three-dimensional graphene network-supported polyimide for lithium-ion batteries. *J. Mater. Chem. A* **2014**, *2,* 10842-10846.

(9) Wu, H.; Shevlin, S. A.; Meng, Q.; Guo, W.; Meng, Y.; Lu, K.; Wei, Z.; Guo, Z. Flexible and binder-free organic cathode for high-performance lithium-ion batteries. *Adv. Mater.* **2014**, *26,* 3338-3343.

(10) Wu, H.; Wang, K.; Meng, Y.; Lu, K.; Wei, Z. An organic cathode material based on a polyimide/CNT nanocomposite for lithium ion batteries. *J. Mater. Chem. A* **2013**, *1,* 6366-6372.

(11) Wu, H. P.; Yang, Q.; Meng, Q. H.; Ahmad, A.; Zhang, M.; Zhu, L. Y.; Liu, Y. G.; Wei, Z. X. A polyimide derivative containing different carbonyl groups for flexible lithium ion batteries. *J. Mater. Chem. A* **2016**, *4,* 2115-2121.

(12) Aldalur, I.; Zhang, H.; Piszcz, M.; Oteo, U.; Rodriguez-Martinez, L. M.; Shanmukaraj, D.; Rojo, T.; Armand, M. Jeffamine® based polymers as highly conductive polymer electrolytes and cathode binder materials for battery application. *J. Power Sources* **2017**, *347,* 37-46.

(13) Zhang, H.; Liu, C.; Zheng, L.; Xu, F.; Feng, W.; Li, H.; Huang, X.; Armand, M.; Nie, J.; Zhou, Z. Lithium bis(fluorosulfonyl)imide/poly(ethylene oxide) polymer electrolyte. *Electrochim. Acta* **2014**, *133,* 529-538.

(14) Xue, Z.; He, D.; Xie, X. Poly(ethylene oxide)-based electrolytes for lithium-ion batteries. *J. Mater. Chem. A* **2015**, *3,* 19218-19253.

(15) Tsao, C.-H.; Hsu, C.-H.; Kuo, P.-L. Ionic conducting and surface active binder of poly(ethylene oxide)-block-poly(acrylonitrile) for high power lithium-ion battery. *Electrochim. Acta* **2016**, *196,* 41-47.

(16) Bouchet, R.; Maria, S.; Meziane, R.; Aboulaich, A.; Lienafa, L.; Bonnet, J.-P.; Phan, T. N. T.; Bertin, D.; Gigmes, D.; Devaux, D.; Denoyel, R.; Armand, M. Single-ion BAB triblock copolymers as highly efficient electrolytes for lithium-metal batteries. *Nat. Mater.* **2013**, *12,* 452-457.

(17) Carretero, P.; Molina, S.; Sandín, R.; Rodríguez-Hernández, J.; Lozano, A. E.; Abajo, J. d. Hydrophilic polyisophthalamides containing poly(ethylene oxide) side chains: Synthesis, characterization, and physical properties. *J. Polym. Sci., Part A: Polym. Chem.* **2013**, *51,* 963-976.

(18) Martínez-Gómez, A.; Alvarez, C.; de Abajo, J.; del Campo, A.; Cortajarena, A. L.; Rodriguez-Hernandez, J. Poly(ethylene oxide) functionalized polyimide-based microporous films to prevent bacterial adhesion. *ACS Appl. Mater. Interfaces* **2015**, *7,* 9716-9724.

(19) Tena, A.; Marcos-Fernández, A.; Palacio, L.; Cuadrado, P.; Prádanos, P.; de Abajo, J.; Lozano, A. E.; Hernández, A. Phase segregation and gas separation properties of thermally treated copoly(ether-imide) from an aromatic dianhydride, an aromatic diamine, and various aliphatic diamines. *Ind. Eng. Chem. Res.* **2012**, *51,* 3766-3775.

(20) Maya, E. M.; Muñoz, D. M.; Lozano, A. E.; de Abajo, J.; de la Campa, J. G. Fluorenyl cardo copolyimides containing poly(ethylene oxide) segments: Synthesis, characterization, and evaluation of properties. *J. Polym. Sci., Part A: Polym. Chem.* **2008**, *46,* 8170-8178.

(21) Djurado, D.; Curtet, J. P.; Bée, M.; Michot, C.; Armand, M. Systematic study of the structure of alternate pyromellitimide–PEO copolymers: Influence of the chain flexibility. *Electrochim. Acta* **2007**, *53,* 1497-1502.

(22) Liang, Y.; Zhang, P.; Chen, J. Function-oriented design of conjugated carbonyl compound electrodes for high energy lithium batteries. *Chem. Sci.* **2013**, *4,* 1330-1337.

(23) Tian, D.; Zhang, H.-Z.; Zhang, D.-S.; Chang, Z.; Han, J.; Gao, X.-P.; Bu, X.-H. Li-ion storage and gas adsorption properties of porous polyimides (PIs). *RSC Adv.* **2014**, *4,* 7506-7510.

(24) Song, Z.; Xu, T.; Gordin, M. L.; Jiang, Y.-B.; Bae, I.-T.; Xiao, Q.; Zhan, H.; Liu, J.; Wang, D. Polymer–graphene nanocomposites as ultrafast-charge and -discharge cathodes for rechargeable lithium batteries. *Nano Lett.* **2012**, *12,* 2205-2211.

(25) Wright, P. V. Electrical conductivity in ionic complexes of poly(ethylene oxide). *Br. Polym. J.* **1975**, *7,* 319-327.

(26) Wright, P. V. Ionic conductivity and organisation of macromolecular polyether-alkali-metal salt complexes. *J. Mater. Chem.* **1995**, *5,* 1275-1283.

CHAPTER 4.

POLYIMIDE-POLYETHER REDOX-ACTIVE BINDERS FOR LITHIUM-SULFUR BATTERIES

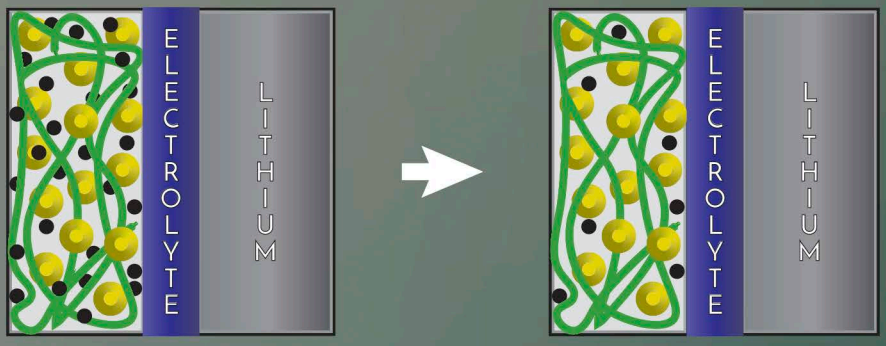

Chapter 4. Polyimide-polyether redox-active binders for lithium-sulfur batteries

4.1. Introduction

In the current search for alternative, sustainable, low cost and clean energy storage systems, lithium-sulfur batteries are an emerging technology able to achieve those demands. Sulfur is an abundant, low cost and environmentally benign element, featuring a high theoretical specific capacity (1675 mA h g^{-1}) and specific energy (2500 W h kg^{-1}).[1-4]

Lithium-sulfur cell consists of a lithium metal anode, an organic electrolyte and a sulfur composite cathode (Figure 4.1a). Because sulfur is in the charged state, the cell operation starts with discharge. Sulfur is reduced at the cathode on

discharge to form various polysulfides that combine with Li to ultimately produce Li_2S.[5] During an ideal discharge process, Octasulfur (*cyclo*-S_8, the most stable allotrope of sulfur at room temperature) is reduced, opening its structure and resulting in the formation of high-order lithium polysulfides Li_2S_x ($6 < x \leq 8$). As the discharge continues, lower order polysulfides Li_2S_x ($2 < x \leq 6$) are formed with the incorporation of additional lithium. At the end of discharge, lithium sulfide Li_2S is formed. These reduction reactions occur in two discharge plateaus at 2.3 and 2.1 V *vs.* Li^+/Li with ether-based liquid electrolyte, as shown in Figure 4.1b. During the following charge, Li_2S is converted to S_8 *via* the formation of the intermediate lithium polysulfides, resulting in a reversible cycle. However, the two charge voltage plateaus are normally overlapped with each other.[3]

Although lithium-sulfur cells are promising devices with greater energy storage and cycle life than conventional Li-ion cells, they have not reached mass commercialization. Several problems inherent in the cell chemistry still remain unsolved. Among such problems are (i) poor electrode rechargeability and limited rate capability owing to the insulating nature of sulfur and the solid reduction products (Li_2S and Li_2S_2); (ii) fast capacity fade due to the generation of soluble polysulfide intermediates, which give rise to a shuttle mechanism; and (iii) a poorly controlled Li/electrolyte interface.[5]

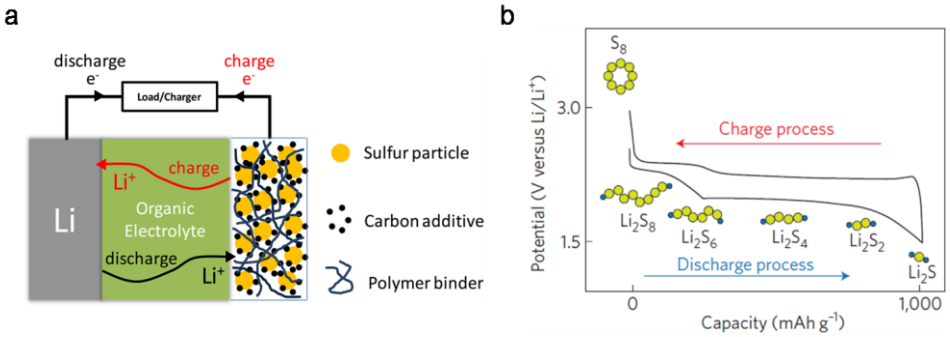

Figure 4.1. (a) Schematic diagram of a lithium-sulfur cell with its charge-discharge operations.[3] (b) Voltage profiles of a lithium-sulfur cell.[5]

During the past decade, substantial progress has been made to mitigate the negative impact of at least some of the problems aforementioned. Research has been mostly focused on developing different ways to avoid the shuttle effect, to increase the conductivity of sulfur cathodes and to accommodate the volume changes of the active material during cycling. The shuttle mechanism results from the dissolution of polysulfides generated at the cathode which are transported back and forth to the anode, reducing the coulombic efficiency and involving the loss of active material. Several strategies have been investigated to avoid this problem; for example, the addition of a porous polysulfide reservoir matrix,[6,7] polymer coatings,[8,9] interlayers[10-12] and surface-coated separators.[13-15] Regarding the insulating behavior of sulfur, incorporation of sulfur into a conductive matrix (*e.g.*, carbon,[8,16,17] polymer[18-20] or metal[21,22]) has been widely studied. However, those additives hinder the fabrication of the cathode as well as they decrease the effective energy density of the battery.[4]

Another electrode additive without energy contribution to the battery is the binder. The main purpose of the binder is to stabilize the electrode, to accommodate the volume changes occurring during the redox reactions and to ensure a good electrical and physical contact between all the components and the current collector. Conventional binders such as polytetrafluoroethylene (PTFE) or poly(vinylidene fluoride) (PVDF) are stable and compatible materials with sulfur electrodes, but they are unable to provide any other advantage.[4] Therefore, alternative binders that can contribute towards improving the battery performance or making the electrode preparation more sustainable are under study. Some examples are poly(ethylene oxide) (PEO),[9,23] poly(vinylpyrrolidone) (PVP),[24] poly(acrylamide-*co*-diallyldimethylammonium chloride) (AMAC),[25] gelatin[26] and carboxymethylcellulose:styrenebutadiene rubber (CMC:SBR).[27] Among them, the most studied one is the first one, PEO. Several groups have demonstrated its ability to increase the specific capacity, reduce the polarization, improve the capacity retention and provide high reaction kinetics.[8,9,23,28]

Recently, a novel approach to enhance the sulfur utilization in the cathode has been reported consisting in the addition of redox-active binders or additives.[29,30] Those materials, based on imide groups, have been studied as redox mediators for the sulfur reactions because both share the same potential range.[30-32] Redox mediators are reversible redox couples able to facilitate the electrochemical reaction of the active material enhancing its utilization and reducing the polarization.[33-36] Furthermore, it has been reported that the strong interaction of the oxygen in the carbonyl groups of the imides (N–C=O groups) with elemental sulfur and lithium sulfides increases the utilization of sulfur and favors the suppression of the shuttle effect.[23-24,29] For these reasons, Gu P.-Y and Zhao Y. *et al.*[29] have studied four different polyimides as hosting matrixes for sulfur cathodes. In comparison with pristine sulfur, they reported a better performance of the cathodes containing redox-active polyimides showing a capacity of 574 mA h g^{-1} at 300 mA g^{-1} (C/5.6) at the 450th cycle. They claimed the high utilization of sulfur is ascribed to the formation of chemical bonds between the polymers and sulfur during the synthesis process. Moreover, Frischmann P.D. and Hwa Y. *et al.*[30] have used cathodes composed of sulfur-graphene oxide nanocomposites with carbon black and a mixture of PVDF with a supramolecular redox-active composite binder. Being the latter a perylene bisimide compound acting as redox mediator to improve the high-rate performance of the sulfur batteries as well as reducing the overpotentials. The sulfur cathode containing PVDF/perylene bisimide composite binder featured a specific capacity of 600 mA h g^{-1} at 1675 mA g^{-1} (1C) at the 150th cycle. In both cases, the amount of carbon in the cathode was 20 and 26 wt%, respectively, which is in agreement with the typical weight ratio of sulfur electrodes reported in the literature.

Although the amount of carbon in the electrode plays an important role in the battery performance, it is a bulky and inactive additive that interferes with the overall energy density of the battery. Thus, for practical applications those

additives should be minimized in the cathode composition.[1,2,37] Thus far, not a lot of effort has been made to decrease the amount of carbon additives.

All in all, polyimide-polyether copolymers synthesized in the third chapter were selected as redox-active binders for sulfur cathodes; aiming to achieve a three-in-one strategy: enhancement of sulfur utilization through the redox mediation of the imide groups, improvement in the cathode stability by the polyether blocks and diminishing the amount of carbon additives without compromising the cell performance. Therefore, in this chapter the amount of conductive carbon was diminished from 30 wt% down to 5 wt% by replacing it with the polyimide-polyether redox-active binder. Furthermore, these cathodes were tested in a solid-state cell with a polymer electrolyte to improve safety and to avoid the shuttle effect.

4.2. Electrochemical performance of lithium-sulfur batteries using redox-active binders

Three polyimide-polyether copolymers synthesized in the third chapter were investigated as redox-active binders for sulfur electrodes. The polymers chosen for this study were Pyromellitic-PEO2000 polyimide, Naphthalene-PEO2000 polyimide and Perylene-PEO2000 polyimide, due to their different electrochemical properties. Two reference binders were used for comparison, poly(vinylidene fluoride-*co*-hexafluoropropylene) (PVDF-HFP) and poly(ethylene oxide) (PEO); the first one as the conventional fluoropolymer mainly used in literature and the second one as a more accurate binder to explore the effect of the redox-active imide groups in the polyimide-polyether copolymers under study.

Sulfur electrodes were fabricated with a typical composition of 60 wt% sulfur, 30 wt% Ketjenblack and 10 wt% binder (PVDF-HFP, PEO, Pyromellitic-

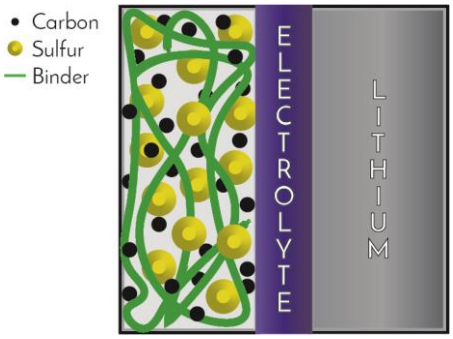

Figure 4.2. Schematic diagram of the lithium-sulfur cell.

PEO2000, Naphthalene-PEO2000 and Perylene-PEO2000 polyimides). A schematic representation of the components in the lithium-sulfur cell studied is depicted in Figure 4.2.

The cell performance of these different cathodes in liquid electrolyte (1M LiTFSI in MeTHF) was evaluated by galvanostatic cycling at C/5 between 1 and 3 V *vs.* Li^+/Li (Figure 4.3). Voltage profiles of the first discharge showed two voltage plateaus for all the cathodes with different binders (Figure 4.3a). Cathode containing PEO binder presented the highest voltage for the first plateau (2.35 V *vs.* Li^+/Li) and the lowest for the second discharge plateau (1.8 V *vs.* Li^+/Li). The cells with the other binders, PVDF-HFP and polyimide-polyether copolymers, featured similar voltage values at discharge, though a slightly higher voltage was observed for the cathode with Naphthalene-PEO2000 polyimide binder (2.26 V and 2.0 V *vs.* Li^+/Li). Furthermore, the sulfur cathode with the latter binder showed the lowest charge voltage, which means lower polarization and higher energy density. Regarding the specific capacity in the first cycle, it was also the cathode containing Naphthalene-PEO2000 polyimide the one with the longest voltage plateaus and highest initial capacity of 1300 mA h g^{-1} (corresponding to 78 % sulfur utilization). It was followed by

Pyromellitic-PEO2000 polyimide (1180 mA h g^{-1}), PVDF-HFP (1160 mA h g^{-1}), Perylene-PEO2000 polyimide (1050 mA h g^{-1}) and PEO (835 mA h g^{-1}). Sulfur cathodes with polyimide-polyether binders showed greater capacity values than pure PEO which could be related to the synergetic effect of imide and PEO groups. Comparison with other reported works is difficult given that electrodes are prepared by different methods and composition. For example, Frischmann *et al.*[30] have reported an initial capacity of 1200 mA h g^{-1} at C/10 using a perylene diimide supramolecular binder and a modified sulfur-graphene oxide nanocomposite. In addition, naphthalene-based polyimides have been reported as hosting matrixes for sulfur cathodes; delivering 1150 mA h g^{-1} initial capacity and 63 % capacity retention after 30 cycles.[29]

Cycling stability of the sulfur cathodes with different binders is shown in Figure 4.3b. All the compositions presented similar capacity retentions, between 63 % and 71 %, after 30 cycles. However, slight differences can be observed for the coulombic efficiency. Sulfur cathode containing PEO binder featured the lowest coulombic efficiency (81 %), requiring greater energy to charge the cell

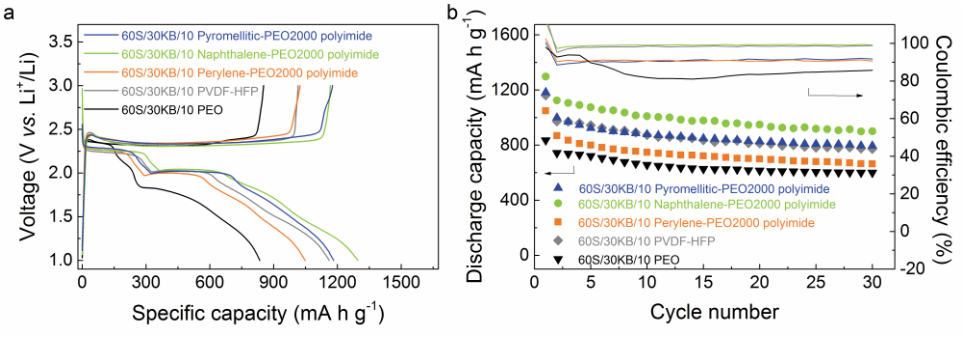

Figure 4.3. (a) Voltage profiles at the first cycle and (b) discharge capacities (left axis) and coulombic efficiency (right axis) of 60S/30KB/10 Pyromellitic-PEO2000 polyimide (blue line/triangles), 60S/30KB/10 Naphthalene-PEO2000 polyimide (green line/circles), 60S30KB/10 Perylene-PEO2000 polyimide (orange line/squares), 60S/30KB/10 PVDF-HFP (grey line/rhombi) and 60S/30KB/10 PEO (black line/inverse triangles) at C/5 using a 1M LiTFSI in MeTHF solution as liquid electrolyte.

than the energy delivered upon discharge. This behavior could be related to the not well defined second voltage plateau observed for this cell. The coulombic efficiency increased when PVDF-HFP and the different polyimide-polyether copolymers were used as binders, approaching 98.5 % for the sulfur cathode comprising Naphthalene-PEO2000 polyimide binder.

Rate capability of sulfur cathodes containing Naphthalene-PEO2000, Perylene-PEO2000 polyimides and PVDF-HFP binders were evaluated at various C-rates from C/5 to 2C (Figure 4.4a). At slow C-rate of C/5, the capacity values have the same trend as in Figure 4.3 where the sulfur cathode with Naphthalene-PEO2000 polyimide binder presented the highest capacity followed by the PVDF-HFP binder and Perylene polyimide. When the C-rate was increased to 2C, discharge capacities of sulfur cathodes with Perylene-PEO2000 polyimide and PVDF-HFP binders decreased rapidly to 110 mA h g^{-1} and 140 mA h g^{-1}, respectively. In contrast, capacity decay of sulfur electrode comprising Naphthalene-PEO2000 polyimide binder was more moderate, delivering a discharge capacity of 260 mA h g^{-1} at 2C corresponding to a 32 % of the initial capacity at C/5. All three cells exhibited very good stability at high currents, as it

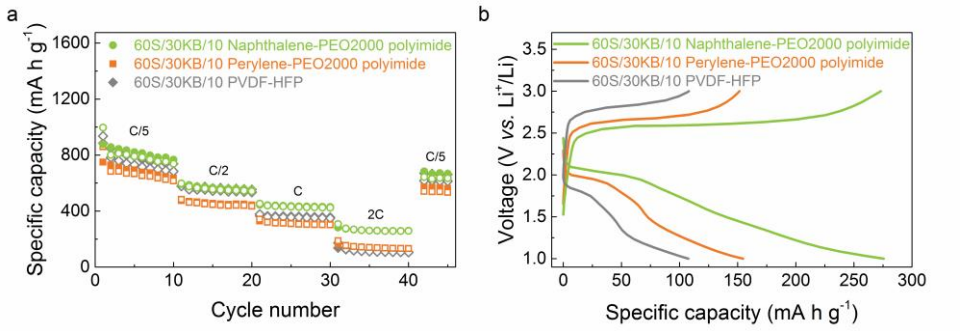

Figure 4.4. (a) Rate capability, charge (filled symbols)-discharge (empty symbols) and (b) voltage profiles at 2C of 60S/30KB/10 Naphthalene-PEO2000 polyimide (green circles/line), 60S30KB/10 Perylene-PEO2000 polyimide (orange squares/line) and 60S/30KB/10 PVDF-HFP (grey rhombi/line), using a 1M LiTFSI in MeTHF solution as liquid electrolyte.

can be seen by the negligible capacity fade during cycling at the same C-rate. Furthermore, the voltage profiles depicted in Figure 4.4b corroborated the better performance of the sulfur cathode with Naphthalene-PEO2000 polyimide binder due to its lower polarization and thus higher energy. These results confirmed the ability of Naphthalene-PEO2000 polyimide binder to act as a redox mediator for lithium-sulfur battery system, providing better results than the reference binder (PVDF-HFP) when cycled at high currents.

4.3. Effect of reducing the amount of carbon content in sulfur cathodes

For practical applications, energy density, in addition to rate capability and safety, is one of the most important characteristics of electrode materials. The incorporation of conductive additives in the cathode not only increases the complexity of this component but also decreases the effective energy density of the cathode significantly.[4,37] Therefore, our aim is to reduce the amount of inactive and bulky carbon in the electrode and to further evaluate the impact on cell performance of redox-active binders in sulfur cathodes. Consequently,

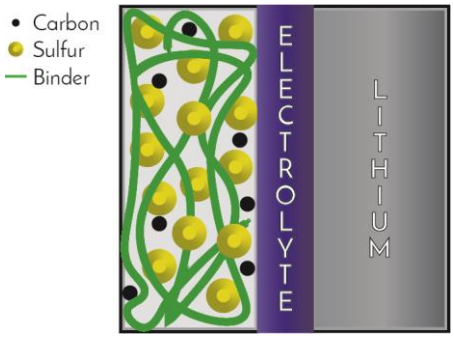

Figure 4.5. Schematic diagram of the lithium-sulfur cell with low amount of carbon.

electrode composition was modified to 45 wt% of sulfur, 5 wt% of Ketjenblack and 50 wt% of binder. In Figure 4.5 the diagram of the lithium-sulfur cell for the new cathode composition with low amount of carbon is represented.

Galvanostatic charge-discharge results at C/5 of sulfur cathodes containing Naphthalene-PEO2000 polyimide and PVDF-HFP reference binder are represented in Figure 4.6. When reducing the amount of carbon in the cathode, the cell containing the PVDF-HFP binder exhibited big polarization with a discharge plateau at 2.0 V *vs.* Li^+/Li and charge plateau at 2.85 V *vs.* Li^+/Li and low sulfur utilization of 450 mA h g^{-1} (grey line in Figure 4.6a). However, the cell with sulfur cathode composed of Naphthalene-PEO2000 polyimide binder was able to improve the cell performance (green line in Figure 4.6a) by reducing polarization and increasing the discharge capacity. This cell featured two discharge plateaus at 2.25 and 1.75 V *vs.* Li^+/Li and a discharge capacity of 550 mA h g^{-1}. Regarding stability of both cells (Figure 4.6b), sulfur cathode with PVDF-HFP binder showed 40 % capacity loss in the first cycle and delivered 185 mA h g^{-1} in the 50th cycle; while sulfur electrode with Naphthalene-PEO2000 binder presented discharge capacity of 388 mA h g^{-1} (70 % capacity retention)

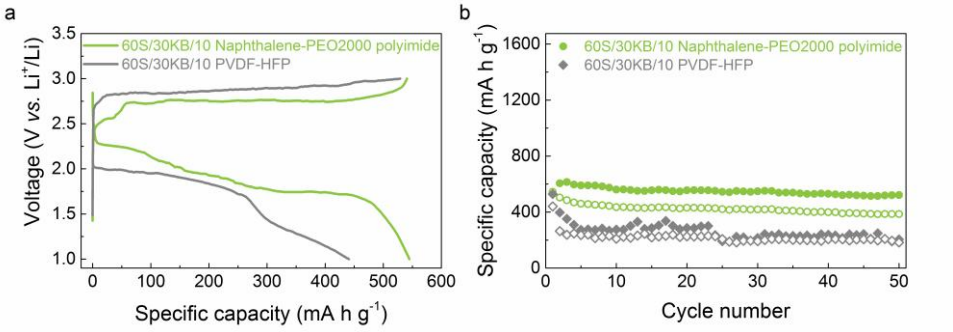

Figure 4.6. (a) Voltage profiles at the first cycle and (b) cycling performances, charge (filled symbols)-discharge (empty symbols) of 45S/5KB/50 Naphthalene-PEO2000 polyimide (green line/circles) and 45S/5KB/50 PVDF-HFP (grey line/rhombi) at C/5 using a 1M LiTFSI in MeTHF solution as liquid electrolyte.

after 50 cycles. These results demonstrated the better performance of the sulfur cathode with redox-active Naphthalene-PEO2000 polyimide and low amount of carbon black in comparison with the reference sulfur cathode containing PVDF-HFP binder. The redox-active polymer binder was able to reduce polarization, increase the sulfur utilization and stabilize the electrode upon cycling.

Regarding cell safety, it can be improved by the removal of the solvents used in liquid electrolytes and the incorporation of solid polymer electrolyte. Furthermore, solid polymer electrolytes are attractive, particularly in lithium-sulfur cells, as they could potentially decrease the extent of active material loss. The polymer used to formulate a solid polymer electrolyte fundamentally must be capable of coordinating Li ions in order to facilitate charge transfer between the cathode and anode. Salts like LiTFSI or LiFSI and PEO polymers are considered to be the best choice.[2,4]

In view of the relatively good electrochemical properties of sulfur cells containing only 5 wt% of carbon black, the next step was to increase the safety and reduce the shuttle effect by using a solid polymer electrolyte. As PEO is a well known polymer electrolyte, not only in Li-S batteries but also in other type of electrochemical energy storage devices,[38-42] it was the polymer of choice for this chapter. An important feature for a good electrochemical performance of the solid-state batteries is the compatibility between the polymer electrolyte and the cathode. Therefore, a mixture of PEO and LiTFSI (12:1, [EO]:[Li]) was used as polymer electrolyte and PEO as the reference binder in the sulfur electrode instead of PVDF-HFP.

The electrochemical behavior of sulfur cathodes with Naphthalene-PEO2000 polyimide and pure PEO binders was investigated using cyclic voltammetry (Figure 4.7). Both cells presented two reduction peaks during the discharge

process at similar potentials, 2.3 and 1.9 V *vs.* Li^+/Li. However, they differ in the position and shape of the oxidation peak during the charge scan. The oxidation potential of the sulfur cathode containing Naphthalene-PEO2000 polyimide binder was lower (2.5 V *vs.* Li^+/Li) than that of PEO binder (2.8 V *vs.* Li^+/Li) indicating the decrease in the polarization of the cell assembled with the redox-active binder. Furthermore, sharper peaks of the cell with the Naphthalene-PEO2000 polyimide binder in contrast with the incomplete and broad peak of the PEO reflected the faster reaction kinetics of the cell with the first binder. Low polarization and high reaction kinetics are two features of a redox mediator, being both accomplished by the redox-active polyimide-polyether copolymer.

The cell performance of the sulfur cathodes containing Naphthalene-PEO2000 polyimide and PEO binders with PEO:LiTFSI (12:1, [EO]:[Li]) as polymer electrolyte was investigated by galvanostatic cycling at C/20 (Figure 4.8). The specific discharge capacity of the sulfur cell comprised of the reference PEO binder decreased from 722 mA h g^{-1} in the first cycle to 232 mA h g^{-1} in the 35th cycle (corresponding to a capacity retention of 32 %). In contrast, the sulfur cathode with Naphthalene- PEO2000 polyimide binder delivered a gradual increase in capacity reaching 333 mA h g^{-1} discharge capacity in the 35th cycle

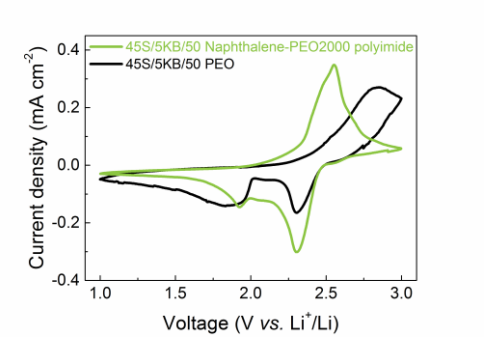

Figure 4.7. Cyclic voltammograms of 45S/5KB/50 Naphthalene-PEO2000 polyimide (green) and 45S/5KB/50 PEO (black) at 0.05 mV s^{-1} using PEO:LiTFSI (12:1, [EO]:[Li]) as polymer electrolyte.

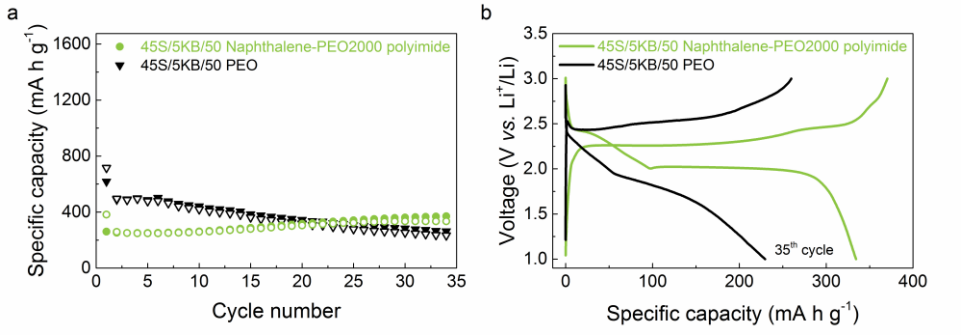

Figure 4.8. (a) Cycling performance charge (filled symbols)-discharge (empty symbols) and (b) voltage profiles at the 35th cycle of 45S/5KB/50 Naphthalene-PEO2000 polyimide (green circles/line) and 45S/5KB/50 PEO (black inverse triangles/line) at C/20 using PEO:LiTFSI (12:1, [EO]:[Li]) as polymer electrolyte.

(Figure 4.8a). This increase in capacity observed over the first 15 cycles might be related with the enhancement of the polymer electrolyte-electrode wetting.[40,43] Furthermore, the cell with sulfur and the redox-active binder featured an improved voltage profile in the 35th cycle (Figure 4.8b) in comparison with the reference cell which showed a dramatic decrease in the voltage plateaus as well as an increase in polarization.

Additionally, galvanostatic charge-discharge experiments at really low C-rate (C/200) were performed on the sulfur cells. Figure 4.9 shows the cycling stability of both sulfur electrodes. On the one hand, sulfur electrode containing PEO reference binder delivered a high initial discharge capacity (830 mA h g^{-1}), however, it was followed by a dramatic capacity fade (293 mA h g^{-1} in the 10th cycle). On the other hand, the cell with sulfur and Naphthalene-PEO2000 polyimide binder featured a better stability over the first 10 cycles, providing 500 mA h g^{-1} discharge capacity corresponding to 83 % capacity retention.

Voltage profiles of the first and tenth cycles provide a better insight into the cell performance (Figure 4.10). While sulfur cathode composed of pure PEO binder

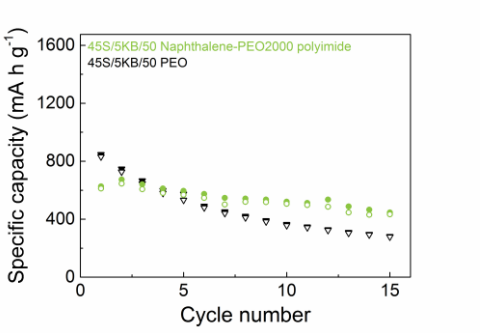

Figure 4.9. Cycling performance, charge (filled symbols)-discharge (empty symbols), of 45S/5KB/50 Naphthalene-PEO2000 polyimide (green circles) and 45S/5KB/50 PEO (black inverse triangles) at C/200 between 1 and 3 V *vs.* Li^+/Li using PEO:LiTFSI (12:1, [EO]:[Li]) as polymer electrolyte.

presented the two characteristic voltages plateaus in the first discharge cycle, the upper voltage was lost and the second one decreased in the 10th cycle (Figure 4.10a). In contrast, sulfur electrode containing Naphthalene-PEO2000 polyimide binder was able to maintain both voltage plateaus in the 10th cycle with only a slight decrease in the capacity (Figure 4.10b).

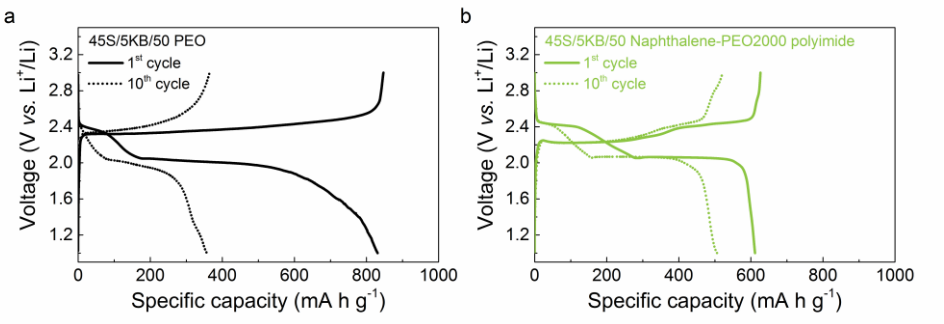

Figure 4.10. Voltage profiles at the 1st cycle (solid line) and the 10th cycle (dotted line) of (a) 45S/5KB/50 PEO (black line) and (b) 45S/5KB/50 Naphthalene-PEO2000 polyimide (green line) at C/200 using PEO:LiTFSI (12:1, [EO]:[Li]) as polymer electrolyte.

4.4. Conclusions

As the redox voltages of polyimides are similar to the ones of sulfur, polyimide-polyether copolymers were proposed as redox-active binders for lithium-sulfur batteries. Among the three polymers investigated varying the conjugation structure of the imides (pyromellitic, naphthalene and perylene), sulfur cathodes containing Naphthalene-PEO2000 polyimide binder showed the best performance in comparison with the other copolymers and the reference binders PVDF-HFP and PEO. The cathode with the electrode composition of 60 wt% sulfur, 30 wt% Ketjenblack and 10% Naphthalene-PEO2000 polyimide cycled in liquid electrolyte showed the best results with an initial capacity of 1300 mA h g^{-1} and 69 % capacity retention after 30 cycles.

Moving towards practical applications where the amount of carbon should be reduced and safety considered, the cathode composition was changed to 45 wt% sulfur, 5 wt% Ketjenblack and 50 wt% of binder and the electrodes were tested using PEO:LiTFSI (12:1, [EO]:[Li]) as polymer electrolyte.

Cyclic voltammetry of the sulfur cathode with Naphthalene-PEO2000 polyimide binder featured lower polarization and higher reaction kinetics than the sulfur electrode with pure PEO binder. Although the specific capacity of the cells decreased due to the low amount of carbon added, the stability of the sulfur cell with Naphthalene-PEO2000 polyimide binder was improved up to 87 % capacity retention.

In this chapter, polyimide-polyether copolymers used as redox-active binders proved the three-in-one strategy: the redox mediating effect which lowered the polarization and increased the sulfur utilization; the higher reaction kinetics as shown with the sharp peaks in the cyclic voltammogram; and the improvement in stability and polarization when the amount of carbon was decreased to 5 wt%.

4.5. Experimental part

4.5.1 Materials

Elemental sulfur (≥99.5 %), poly(ethylene oxide) (PEO) (M_W = 5 x 10^6 g mol^{-1}), *N*-Methyl-2-pyrrolidone (NMP), 2-methyltetrahydrofuran (MeTHF) and acetonitrile (ACN) were purchased from Sigma-Aldrich and used as received. Lithium bis(trifluoromethanesulfonyl)imide (LiTFSI) was purchased from Solvionic®. Poly(vinylidene difluoride-*co*-hexafluoropropylene) (PVDF-HFP, kynar®) was received from Arkema.

4.5.2 Electrode preparation and cell assembly

Two types of sulfur cathodes were prepared with different sulfur/carbon/binder compositions. One of the compositions consisted in mixing 60 wt% of sulfur, 30 wt% of Ketjenblack and 10 wt% of binder while the other one was 45 wt% of sulfur, 5 wt% of Ketjenblack and 50 wt% of binder. The sulfur electrodes were prepared by dissolving the corresponding binder in NMP for PVDF-HFP or acetonitrile for the other binders. Afterwards, sulfur and carbon black were added and mixed by planetary ball milling. The obtained slurry was casted over an aluminum carbon coated foil and dried under vacuum at 70 °C overnight. The films were punched into 13 mm diameter discs with a sulfur loading of 0.8 - 1.0 mg cm^{-2} for the 60/30/10 composition and 1.2 - 1.5 mg cm^{-2} for 45/5/50.

Coin cells (CR2032) were assembled in an argon-filled glove box. Lithium foil (Rockwood lithium) used as anode electrode was separated from the cathode by glass fiber (Glass fiber GFD/55, Whatman) imbibed with 1 M LiTFSI in MeTHF solution. For solid-state batteries PEO:LiTFSI as polymer electrolyte was used. It was prepared by dissolving PEO and LiTFSI (12:1, [EO]:[Li]) in acetonitrile and solvent-casted over a teflon substrate. The membranes were further hot-pressed at 70 °C with a final thickness of 250 µm.

4.5.3 Methods

Cyclic voltammetry (CV) measurements were carried out on a VMP3 (Biologic®) electrochemical workstation. Scan rates of 0.05 mV s^{-1} were used between 1 and 3 V *vs.* Li^+/Li.

Galvanostatic charge-discharge experiments were conducted on a MACCOR® battery tester between 1 and 3 V *vs.* Li^+/Li and the current density was based on the sulfur mass (1C = 1675 mA g^{-1}). Cells with liquid electrolyte were cycled at 20 °C whereas cells with polymer electrolyte were cycled at 70 °C.

4.6. References

(1) Manthiram, A.; Chung, S.-H.; Zu, C. Lithium–Sulfur batteries: progress and prospects. *Adv. Mater.* **2015**, *27,* 1980-2006.

(2) Urbonaite, S.; Poux, T.; Novák, P. Progress towards commercially viable Li–S battery cells. *Adv. Energy Mater.* **2015**, *5,* 1500118.

(3) Manthiram, A.; Fu, Y.; Chung, S.-H.; Zu, C.; Su, Y.-S. Rechargeable lithium–sulfur batteries. *Chem. Rev.* **2014**, *114,* 11751-11787.

(4) Dirlam, P. T.; Glass, R. S.; Char, K.; Pyun, J. The use of polymers in Li-S batteries: A review. *J. Polym. Sci., Part A: Polym. Chem.* **2017**, *55,* 1635-1668.

(5) Bruce, P. G.; Freunberger, S. A.; Hardwick, L. J.; Tarascon, J.-M. Li-O_2 and Li-S batteries with high energy storage. *Nat. Mater.* **2012**, *11,* 19-29.

(6) Wei, S.; Zhang, H.; Huang, Y.; Wang, W.; Xia, Y.; Yu, Z. Pig bone derived hierarchical porous carbon and its enhanced cycling performance of lithium-sulfur batteries. *Energy Environ. Sci.* **2011**, *4,* 736-740.

(7) Ji, X.; Evers, S.; Black, R.; Nazar, L. F. Stabilizing lithium–sulphur cathodes using polysulphide reservoirs. *Nat. Commun.* **2011**, *2,* 325.

(8) Ji, X.; Lee, K. T.; Nazar, L. F. A highly ordered nanostructured carbon-sulphur cathode for lithium-sulphur batteries. *Nat. Mater.* **2009**, *8,* 500-506.

(9) Fu, Y.; Su, Y.-S.; Manthiram, A. Sulfur–carbon nanocomposite cathodes improved by an amphiphilic block copolymer for high-rate lithium–sulfur batteries. *ACS Appl. Mater. Interfaces* **2012**, *4,* 6046-6052.

(10) Ma, G.; Wen, Z.; Jin, J.; Wu, M.; Wu, X.; Zhang, J. Enhanced cycle performance of Li–S battery with a polypyrrole functional interlayer. *J. Power Sources* **2014**, *267,* 542-546.

(11) Su, Y.-S.; Manthiram, A. A new approach to improve cycle performance of rechargeable lithium-sulfur batteries by inserting a free-standing MWCNT interlayer. *Chem. Commun.* **2012**, *48,* 8817-8819.

(12) Zhang, K.; Qin, F.; Fang, J.; Li, Q.; Jia, M.; Lai, Y.; Zhang, Z.; Li, J. Nickel foam as interlayer to improve the performance of lithium–sulfur battery. *J. Solid State Electrochem.* **2014**, *18,* 1025-1029.

(13) Huang, J.-Q.; Zhang, Q.; Peng, H.-J.; Liu, X.-Y.; Qian, W.-Z.; Wei, F. Ionic shield for polysulfides towards highly-stable lithium-sulfur batteries. *Energy Environ. Sci.* **2014**, *7,* 347-353.

(14) Chung, S.-H.; Manthiram, A. A polyethylene glycol-supported microporous carbon coating as a polysulfide trap for utilizing pure sulfur cathodes in lithium–sulfur batteries. *Adv. Mater.* **2014**, *26,* 7352-7357.

(15) Zhang, Z.; Lai, Y.; Zhang, Z.; Zhang, K.; Li, J. Al_2O_3-coated porous separator for enhanced electrochemical performance of lithium sulfur batteries. *Electrochim. Acta* **2014**, *129,* 55-61.

(16) Wang, H.; Yang, Y.; Liang, Y.; Robinson, J. T.; Li, Y.; Jackson, A.; Cui, Y.; Dai, H. Graphene-wrapped sulfur particles as a rechargeable lithium–sulfur battery cathode material with high capacity and cycling stability. *Nano Lett.* **2011**, *11,* 2644-2647.

(17) Jayaprakash, N.; Shen, J.; Moganty, S. S.; Corona, A.; Archer, L. A. Porous hollow carbon@sulfur composites for high-power lithium–sulfur batteries. *Angew. Chem. Int. Ed.* **2011**, *50,* 5904-5908.

(18) Ma, G.; Huang, F.; Wen, Z.; Wang, Q.; Hong, X.; Jin, J.; Wu, X. Enhanced performance of lithium sulfur batteries with conductive polymer modified separators. *J. Mater. Chem. A* **2016**, *4,* 16968-16974.

(19) Xiao, L.; Cao, Y.; Xiao, J.; Schwenzer, B.; Engelhard, M. H.; Saraf, L. V.; Nie, Z.; Exarhos, G. J.; Liu, J. A soft approach to encapsulate sulfur: Polyaniline nanotubes for lithium-sulfur batteries with long cycle life. *Adv. Mater.* **2012**, *24,* 1176-1181.

(20) Li, W.; Zhang, Q.; Zheng, G.; Seh, Z. W.; Yao, H.; Cui, Y. Understanding the role of different conductive polymers in improving the nanostructured sulfur cathode performance. *Nano Lett.* **2013**, *13,* 5534-5540.

(21) Wei Seh, Z.; Li, W.; Cha, J. J.; Zheng, G.; Yang, Y.; McDowell, M. T.; Hsu, P.-C.; Cui, Y. Sulphur–TiO_2 yolk–shell nanoarchitecture with internal void space for long-cycle lithium–sulphur batteries. *Nat. Commun.* **2013**, *4,* 1331.

(22) Pang, Q.; Kundu, D.; Cuisinier, M.; Nazar, L. F. Surface-enhanced redox chemistry of polysulphides on a metallic and polar host for lithium-sulphur batteries. *Nat. Commun.* **2014**, *5,* 4759.

(23) Lacey, M. J.; Jeschull, F.; Edström, K.; Brandell, D. Functional, water-soluble binders for improved capacity and stability of lithium–sulfur batteries. *J. Power Sources* **2014**, *264,* 8-14.

(24) Seh, Z. W.; Zhang, Q.; Li, W.; Zheng, G.; Yao, H.; Cui, Y. Stable cycling of lithium sulfide cathodes through strong affinity with a bifunctional binder. *Chem. Sci.* **2013**, *4,* 3673-3677.

(25) Zhang, S. S. Binder based on polyelectrolyte for high capacity density lithium/sulfur battery. *J. Electrochem. Soc.* **2012**, *159,* A1226-A1229.

(26) Wang, Q.; Wang, W.; Huang, Y.; Wang, F.; Zhang, H.; Yu, Z.; Wang, A.; Yuan, K. Improve rate capability of the sulfur cathode using a gelatin binder. *J. Electrochem. Soc.* **2011**, *158,* A775-A779.

(27) Rao, M.; Song, X.; Liao, H.; Cairns, E. J. Carbon nanofiber–sulfur composite cathode materials with different binders for secondary Li/S cells. *Electrochim. Acta* **2012**, *65,* 228-233.

(28) Lacey, M. J.; Jeschull, F.; Edstrom, K.; Brandell, D. Why PEO as a binder or polymer coating increases capacity in the Li-S system. *Chem. Commun.* **2013**, *49,* 8531-8533.

(29) Gu, P.-Y.; Zhao, Y.; Xie, J.; Binte Ali, N.; Nie, L.; Xu, Z. J.; Zhang, Q. Improving the performance of lithium–sulfur batteries by employing polyimide particles as hosting matrixes. *ACS Appl. Mater. Interfaces* **2016**, *8,* 7464-7470.

(30) Frischmann, P. D.; Hwa, Y.; Cairns, E. J.; Helms, B. A. Redox-active supramolecular polymer binders for lithium–sulfur batteries that adapt their transport properties in operando. *Chem. Mater.* **2016**, *28,* 7414-7421.

(31) Chen, Y.; Freunberger, S. A.; Peng, Z.; Fontaine, O.; Bruce, P. G. Charging a Li–O_2 battery using a redox mediator. *Nat. Chem.* **2013**, *5,* 489-494.

(32) Frischmann, P. D.; Gerber, L. C. H.; Doris, S. E.; Tsai, E. Y.; Fan, F. Y.; Qu, X.; Jain, A.; Persson, K. A.; Chiang, Y.-M.; Helms, B. A. Supramolecular perylene bisimide-polysulfide gel networks as nanostructured redox mediators in dissolved polysulfide lithium–sulfur batteries. *Chem. Mater.* **2015**, *27,* 6765-6770.

(33) Li, J.; Yang, L.; Yang, S.; Lee, J. Y. The application of redox targeting principles to the design of rechargeable Li–S flow batteries. *Adv. Energy Mater.* **2015**, *5,* 1501808.

(34) Gerber, L. C. H.; Frischmann, P. D.; Fan, F. Y.; Doris, S. E.; Qu, X.; Scheuermann, A. M.; Persson, K.; Chiang, Y.-M.; Helms, B. A. Three-Dimensional growth of Li_2S in lithium–sulfur batteries promoted by a redox mediator. *Nano Lett.* **2016**, *16,* 549-554.

(35) Moshurchak, L. M.; Buhrmester, C.; Dahn, J. R. Triphenylamines as a class of redox shuttle molecules for the overcharge protection of lithium-ion cells. *J. Electrochem. Soc.* **2008**, *155,* A129-A131.

(36) Meini, S.; Elazari, R.; Rosenman, A.; Garsuch, A.; Aurbach, D. The use of redox mediators for enhancing utilization of Li_2S cathodes for advanced Li–S battery systems. *J. Phys. Chem. Lett.* **2014**, *5,* 915-918.

(37) Chen, Z.; Dahn, J. R. Reducing carbon in $LiFePO_4$ / C composite electrodes to maximize specific energy, volumetric energy, and tap density. *J. Electrochem. Soc.* **2002**, *149,* A1184-A1189.

(38) Croce, F.; Appetecchi, G. B.; Persi, L.; Scrosati, B. Nanocomposite polymer electrolytes for lithium batteries. *Nature* **1998**, *394,* 456-458.

(39) Marmorstein, D.; Yu, T. H.; Striebel, K. A.; McLarnon, F. R.; Hou, J.; Cairns, E. J. Electrochemical performance of lithium/sulfur cells with three different polymer electrolytes. *J. Power Sources* **2000**, *89,* 219-226.

(40) Aldalur, I.; Zhang, H.; Piszcz, M.; Oteo, U.; Rodriguez-Martinez, L. M.; Shanmukaraj, D.; Rojo, T.; Armand, M. Jeffamine® based polymers as highly conductive polymer electrolytes and cathode binder materials for battery application. *J. Power Sources* **2017**, *347,* 37-46.

(41) Porcarelli, L.; Shaplov, A. S.; Bella, F.; Nair, J. R.; Mecerreyes, D.; Gerbaldi, C. Single-ion conducting polymer electrolytes for lithium metal polymer batteries that operate at ambient temperature. *ACS Energy Lett.* **2016**, *1,* 678-682.

(42) Zhang, Y.; Zhao, Y.; Gosselink, D.; Chen, P. Synthesis of poly(ethylene-oxide)/nanoclay solid polymer electrolyte for all solid-state lithium/sulfur battery. *Ionics* **2015**, *21,* 381-385.

(43) Carbone, L.; Hassoun, J. A low-cost, high-energy polymer lithium-sulfur cell using a composite electrode and polyethylene oxide (PEO) electrolyte. *Ionics* **2016**, *22,* 2341-2346.

CHAPTER 5.

HIGH POWER DENSITY POLYIMIDE-POLYETHER ANODES FOR SODIUM AQUEOUS BATTERIES

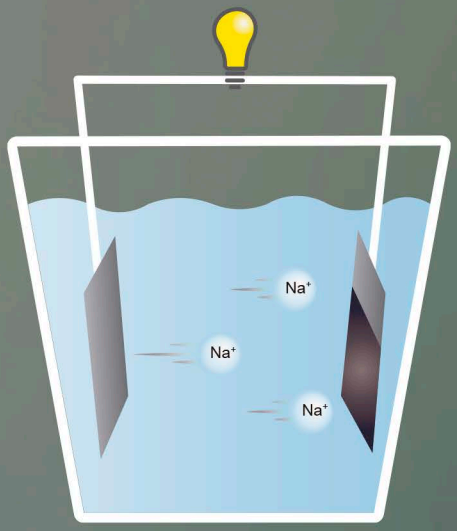

Chapter 5. High power density polyimide-polyether anodes for sodium aqueous batteries

5.1. Introduction

Energy storage devices are a key component of numerous emerging and existing technologies ranging from electric vehicles to wearable electronics.[1,2] In addition to high energy density, novel energy storage devices should fulfill other demands such as power density, safety, low-cost and environmental friendliness.[3,4] Aqueous sodium-ion batteries offer the potential to meet the above requirements since sodium is a non-toxic, low cost and abundant element and aqueous electrolytes are inherently safer and more environmentally friendly when compared to their organic counterparts which are often flammable and toxic.[5-8]

One of the challenges in developing batteries based on aqueous electrolytes is the scarce availability of electrode materials with a redox reaction within the oxygen and hydrogen evolution potentials.[9] Significant progress has been achieved in developing cathode materials for aqueous sodium-ion battery electrodes.[10-12] However, advancement in the anode side with stable electrochemical performance is still a challenge.[9,13] Amongst the inorganic anode materials reported, Sodium Super Ionic Conductor (NASICON-type), $NaTi_2(PO_4)_3$, demonstrated high specific capacity of 123 mA h g^{-1} for 30 electrochemical cycles.[14] Prussian blue analogues with stability for up to 1000 electrochemical cycles were also reported although in highly saturated electrolytes.[15] Nevertheless, such inorganic materials based on transition metals may suffer structural changes during the redox processes resulting in capacity fade while cycling. Besides, their high cost and scarcity introduce additional challenges for their widespread utilization.[16,17]

The aforementioned limitations can be addressed by the investigation of new classes of battery electrodes based on organic/polymeric materials.[18] Redox polymers offer versatile properties that can be tuned with the chemical structure. In addition, they are abundant, environmentally friendly and they can readily accommodate ions, not only lithium but also sodium, magnesium or aluminum.[18-21] In spite of the large number of polymer electrode materials investigated up to date, only few exhibited electrochemical activity as anode materials in aqueous sodium electrolytes. One example is poly(2-vinylanthraquinone) which was utilized as an anode material in an aqueous polymer/air battery with high specific capacity of 217 mA h g^{-1} for 300 cycles in basic media at a current density of 22C.[13] Other examples are naphthalene-based polyimides which are able to cycle in neutral media. The highest current density used to cycle these materials was 20C showing a specific capacity of 95 mA h g^{-1}.[17,22,23]

The conjugated chemical structure of redox-active polyimides stabilizes the reduced species resulting in fast redox kinetics of the polymer.[24] It has been reported and studied along this thesis that increasing the conjugation (from pyromellitic, naphthalene to perylene polyimides) improves the redox properties of the polymer.[21,25,26] Furthermore, the incorporation of polyether segments to polyimides not only improved their tractability but also promoted ion mobility making ions more accessible to the redox-active imide groups.[25-29] Therefore, polyimide-polyether copolymers might be promising candidates as anode materials for high-rate aqueous sodium-ion batteries. Up to date, only naphthalene-based polyimides have been investigated for this system, however, their performance at high current densities was not studied.

In this chapter, naphthalene as well as perylene polyimides bearing PEO units of 2000 g mol^{-1} were investigated and compared as anode materials for aqueous sodium batteries. Electrochemical performance and kinetics of both polymers was investigated. Furthermore, rate performance and cycling stability at high current densities of Perylene-PEO2000 polyimide were studied.

5.2. Electrochemical characterization of polyimides

The electrochemical properties of Naphthalene-PEO2000 and Perylene-PEO2000 polyimides were investigated by cyclic voltammetry in a three-electrode cell with 1M Na_2SO_4 aqueous electrolyte (Figure 5.1). The slurries containing 85 wt% of polymer and 15 wt% of carbon Ketjenblack were deposited on a platinum electrode with an active surface area of 1 cm^2. Platinum was also used as counter electrode and the reference electrode was Ag/AgCl.

Cyclic voltammogram of Naphthalene-PEO2000 polyimide (Figure 5.2a) showed two reversible reduction/oxidation peaks at -0.41/-0.3 V and -0.66/-0.61 V

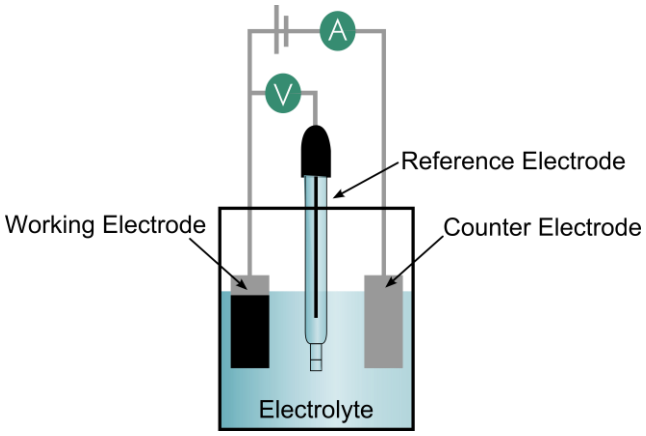

Figure 5.1. Schematic representation of a three electrode cell.

vs. Ag/AgCl. Each redox peak corresponded to one-electron reaction leading to a two-step reaction following the mechanism depicted on the right side of Figure 5.2a. In the first step one electron is gained forming a radical anion, followed by another electron generating a dianion specie. In contrast, Perylene-PEO2000 featured only one redox peak at -0.56/-0.51 V *vs.* Ag/AgCl (Figure 5.2b). This change in the redox mechanism, from one-electron two-step reaction for Naphthalene-PEO2000 polyimide to two-electron one-step reaction for Perylene-PEO2000 polyimide can be explained by the high delocalization of the perylene moieties which favors the fast transformation between the radical anion and dianion species resulting in one broader peak involving two electrons.[24,26]

The kinetics of the redox reactions for both polymers was investigated using cyclic voltammetry at different scan rates, from 1 to 20 mV s^{-1}. Naphthalene-PEO2000 polyimide (Figure 5.3a) showed the two characteristic redox peaks whereas Perylene-PEO2000 polyimide (Figure 5.3b) presented only one. In both cases, a slight decrease (increase) in the reduction (oxidation) potentials was observed with the scan rate; indicating there is a competition between the

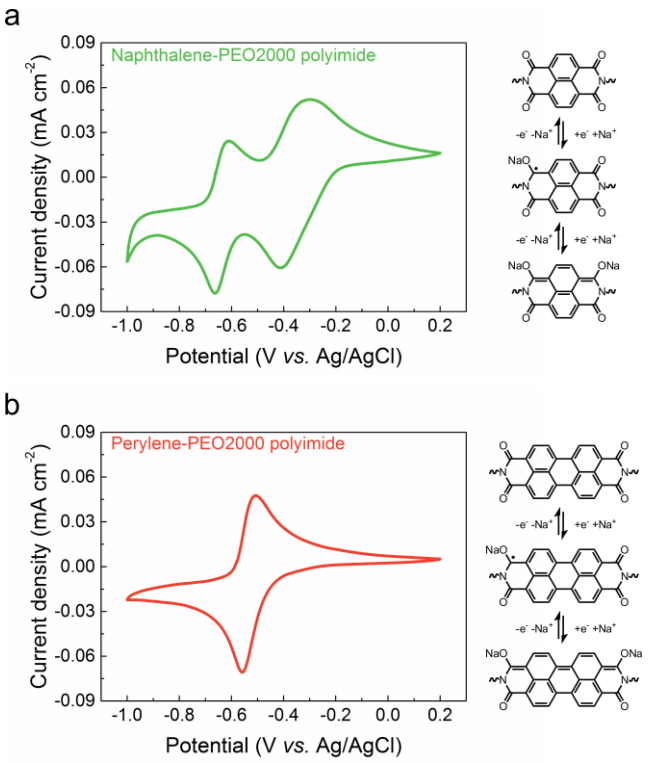

Figure 5.2. Cyclic voltammograms at 1 mV s^{-1} and redox mechanisms of (a) Naphthalene-PEO2000 (green) and (b) Perylene-PEO2000 (red) polyimides.

electrode kinetics and mass transport. Faster scan rates encourage greater electrochemical irreversibility.[30] Considering that the current follows the power-law equation, it can be related to the scan rate by Equation 5-1:

$$i = av^b \qquad \text{Equation 5-1}$$

where i is the current peak, v the scan rate and a and b are adjustable parameters. The slope (value of parameter b) of a log(v)-log(i) plot provides information about the redox mechanism. For b equal 0.5 the electrochemical process is diffusion-controlled whereas for a value of 1 corresponds to an

adsorption-controlled behavior.[31,32] On the one hand, Naphthalene-PEO2000 polyimide featured b values of 0.6 and 0.7 for the first and second redox peaks, respectively, indicating a diffusion-controlled mechanism (Figure 5.3c). On the other hand, Perylene-PEO2000 presented a b value of 1 (Figure 5.3d) suggesting an adsorption-controlled behavior, in which mass transfer might not be rate-determining.[21]

To further investigate the electrochemical performance of both polyimides, galvanostatic charge-discharge experiments were conducted using the same three-electrode cell. Naphthalene-PEO2000 polyimide presented two plateaus at around -0.4 V and -0.7 V *vs.* Ag/AgCl (Figure 5.4a). The capacity observed at the

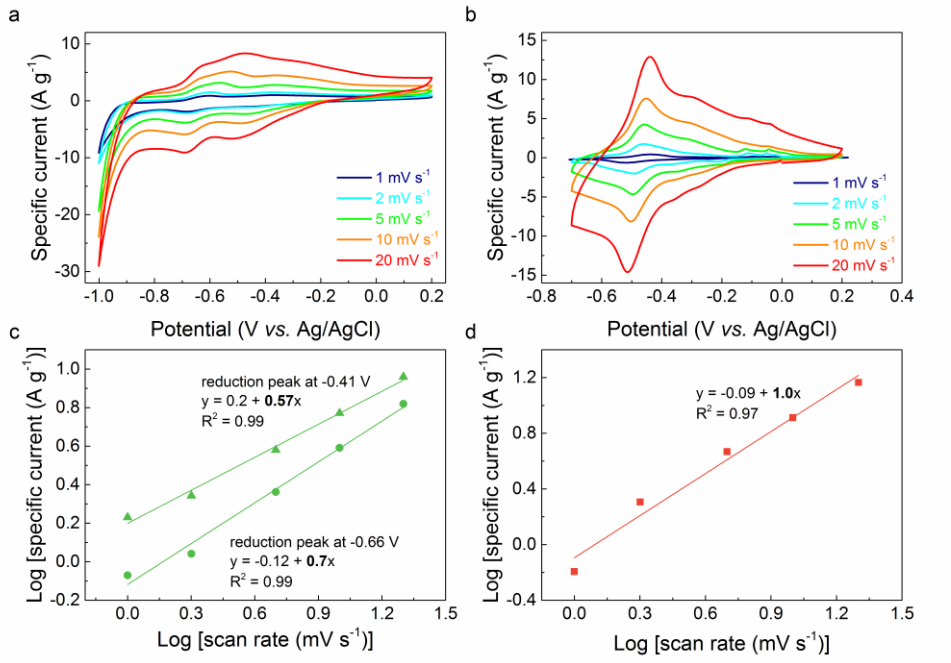

Figure 5.3. Cyclic voltammograms at increasing scan rates of (a) Naphthalene-PEO2000 polyimide and (b) Perylene-PEO2000 polyimide. And b value determined by the relationship between current and scan rate for (c) Naphthalene-PEO2000 polyimide, for the first reduction peak (green triangles) and second reduction peak (green circles) and (d) for Perylene-PEO2000 polyimide (red squares).

end of each plateau indicated that one electron was transferred in each one. This is in agreement with the corresponding cyclic voltammogram in Figure 5.2a. The theoretical capacity of the naphthalene imide units, which are the redox-active species, is 200 mA h g^{-1}. As it can be seen in Figure 5.4b, this polyimide was able to deliver 186 mA h g^{-1} at 20C, (93 % material activity) with coulombic efficiency approaching 100 % and 94 % capacity retention after 25 cycles. A material activity of 93 % at 20C is higher than previous literature reports of 52-60 % at the same C-rate.[17,22,23]

In contrast, Perylene-PEO2000 polyimide was able to reversibly exchange two

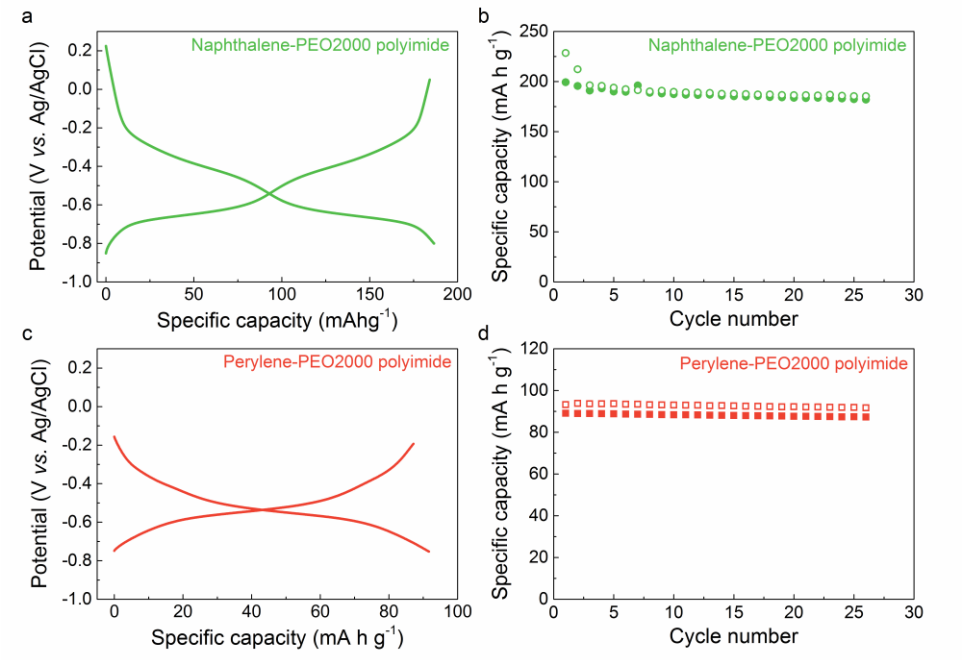

Figure 5.4. (a) Voltage profile and (b) charge (filled circles)-discharge (empty circles) capacities for Naphthalene-PEO2000 polyimide at 20C (1C = 200 mA g^{-1}). (c) Voltage profile and (b) charge (filled squares)-discharge (empty squares) capacities for Perylene-PEO2000 polyimide at 20C (1C = 140 mA g^{-1}).

electrons in one voltage plateau at around -0.5 V *vs.* Ag/AgCl, as seen from the voltage profile in Figure 5.4c and confirmed by the cyclic voltammogram in Figure 5.2b. The specific capacity provided by Perylene-PEO2000 polyimide was 92 mA h g^{-1} (theoretical capacity of perylene units is 140 mA h g^{-1}). Coulombic efficiency also approached 100 % and the material retained 98 % of its capacity after 25 cycles (Figure 5.4d). Therefore, Perylene-PEO2000 polyimide electrode accessed ~67 % of its theoretical capacity when cycled at 20C rate. Although perylene polyimides in sodium aqueous batteries have not been reported, to the best of our knowledge, when compared to the naphthalene analogous a material utilization of 67 % is still higher at 20C.

5.3. High rate performance of perylene polyimide

Due to the novelty of perylene polyimide and its good electrochemical performance, we chose this material to further study its properties at high current rates. Additionally, the fact that this polymer exhibited one charge/discharge plateau instead of two is advantageous from the system engineering perspective for integration of the electrode into practical systems. Redox reactions occurring at one potential would deliver constant energy values. Thus, further characterization of the rate capability and cycle life was carried out for Perylene-PEO2000 polyimide. The processability of the electrode was enhanced by changing the current collector of the working electrode from a platinum metal sheet to a silver ink casted over a polyethylene naphthalate (PEN) substrate. The experiments were also carried out in a three-electrode cell with platinum as counter electrode and Ag/AgCl as reference electrode.

The performance of Perylene-PEO2000 polyimide for high power applications was studied. The capacity was measured at increasing current densities from 10C to 600C which correspond to discharge times of 6 minutes to 6 seconds,

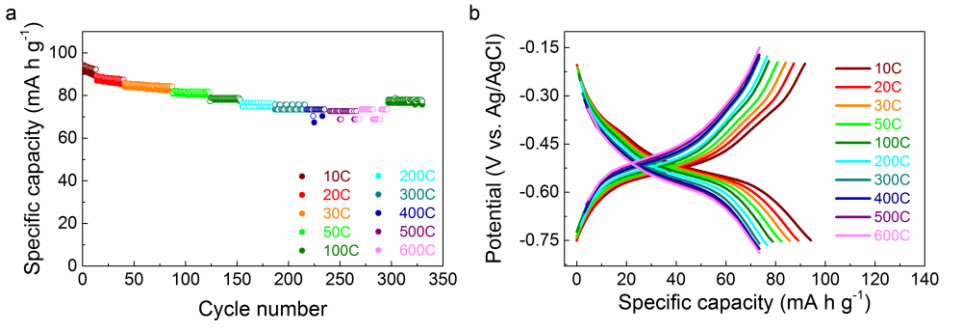

Figure 5.5. (a) Rate capability charge (filled circles)-discharge (empty circles) and (b) voltage profiles at different C-rates for Perylene-PEO2000 polyimide.

respectively. As depicted in Figure 5.5a, the electrode delivered a specific capacity of 94 mA h g^{-1} at 10C and 73 mA h g^{-1} at 600C (78 % capacity retention), without notable increase in polarization (Figure 5.5b) with coulombic efficiency approaching 100 %.

Additionally, cycling stability was studied at 600C for 2000 cycles (Figure 5.6). When cycled at 600C, Perylene-PEO2000 polyimide delivered 54 mA h g^{-1} specific capacity with 100 % coulombic efficiency and 98 % capacity retention

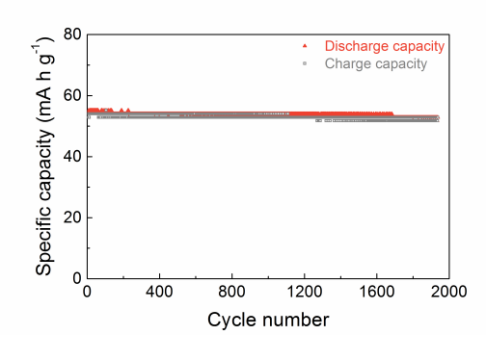

Figure 5.6. Cycling stability of Perylene-PEO2000 polyimide at 600C, charge (grey empty squares)-discharge (red filled triangles).

after 2000 cycles, indicating the high stability of the material when cycled at high currents. This makes Perylene-PEO2000 polyimide a promising anode candidate for high-rate aqueous sodium-ion batteries.

5.4. Conclusions

Naphthalene- and perylene-based polyimides combined with oligoether groups yielded soluble polymers in some organic solvents which facilitated its processability and preparation of the final electrode. Both materials presented electrochemical activity in sodium aqueous electrolyte in the negative side (*vs.* Ag/AgCl) making them good candidates for anode applications. On the one hand, Naphthalene-PEO2000 showed two redox peaks corresponding to one-electron two-step reaction undergoing a diffusion-controlled mechanism. On the other hand, Perylene-PEO2000 polyimide presented one peak indicating a redox mechanism of two-electrons in one-step with an adsorption-controlled behavior. Both polyimides featured stable electrochemical performance with capacity retentions higher than 94 % at 20C.

High power applications were studied for Perylene-PEO2000 polyimide. This polymer retained 78 % of its capacity when the C-rate was increased from 10C to 600C and exhibited stable cycling at 600C for up to 2000 charge-discharge cycles without significant capacity fade (98 % capacity retention). These results make perylene-based polyimide a promising candidate for application in high power aqueous sodium-ion batteries.

5.5. Experimental part

5.5.1. Materials

N-Methyl-2-pyrrolidone (NMP) and sodium sulfate (Na_2SO_4) (≥ 99 %) were purchased from Sigma-Aldrich and used as received. Conductive silver ink was purchased from Creative Materials, Inc.

5.5.2. Electrode preparation

Polymer electrodes were prepared by mixing active material (85 wt% polyimide-polyether copolymer) and Ketjenblack (15 wt%) in NMP. The slurry containing active material was uniformly casted over current collectors to create the working electrodes. Platinum metal was used as current collector with a polymer mass loading of 1 mg over 1.6 cm^2 area. Conductive silver ink casted over a PEN substrate was also used as current collector with 0.5 mg polymer mass loading over 1 cm^2 area.

5.5.3. Methods

Electrochemical tests were carried out using a three-electrode cell with platinum as counter electrode and Ag/AgCl as reference electrode. The electrolyte solution was a 1 M Na_2SO_4 solution purged with nitrogen for 30 minutes.

Electrochemical measurements were carried out on an Ivium-n-Stat electrochemical analyzer. Cyclic voltammetry was performed at different scan rates and galvanostatic charge-discharge measurements at various C-rates (1C refers to 200 mA g^{-1} for Naphthalene-PEO2000 polyimide and to 138 mA g^{-1} for Perylene-PEO2000 polyimide).

5.6. References

(1) Ostfeld, A. E.; Gaikwad, A. M.; Khan, Y.; Arias, A. C. High-performance flexible energy storage and harvesting system for wearable electronics. *Sci. Rep.* **2016**, *6,* 26122.

(2) Zamarayeva, A. M.; Gaikwad, A. M.; Deckman, I.; Wang, M.; Khau, B.; Steingart, D. A.; Arias, A. C. Fabrication of a high-performance flexible silver–zinc wire battery. *Adv. Electron. Mater.* **2016**, *2,* 1500296.

(3) Oltean, V.-A.; Renault, S.; Valvo, M.; Brandell, D. Sustainable Materials for Sustainable Energy Storage: Organic Na Electrodes. *Materials* **2016**, *9,* 142.

(4) Poizot, P.; Dolhem, F. Clean energy new deal for a sustainable world: from non-CO_2 generating energy sources to greener electrochemical storage devices. *Energy Environ. Sci.* **2011**, *4,* 2003-2019.

(5) Hong, S. Y.; Kim, Y.; Park, Y.; Choi, A.; Choi, N.-S.; Lee, K. T. Charge carriers in rechargeable batteries: Na ions vs. Li ions. *Energy Environ. Sci.* **2013**, *6,* 2067-2081.

(6) Palomares, V.; Serras, P.; Villaluenga, I.; Hueso, K. B.; Carretero-Gonzalez, J.; Rojo, T. Na-ion batteries, recent advances and present challenges to become low cost energy storage systems. *Energy Environ. Sci.* **2012**, *5,* 5884-5901.

(7) Pan, H.; Hu, Y.-S.; Chen, L. Room-temperature stationary sodium-ion batteries for large-scale electric energy storage. *Energy Environ. Sci.* **2013**, *6,* 2338-2360.

(8) Yabuuchi, N.; Kubota, K.; Dahbi, M.; Komaba, S. Research development on sodium-ion batteries. *Chem. Rev.* **2014**, *114,* 11636-11682.

(9) Kim, H.; Hong, J.; Park, K.-Y.; Kim, H.; Kim, S.-W.; Kang, K. Aqueous rechargeable Li and Na ion batteries. *Chem. Rev.* **2014**, *114,* 11788-11827.

(10) Whitacre, J. F.; Tevar, A.; Sharma, S. $Na_4Mn_9O_{18}$ as a positive electrode material for an aqueous electrolyte sodium-ion energy storage device. *Electrochem. Commun.* **2010**, *12,* 463-466.

(11) Winsberg, J.; Stolze, C.; Schwenke, A.; Muench, S.; Hager, M. D.; Schubert, U. S. Aqueous 2,2,6,6-Tetramethylpiperidine-N-oxyl catholytes for a high-capacity and uigh current density oxygen-insensitive hybrid-flow battery. *ACS Energy Lett.* **2017**, *2,* 411-416.

(12) Zhou, M.; Li, W.; Gu, T.; Wang, K.; Cheng, S.; Jiang, K. A sulfonated polyaniline with high density and high rate Na-storage performances as a flexible organic cathode for sodium ion batteries. *Chem. Commun.* **2015**, *51,* 14354-14356.

(13) Choi, W.; Harada, D.; Oyaizu, K.; Nishide, H. Aqueous electrochemistry of poly(vinylanthraquinone) for anode-active materials in high-density and rechargeable polymer/air batteries. *J. Am. Chem. Soc.* **2011**, *133,* 19839-19843.

(14) Park, S. I.; Gocheva, I.; Okada, S.; Yamaki, J.-i. Electrochemical Properties of $NaTi_2(PO_4)_3$ Anode for Rechargeable Aqueous Sodium-Ion Batteries. *J. Electrochem. Soc.* **2011**, *158,* A1067-A1070.

(15) Pasta, M.; Wessells, C. D.; Liu, N.; Nelson, J.; McDowell, M. T.; Huggins, R. A.; Toney, M. F.; Cui, Y. Full open-framework batteries for stationary energy storage. *Nat. Commun.* **2014**, *5,* 3007.

(16) Mike, J. F.; Lutkenhaus, J. L. Electrochemically active polymers for electrochemical energy storage: Opportunities and challenges. *ACS Macro Lett.* **2013**, *2,* 839-844.

(17) Qin, H.; Song, Z. P.; Zhan, H.; Zhou, Y. H. Aqueous rechargeable alkali-ion batteries with polyimide anode. *J. Power Sources* **2014**, *249,* 367-372.

(18) Häupler, B.; Wild, A.; Schubert, U. S. Carbonyls: Powerful organic materials for secondary batteries. *Adv. Energy Mater.* **2015**, *5,* 1402034.

(19) Casado, N.; Hernández, G.; Sardon, H.; Mecerreyes, D. Current trends in redox polymers for energy and medicine. *Prog. Polym. Sci.* **2016**, *52,* 107-135.

(20) Song, Z.; Zhou, H. Towards sustainable and versatile energy storage devices: an overview of organic electrode materials. *Energy Environ. Sci.* **2013**, *6,* 2280-2301.

(21) Wang, H.-g.; Yuan, S.; Ma, D.-l.; Huang, X.-l.; Meng, F.-l.; Zhang, X.-b. Tailored aromatic carbonyl derivative polyimides for high-power and long-cycle sodium-organic batteries. *Adv. Energy Mater.* **2014**, *4,* 1301651.

(22) Deng, W.; Shen, Y.; Qian, J.; Yang, H. A polyimide anode with high capacity and superior cyclability for aqueous Na-ion batteries. *Chem. Commun.* **2015**, *51,* 5097-5099.

(23) Gu, T.; Zhou, M.; Liu, M.; Wang, K.; Cheng, S.; Jiang, K. A polyimide-MWCNTs composite as high performance anode for aqueous Na-ion batteries. *RSC Adv.* **2016**, *6,* 53319-53323.

(24) Song, Z.; Zhan, H.; Zhou, Y. Polyimides: Promising energy-storage materials. *Angew. Chem. Int. Ed.* **2010**, *49,* 8444-8448.

(25) Hernández, G.; Casado, N.; Coste, R.; Shanmukaraj, D.; Rubatat, L.; Armand, M.; Mecerreyes, D. Redox-active polyimide-polyether block copolymers as electrode materials for lithium batteries. *RSC Adv.* **2015**, *5,* 17096-17103.

(26) Michot, C.; Baril, D.; Armand, M. Polyimide polyether mixed conductors as switchable materials for electrochromic devices. *Sol. Energy Mater. Sol. Cells* **1995**, *39,* 289-299.

(27) Lacey, M. J.; Jeschull, F.; Edstrom, K.; Brandell, D. Why PEO as a binder or polymer coating increases capacity in the Li-S system. *Chem. Commun.* **2013**, *49,* 8531-8533.

(28) Porcarelli, L.; Shaplov, A. S.; Bella, F.; Nair, J. R.; Mecerreyes, D.; Gerbaldi, C. Single-ion conducting polymer electrolytes for lithium metal polymer batteries that operate at ambient temperature. *ACS Energy Lett.* **2016**, *1,* 678-682.

(29) Wright, P. V. Ionic conductivity and organisation of macromolecular polyether-alkali-metal salt complexes. *J. Mater. Chem.* **1995**, *5,* 1275-1283.

(30) Brownson, D. A. C.; Banks, C. E., Interpreting Electrochemistry. In *The Handbook of Graphene Electrochemistry*, Springer London: London, 2014, 23-77.

(31) Lindström, H.; Södergren, S.; Solbrand, A.; Rensmo, H.; Hjelm, J.; Hagfeldt, A.; Lindquist, S.-E. Li^+ Ion Insertion in TiO_2 (Anatase). 2. Voltammetry on Nanoporous Films. *J. Phys. Chem. B* **1997**, *101,* 7717-7722.

(32) Simon, P.; Gogotsi, Y.; Dunn, B. Where do batteries end and supercapacitors begin? *Science* **2014**, *343,* 1210-1211.

CHAPTER 6.
CONCLUSIONS

Chapter 6. Conclusions

This PhD thesis aimed at designing polyimides with improved electrochemical properties as well as enhanced tractability. The synthesized polyimides were characterized as electrode materials for electrochemical cells, such as lithium batteries, lithium-sulfur batteries and aqueous sodium batteries.

First, redox-active polyimides bearing different imide structures as well as additional electroactive moieties and flexible groups were synthesized and characterized as cathode materials in lithium batteries. Cyclic voltammetry of polyimides varied depending on the chemical structure of the starting dianhydrides. Polyimides based on pyromellitic dianhydride showed two redox peaks whereas naphthalene-based polyimides featured only one at higher voltages. Galvanostatic charge-discharge experiments suggested a three-electron redox reaction for polyimides prepared from naphthalene dianhydride and electroactive diamines. Among the different polymers, anthrone-based naphthalene polyimide featured the best results regarding cycling stability and rate performance. In contrast, flexible polyimides bearing aliphatic diamines with

ether functionalities were able to access the complete theoretical capacity of the material.

Secondly, soluble polyimide-polyether copolymers were successfully synthesized through a straightforward polycondensation reaction. Three different dianhydrides (pyromellitic, naphthalene and perylene) were used as starting monomers with linear oligoether diamines (Jeffamines® of 600, 900 and 2000 g mol^{-1}). Solubility in acetonitrile and film forming properties facilitated the electrode preparation of these copolymers, avoiding the use of toxic and high boiling point solvents. Increasing conjugation from pyromellitic, to naphthalene and to perylene imide structures resulted in higher redox voltages and greater stability of the electrodes. However, the highest active mass utilization was achieved by Naphthalene-PEO2000 polyimide. Furthermore, lengthening the PEO chains from 600 to 2000 g mol^{-1} led to higher accessibility of the redox-active imide moieties, thus increasing the specific capacity.

Beyond conventional lithium-ion batteries, lithium-sulfur cells are arising as promising devices with high specific capacity. However, several challenges such as poor electrode rechargeability and fast capacity fade are still unsolved. Incorporation of redox mediators, such as imide groups, to the electrode formulation is an interesting approach to solve those problems. Therefore, the synthesized polyimide-polyether copolymers were investigated as redox-active binders for sulfur cathodes. In particular, sulfur cathode containing Naphthalene-PEO2000 polyimide binder was able to increase the sulfur utilization in addition to improve the rate performance when compared to conventional binders, such as PVDF-HFP or PEO. Additionally, to explore more practical applications the amount of carbon in the electrode composition was reduced from 30 wt% to 5 wt% and PEO:LiTFSI was used as polymer electrolyte to improve the cell safety. Sulfur cathode with Naphthalene-PEO2000 binder presented lower polarization, higher reaction kinetics and increased cycling stability in comparison

to the reference sulfur electrode with PEO binder, suggesting a redox mediating effect of the imide groups.

Finally, electrochemical properties of polyimide-polyether copolymers were studied in sodium aqueous electrolyte due to their safety, low cost and environmentally friendly characteristics. While Naphthalene-PEO2000 polyimide presented two pairs of redox peaks involving one-electron each, Perylene-PEO2000 polyimide showed only one pair corresponding to two-electron redox reaction. Investigation on the kinetics of the redox reactions determined a diffusion-controlled mechanism for Naphthalene-PEO2000 polyimide and an adsorption-controlled behavior for the analogous perylene polyimide. Galvanostatic charge-discharge measurements at 20C demonstrated that Naphthalene-PEO2000 polyimide featured better electrochemical performance in terms of active mass utilization. In contrast, Perylene-PEO2000 polyimide presented outstanding rate performance when increasing C-rate from 10C to 600C. Regarding cycling stability, the latter polymer delivered stable capacity at 600C for 2000 cycles.

Resumen

La transición de combustibles fósiles a energías renovables es uno de los desafíos más importantes e inminentes para combatir el cambio climático y el calentamiento global. Una sociedad moderna y sostenible debe ser capaz de almacenar energía proveniente de energías renovables como la eólica o la solar. Desafortunadamente, estas fuentes de obtención de energía son intermitentes e imprevisibles. Por ello, es importante y necesario el desarrollo de tecnologías de almacenamiento de energía que sean eficientes para sacar el mayor provecho de dichas energías renovables.

Además, las aplicaciones que requieren sistemas de almacenamiento están creciendo enormemente desde los dispositivos electrónicos portátiles, hasta la implementación de una red de transporte eléctrico e incluso a gran escala en el caso de la red eléctrica. Actualmente, la mayor parte de las baterías comerciales son de litio-ion basadas en óxidos inorgánicos como materiales activos. Sin embargo, a pesar de su excelente densidad energética y potencia, contienen metales tóxicos y disolventes orgánicos inflamables. Por ello, se están investigando nuevos materiales electroquímicamente activos que no sean tóxicos, que permitan su reciclaje y que almacenen energía sin dañar el medio ambiente, de manera sostenible, con bajo coste y que sea seguro (Figure R.1).

Figure R.1. Esquema representando los futuros retos en el campo del almacenamiento de energía electroquímica.

En este contexto, los polímeros con propiedades redox están ganando interés como materiales alternativos a los utilizados convencionalmente para almacenamiento de energía electroquímica. Asimismo, los polímeros ofrecen otras ventajas como la gran variedad estructural disponible, su bajo peso y flexibilidad. Dentro de la gran variedad de polímeros electroactivos, los polímeros con grupos carbonilo y, en concreto, las poliimidas han ganado interés en los últimos años debido a su marcado potencial redox y alta capacidad específica. Las poliimidas son buenas candidatas para almacenamiento de energía electroquímica debido a que pueden ser sintetizadas de manera fácil y en grandes cantidades, a la vez que poseen excelentes propiedades térmicas. Sin embargo, la desventaja de las poliimidas electroactivas es que normalmente son polvos insolubles que dificultan su procesado. Por ello, el objetivo principal de esta tesis es la síntesis de poliimidas solubles, con propiedades electroquímicas mejoradas, así como su utilización en diferentes sistemas de

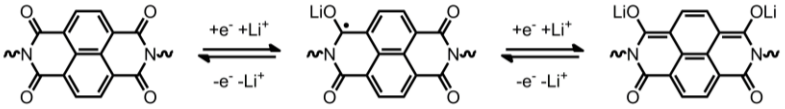

Figure R.2. Mecanismo de la reacción redox de una poliimida basada en naftaleno.

almacenamiento de energía electroquímica como las baterías de litio, de litio-azufre y de sodio en medio acuoso.

Las poliimidas se sintetizan a partir de dianhídridos y diaminas. Las propiedades electroquímicas vienen dadas principalmente por los grupos imida, que por norma general, son capaces de reducirse y oxidarse reversiblemente transfiriendo un electrón por cada grupo (Figure R.2). Así, las poliimidas son capaces de intercambiar dos electrones por cada unidad repetitiva. En el segundo capítulo de esta tesis, se han sintetizado poliimidas con diaminas electroactivas incrementando el número de electrones intercambiados y, consecuentemente, la energía que pueden almacenar. Entre todas las estructuras estudiadas, la poliimida preparada con una diamina derivada del grupo antrona (antraceno con una cetona) mostró los mejores resultados en cuanto a estabilidad en el ciclado de la batería y capacidad a elevadas velocidades de carga-descarga. Por otro lado, el uso de diaminas alifáticas, y en particular las que contienen grupos éter, dan lugar a poliimidas más flexibles capaces de acceder a toda la capacidad teórica del material.

En el tercer capítulo se sintetizaron copolímeros de poliimida y poliéter mediante una sencilla reacción de policondensación. Los polímeros obtenidos, solubles en acetonitrilo, facilitaron la preparación de los electrodos debido a su habilidad para formar filmes. El aumento de la conjugación en la estructura de la imida (desde el piromelítico, pasando por el naftaleno hasta el perileno) resultó en un incremento sucesivo del voltaje y de la estabilidad de la batería. Sin embargo, el

copolímero que presentó mayor porcentaje de masa activa fue la polimida basada en naftaleno y poliéter de 2000 g mol^{-1}. Además, se observó que al aumentar la longitud de las cadenas de poliéter desde 600, 900 hasta 2000 g mol^{-1} supuso una mayor accesibilidad de los grupos imida electroactivos.

Una vez que las propiedades electroquímicas de las poliimidas fueron estudiadas, se prosiguió a su empleo en diferentes tipos de baterías. Por ejemplo, las baterías de litio-azufre poseen una elevada densidad energética y utilizan azufre que es un material activo barato y con baja toxicidad. Sin embargo, algunos de los problemas que están sin resolver en esta aplicación son la pérdida de capacidad durante el ciclado y la necesidad de incorporar grandes cantidades de carbón conductor debido a su carácter aislante. Las poliimidas presentan potenciales redox muy parecidos a los del azufre, por lo que pueden actuar como mediadores redox mejorando la reacción electroquímica del azufre. Dada la solubilidad y la posibilidad de formar filmes de los copolímeros de poliimida y poliéter, éstos fueron investigados como aglutinantes electroactivos en electrodos de azufre.

El cátodo de azufre compuesto de la poliimida Naftaleno-PEO2000 presentó un aumento de la utilización del azufre y un mejor funcionamiento a altas velocidades de carga-descarga en comparación con electrodos de azufre preparados con aglutinantes convencionales como PVDF-HFP o PEO. Para llevar a cabo aplicaciones más prácticas, la cantidad de carbón conductor se redujo desde un 30 % en peso hasta un 5 % en peso y, además, se utilizó una mezcla de PEO:LiTFSI como electrolito polimérico para aumentar la seguridad de la batería. De nuevo, el cátodo de azufre con poliimida Naftaleno-PEO2000 como aglutinante demostró una menor polarización, cinéticas redox más rápidas y un aumento en la estabilidad durante el ciclado en comparación con el aglutinante de poliéter, sugiriendo la habilidad de la imida para actuar como mediador redox del azufre.

Por último, los copolímeros de poliimida-poliéter fueron estudiados como ánodos de baterías de sodio acuosas caracterizadas por su bajo coste, seguridad y sostenibilidad. Por un lado, la poliimida de Naftaleno-PEO2000 dio lugar a dos pares de picos redox intercambiando un electrón en cada uno ellos. Por otro lado, la poliimida de Perileno-PEO2000 mostró un solo par de picos redox con el intercambio de dos electrones. Éste último material presentó un excelente funcionamiento a elevadas velocidades de carga-descarga, proporcionando estabilidad electroquímica durante 2000 ciclos a una velocidad de carga-descarga de 6 segundos (600C).

Para concluir, en esta tesis doctoral se han desarrollado poliimidas electroactivas con diferentes estructuras y sus propiedades electroquímicas han sido estudiadas. Los copolimeros de poliimida-poliéter se han investigado como materiales activos de cátodos en baterías de litio, como aglutinantes electroactivos en baterías de litio-azufre y como ánodos en baterías de sodio acuosas.

List of acronyms

6F	Hexafluoroisopropylidene moiety
6FDA	4,4’-(hexafluoroisopropylidene) diphthalic anhydride
AAn	Aniline anthrone
ACN	Acetonitrile
AFM	Atomic Force Microscopy
AMAC	Poly(acrylamide-*co*-diallyldimethylammonium chloride)
APh	Aniline phthalein
AphI	Aniline phthalimidine
ATR-FTIR	Attenuated Total Reflectance Fourier Transform Infrared Spectroscopy
CMC	Carboxymethylcellulose
CNT	Carbonnanotube
CV	Cyclic Voltammetry

Đ	Dispersity
DDA	1,12-dodecanediamine
DMAc	N,N-dimethylacetamide
DMAc	*N,N*-dimethylacetamide
DME	Dimethoxyethane
DMF	*N,N*-dimethylformamide
DMSO-d_6	Deuterated dimethyl sulfoxide
DODDA	4,9-dioxa-1,12-dodecanediamine
DOL	1,3-dioxolane
DSC	Differential Scanning Calorimetry
EO	Ethylene oxide
GPC	Gel Permeation Chromatography
IoT	Internet of Things
KB	Ketjenblack
Li-air	Lithium-air
LiFSI	Lithium bis(fluorosulfonyl)imide
Li-S	Lithium-sulfur
LiTFSI	Lithium bis(trifluoromethanesulfonyl)imide
LUMO	Lower Unoccupied Molecular Orbital

MeTHF	2-methyltetrahydrofuran
MW	Molar mass of the repeating unit
M_w	Molecular weight
MWCNT	Multi-walled carbon nanotube
Na-ion	Sodium-ion
NASICON	Sodium Super Ionic CONductor
NMP	*N*-methyl-2-pyrrolidone
NMR	Nuclear Magnetic Resonance
NTDA	1,4,5,8-naphthalenetetracarboxylic dianhydride
PANI	Polyaniline
PEDOT	Poly(3,4-ethylenedioxythiophene)
PEN	Polyethylene naphthalate
PEO	Poly(ethylene oxide)
PLDA	Perylene-3,4,9,10-tetracarboxylic dianhydride
PMDA	Pyromellitic dianhydride
PPO	Poly(propylene oxide)
Ppy	Polypyrrole
PTFE	Poly(tetrafluoroethylene)
PVDF	Poly(vinylidene fluoride)

PVDF-HFP	Poly(vinylidene difluoride-*co*-hexafluoropropylene)
PVP	Poly(vinylpyrrolidone)
QN-TFSI	Quinuclidine-TFSI
RFB	Redox Flow Batteries
SBR	Styrenebutadiene rubber
SCE	Saturated Calomel Electrode
SWCNT	Single-walled carbon nanotube
T_d	Degradation temperature
TEMPO	2,2,6,6-tetramethylpiperidine-1-oxyl
T_g	Glass transition temperature
TGA	Thermogravimetric analysis
THF	Tetrahydrofuran
T_m	Melting temperature

List of publications

1. **Guiomar Hernández**, Mehmet Işik, Daniele Mantione, Afshin Pendashteh, Paula Navalpotro, Devaraj Shanmukaraj, Rebeca Marcilla, David Mecerreyes. Redox-active poly(ionic liquid)s as active materials for energy storage applications. Journal of Materials Chemistry A, 2017, Advance Article, DOI: 10.1039/C6TA10056B.

2. Nerea Casado, **Guiomar Hernández**, Antonio Veloso, Devaraj Shanmukaraj, David Mecerreyes, Michel Armand. PEDOT radical polymer with synergetic redox and electrical properties. ACS Macro Letters, 2016, 5, 59-64.

3. Nerea Casado, **Guiomar Hernández**, Haritz Sardon, David Mecerreyes. Current trends in redox polymers for energy and medicine. Progress in Polymer Science, 2016, 52, 107-135.

4. **Guiomar Hernández**, Nerea Casado, Raphaël Coste, Devaraj Shanmukaraj, Laurent Rubatat, Michel Armand, David Mecerreyes. Redox-active polyimide-polyether block copolymers as electrode materials for lithium batteries. RSC Advances, 2015, 5, 17096-17103.

5. M. Ali Aboudzadeh, Alexander S. Shaplov, **Guiomar Hernández**, Ptr S. Vlasov, Elena I. Lozinskaya, Cristina Pozo-Gonzalo, Maria Forsyth, Yakov s. Vygodskii, David Mecerreyes. Supramolecular ionic networks with superior thermal and transport properties based on novel delocalized di-anionic compounds. Journal of Materials Chemistry A, 2015, 3, 2338-2343.

6. Nerea Casado, **Guiomar Hernández**, David Mecerreyes, Michel Armand. Polímeros innovadores para almacenamiento de energía. cicNetwork, 2013,14, 52-55.

List of presentations

1. 18th IMLB Meeting, Chicago, USA, 19th – 24th June 2016.
   Poster Presentation: New polyimides as electrode materials for Li-ion batteries. Guiomar Hernández, Sofia M. Morozova, Alexander S. Shaplov, Elena I. Lozinskaya, Yakov S. Vygodskii, Devaraj Shanmukaraj, Michel Armand, David Mecerreyes.

2. 229th ECS Meeting, San Diego, USA, 29th May – 2nd June 2016.
   Oral presentation: Redox-active poly(ionic liquid)s as active materials in energy devices. Guiomar Hernández, Mehmet Işik, David Mecerreyes.

3. EUPOC, Gargnano, Italy, 24th – 28th May 2015.
   Poster presentation: Redox-active polyimide-polyether block copolymers as electrode materials for lithium batteries. Guiomar Hernández, Nerea Casado, Raphaël Coste, Devaraj Shanmukaraj, Laurent Rubatat, Michel Armand, David Mecerreyes.

4. JIP-JEPO, Donostia-San Sebastián, Spain, 14th – 18th September 2015.
   Oral presentation: Redox-active polymers for batteries. Guiomar Hernández, Nerea Casado, Laurent Rubatat, Devaraj Shanmukaraj, Michel Armand, David Mecerreyes.

5. Polycondensation, Tokyo, Japan, 8th – 11th September 2014.
   Poster presentation: Polyimide/polyether block copolymers for electrochemical energy storage. Guiomar Hernández, Nerea Casado, Michel Armand, David Mecerreyes.

6. ISPE, Geelong, Australia, 24th – 29th August 2014.
   Poster presentation: Polyimide/polyether block copolymers for energy storage. Guiomar Hernández, Nerea Casado, Michel Armand, David Mecerreyes.

7. Power Our Future 2014, Vitoria-Gasteiz, Spain, 2nd – 4th April 2014.
   Poster presentation: Polyimide/polyether block copolymers for energy storage. Guiomar Hernández, Nerea Casado, Michel Armand, David Mecerreyes.

Collaborations

This thesis has been done in close collaboration with several universities and research centers. Firstly, polyimides presented in chapter 1 were synthesized by Sofia M. Morozova and Dr. Alexander S. Shaplov from A. N. Nesmeyanov Institute of Organoelement Compounds of Russian Academy of Sciences (INEOS RAS) (Moscow, Russia).

Besides, I regularly moved to CIC EnergiGUNE (Vitoria-Gasteiz, Spain) to assemble the batteries and perform the electrochemical characterization reported in chapters 2, 3 and 4. This part was supervised by Dr. Devaraj Shanmukaraj and Prof. Michel Armand. Additionally, morphology of samples reported in chapter 3 was studied by AFM in collaboration with Raphaël Coste and Dr. Laurent Rubatat from the University of Pau.

Finally, chapter 5 was developed at the University of California at Berkeley (Berkeley, USA) during a 6-month stay under the supervision of Dr. Abhinav M. Gaikwad and Prof. Ana C. Arias.